Chemical Analysis of *Dacrydium cupressinum* to Help Save the Kākāpō

BY

DANIEL STEVEN HARRINGTON

A thesis submitted to the Victoria University of Wellington in fulfilment of the requirements for the degree of Master of Drug Discovery and Development

The Ferrier Research Institute

2022

Abstract

The world's largest flightless parrot, the kākāpō, are a critically endangered species with 209 individuals remaining. Conservation efforts involving close monitoring, supplementary feeding, genetic analysis, and artificial insemination have increased the kākāpō population from a low of 51 individuals in 1995. Slow breeding cycles, low fertility, and a lack of available predator free habitat currently hinder recovery efforts.

Rimu (*Dacrydium cupressinum*) berries are a favourite food of kākāpō. Breeding generally coincides with rimu masting which limits the kākāpō reproductive cycle to approximately once every three years. The breeding triggers for kākāpō are not yet fully understood. It has been hypothesised that phytoestrogens present in rimu fruit act as a breeding trigger by increasing the fecundity of both females and males.

Natural products extraction and chromatography techniques guided by nuclear magnetic resonance (NMR) spectroscopy were used to search for potential phytoestrogens. Aided by an oestrogenic bioassay, phytoestrogenic compounds were detected in the water and methanol extracts of rimu plant structures consumed by kākāpō. Compound **48** was isolated, a compound that shares structural similarity with the known phytoestrogen podocarpic acid (**27**), a known high-level constituent of rimu heartwood. Spectroscopic evidence for other compounds sharing structural similarity to **27** was also detected in fractions of rimu plant structures.

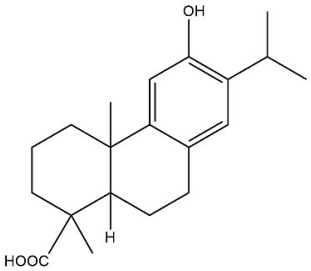

48

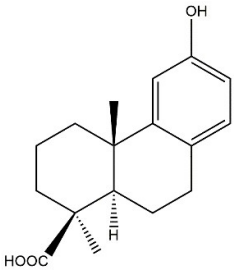

27

Carbohydrate analysis of rimu berries was conducted to characterise the individual sugar composition as nutritional and prebiotic chemical characterisation will inform supplementary feed formulations. This study examined the simple sugars, starch, and monomer compositions of alcohol and warm water extracts of rimu berries.

Rimu plant structures from the island sanctuaries where kākāpō currently reside were examined for their iodine content and were found to be relatively high in iodine. This finding may influence further studies examining kākāpō thyroid health and fecundity which is influenced by iodine intake.

Acknowledgements

First and foremost, I wish to express my deepest gratitude to Simon Hinkley and Janet Pitman for providing me with this opportunity to work on this project.

Simon, your infectious curiosity, consistent positivity, and encouraging nature has made working with you an absolute pleasure. I really appreciate how you managed to understand me as a person, trust me to work independently, and would happily take time to hang out and chat. You have gone beyond your duties as a supervisor; you have truly been a mentor.

I would like to express how much I have enjoyed my time working at the Ferrier Institute. The collaborative and supportive culture of the Ferrier Institute has been evident throughout my studies.

I would also like to extend my thanks for the Marsden Fund for selecting this project for funding.

Tracy Bell, your advice and support with the carbohydrate analysis is very much appreciated. Your knowledge as a botanist and of plant cell walls was extremely helpful.

Jono Singh and Peter Northcote, not only do I thank you for your continued support throughout this entire project, but also for the many laughs and good chats. Jono, I thank you for being there to answer all my questions, no matter how trivial or endless they were. Peter, your spectroscopic wizardry not only amazed me, but has also taught me a lot. I'm thankful for all your help and advice.

I would like to thank Janet Pitman and Amey Hughes at the Victoria School of Biological Sciences for providing the bioassay which was incredibly valuable to this study.

Andrew Digby, thank you for your assistance in providing current data for kākāpō populations and nutrient compositions of rimu berries and supplementary food which

has extended the information in this study beyond what is currently reported in the published literature.

Thanks to Malcolm Reid at the University of Otago for his assistance with the iodine analysis.

Thanks to Yinrong Lu for high resolution mass spectrometry.

I would also like to thank all of the A-block team for always being friendly, approachable, and supportive. Rob Keyzers, I thank you for your support on MS and for igniting my passion for natural products chemistry during my undergraduate studies. Benji Compton, thanks for taking me on as a summer student at the Ferrier Institute. Thanks to the F-block team who helped me as summer student and during this study.

Finally, I would like to thank all my friends and family for their continued support and encouragement.

Declaration and copyright

The work in this thesis was completed by the author at Victoria University of Wellington, New Zealand. It has not been submitted before, in part or in whole, for a higher degree at this university or any other.

Contents

List of Figures

List of Tables

List of Schemes

Glossary

1D	One-dimensional
2D	Two-dimensional
ADF	Acid detergent fibre
ADP	Adenosine diphosphate
AGP	Arabinogalactan protein
AIR	Alcohol insoluble residue
AOAC	Association of official agricultural chemists
aq.	Aqueous
Arg	Arginine
ATP	Adenosine triphosphate
br	Broad
C18	Octadecyl derivatised silica gel
CC	Circadian clock
$CDCl_3$	Chloroform (deuterated)
CE	Chloroform extract
COSY	Correlation spectroscopy
CV	Column volume
d	Doublet
dd	Doublet of doublets
ddd	Doublet of doublet of doublets
DCM	Dichloromethane
DMSO	Dimethyl sulfoxide
DNA	Deoxyribonucleic acid
DP	Degree of polymerisation
DPC	Dietary phytochemicals
dquin	Doublet of quintets
E1	Oestrone
E2	Oestradiol
E3	Oestriol
ELSD	Evaporative light scattering detector
ER	Oestrogen receptor
EtOAc	Ethyl acetate
EtOH	Ethanol
EYPG	Egg yolk protein genes
F-6-P	Fructose-6-phosphate
FA	Fatty acid
Fol	Foliage
FSH	Follicle stimulating hormone
G-6-P	Glucose-6-phosphate

GC	Gas chromatography
GC-MS	Gas chromatography-mass spectrometry
Glu	Glutamic acid
H	Hypothalamus
H2SO4	Sulfuric acid
hER	Human oestrogen receptor
His	Histidine
HMBC	Heteronuclear multiple bond correlation
HPAEC-PAD	High-performance anion exchange chromatography with pulsed amperometric detection
HPLC	High-performance liquid chromatography
HSQC	Heteronuclear single-quantum correlation
ICP-MS	Inductively coupled plasma mass spectrometry
ICP-OES	Inductively coupled plasma optical emission spectrometry
Ile	Isoleucine
kER	Kākāpō oestrogen receptor
LBD	Ligand binding domain
LC-MS	Liquid chromatography-mass spectrometry
LH	Luteinising hormone
m	Multiplet
m/z	Mass to charge ratio
ME	Methanol extract
MeHCl	Methanolic hydrochloric acid
MeOH	Methanol
Met	Methionine
MS	Mass spectrometry
MW	Molecular weight
NADP+	Nicotinamide adenine dinucleotide phosphate (oxidised)
NADPH	Nicotinamide adenine dinucleotide phosphate (reduced)
NaOH	Sodium hydroxide
NDF	Neutral detergent fibre
NMR	Nuclear magnetic resonance
NOESY	Nuclear Overhauser effect spectroscopy
P	Pituitary
Phe	Phenylalanine
ppm	Parts per million (NMR chemical shift)
PSDVB	Poly(styrene-divinyl benzene)
RB	Rimu berry
R_f	Retention factor
RS	Rimu seed
RUO	Rimu unfertilised ovule
s	Singlet
SDG	Secoisolariciresinol diglucoside
SERM	Selective oestrogen receptor modulator

sept	Septet
SHBG	Sex hormone binding globulin
SOF	Small ovarian follicles
SS	Alcohol soluble solution
t	Triplet
td	Triplet of doublets
TFA	Trifluoroacetic acid
TLC	Thin-layer chromatography
TMAH	Tetramethylammonium hydroxide
UV	Ultraviolet
WE	Water extract
WWE_Insol	Warm water extract insoluble
WWE_Sol	Warm water extract soluble
YF	Yolk-filled follicles
δ	Chemical shift (ppm)

Chapter 1. Introduction

1.1 Kākāpō

Kākāpō (*Strigops habroptilus*) are a critically endangered, flightless, nocturnal parrot species, native to New Zealand. Kākāpō are the heaviest parrot species in the world and are possibly the longest living bird species in the world with recorded lifespans of 90 years.[1] Kākāpō previously occupied mountain, forest, and grassland habitats across the entire country but habitat destruction and the introduction of predators had reduced their known population to 51 in 1995. The entire remaining population of kākāpō was transferred to Whenua Hou/Codfish Island, Maud Island, and Hauturu/Little Barrier Island in the 1980s and 1990s. Since then, the population has been managed on five managed predator-free islands including Whenua Hou/Codfish Island, Maud Island, Hauturu/Little Barrier Island, Chalky Island, and Pukenui/Anchor Island.[1]

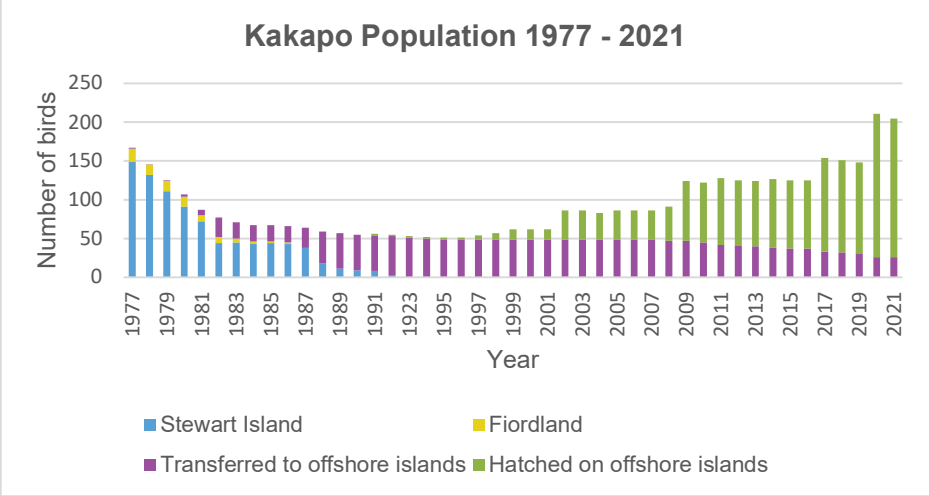

Figure 1. Kākāpō population 1977 – 2021. Reproduced from personal communication with kākāpō science advisor Andrew Digby from the Department of Conservation.

Kākāpō population recovery efforts are hindered by high levels of infertility, egg hatching failures, abnormal sperm, and genetic bottlenecks.[2,3] Thanks to recovery efforts including supplementary feeding, genetic studies, and artificial insemination, the population of kākāpō reached a record 70 year high of 213 birds in December 2019.[3,4] Creating larger areas of predator free land and improving the fertility and successful reproduction of kākāpō is a high priority if conservation efforts are to save this precious species from extinction.

Figure 2. Map of New Zealand displaying the locations of the five managed predator free islands where kākāpō currently reside.

Figure 3. Illustration of a kākāpō. Reproduced from “A History of the Birds of New Zealand” by J. G. Keulemans, in W.L. Buller's 2nd edition, published 1888. (Public domain).

Kākāpō have an annual gonadal cycle in which male testosterone, and female 17β-oestradiol (E2), levels are elevated during the spring and summer of the breeding season.[2] Despite this, kākāpō usually breed only once every 2-5 years in a lek mating system.[3] Lek mating consists of an aggregation of males engaging in competitive displays and courtship rituals to attract prospecting females.[4] For male kākāpō, this consists of a bowl and track system in which each male kākāpō excavates and maintains one or multiple shallow depressions, known as bowls,

which are linked by tracks. The bowls act to help resonate the low-frequency booming call of male kākāpō which serves to attract prospective mates who assess bowl location, acoustic quality and booming efficiency, amongst other characteristics, for mate suitability.[5] Kākāpō are capable of annual breeding as egg laying has been observed on two successive seasons on Little Barrier Island, but the appropriate stimuli are evidently not naturally present every year.[2] Kākāpō breeding has been linked to territorial behaviour, seasonal changes in photoperiod, and annual variations in the abundance of food.[3] It is unknown what induces kākāpō to breed, but triggers may include cognitive stimulus, nutritional status, weight gain, or hormonal stimulation.[3] Booming behaviour from male kākāpō coincides with elevated male testosterone levels and begins many weeks before the females lay eggs.[2] In some years, the males will boom without egg-laying occurring, possibly indicating that there is a difference between the breeding triggers which male and female kākāpō respond to.[3]

Successful breeding in kākāpō has been linked to larger foraging home ranges and a higher quality of breeding habitat characterised by the prevalence of mature rimu forest.[6] The successful breeding season of 2018/2019 resulted in 71 chicks surviving through to juvenile age and has been linked to the rimu mast year (refer to **Section 1.2**) leading to large amounts of rimu fruit being available on the predator free islands where kākāpō populations are managed.[7] Tracking mast years in a range of forest trees and plants such as rimu (*Dacrydium cupressinum*), beech (*Nothofagus* sp.), and snow tussock (*Chionochloa rigida*), has shown that masting is linked to the timing of kākāpō breeding on Stewart, Little Barrier, and Codfish islands.[3]

Kākāpō are entirely herbivorous and feed on a wide range of leaves, twigs, bark, roots, fern rhizome, fungi, fruit, nectar, and seeds from a number of plant species.[8,9] The most sought after parts of plants are either subterranean or new growth leaves, bark, and fruit-seeds, which are possibly selected due to containing the highest nutrient levels.[9] The preferred food of female kākāpō and developing chicks is the fruit of podocarps (Podocarpaceae family) such as rimu.[10,11] It has been suggested that the development of green ovules on rimu trees during the middle of the year

may serve as a potential trigger for kākāpō in order to breed in the following autumn,[12] yet, kākāpō have also been found to successfully live in vegetation less than a metre high in habitats that are devoid of podocarps.[8] While rimu may provide a major cue for kākāpō breeding it is not essential. Increases in the intake of specific nutrients combined with visual and tactile cues from the sight and ingestion of particular foods likely produces a range of effects which kākāpō respond to.[3]

Supplementary food has been tested on populations of low body mass kākāpō on Little Barrier Island and was found to induce the first breeding in 7 years which indicates that the availability of food plays an important role in breeding.[13] The supplementary food provided to kākāpō included almonds, Brazil nuts, walnuts, sunflower seeds, apples, sweet potato, and honey/water (3:1) solution. Supplementary feeding resulted in an average increase in 15% of the body mass of female kākāpō with the supplementary feed making up on average 55% of the daily metabolised energy.[14]

When supplementary feeding was provided to kākāpō of adequate body mass on Codfish Island, there was no increase in breeding frequency, and heavy supplementary feeding was found to decrease breeding frequency and bias the offspring ratio towards males.[14,15] The reduction in breeding frequency has been suggested to be due to high concentrations of leptin produced from adipose tissue which mediates the undernutrition-induced alternations of the reproductive-axis in the hypothalamus.[16] The bias towards male progeny is thought to occur through maternal control of offspring sex ratio where well-nourished reproducing females are able to invest in the greater energy requirements to raise the larger and faster growing males, whereas the production of female offspring is advantageous during times of lesser food availability.[14] There is also the hypothesis that female kākāpō bias their production towards the more dispersive sex when competition for resources is greater. For many bird species, the females are more likely to disperse from their natal area than the males, but it is unknown how this occurs in kākāpō due to the limited number that have been raised to independence and the lack of available habitat for dispersion.[14]

1.2 *Dacrydium cupressinum* (Rimu)

Dacrydium cupressinum, commonly known as rimu, is a large evergreen coniferous tree endemic to New Zealand belonging to the family Podocarpaceae. Other names for rimu include red pine, huarangi, puaka, and Southern conifer.[17] Rimu trees generally will grow to a height of 20-35 m with a life span of 550 – 650 years, but some specimens may grow to reach heights of up to 60 m and have lifespans exceeding 1000 years.[18]

Rimu are dioicous, with male and female cones occurring on different trees.[17] Reproduction occurs at irregular intervals, commonly known as mast seeding, in which heavy seed crops are produced by the majority of trees in some years (mast years), while other years see little or no seed production. Mast seeding has been hypothesised to be an evolutionary response to seed predation, or may be due to climatic cues and a greater abundance of resources.[19] Reproduction in rimu spans three growing seasons (24 – 30 months) with both sexes exhibiting a synchronised reproductive effort with cone production beginning late in the summer of the first season, followed by pollination in the second season, fertilisation in spring to early summer of the third season, and seed fall occurring during autumn at the end of the third season.[19] Seeds can be dispersed by gravity up to 20 m from the parent tree, but are also well suited to dispersal by birds who swallow both the seed and the swollen red or pink fleshy receptacle which subtends the ovule, allowing the seed to pass through the digestive system intact and be dispersed in the bird's effluent large distances away from the parent tree.[20]

Figure 4. Illustrations of rimu. **(A)** Mature rimu tree. **(B)** Juvenile rimu tree. **(C)** Pendulous branch with mature cones on the tips. **(D)** Mature cone with swollen red fleshy receptacle with elliptic-oblong seed. Reproduced from “2007 in Flowering Plants – Native and Introduced”, by N. Adams, from TePapa Archives Collection. (CC BY-NC-ND 4.0).

A number of compounds have been isolated from the essential oil, leaves, branchlets, bark, and heartwood of rimu. The essential oil has been reported to contain a number of sesquiterpene and diterpenes including (+)-α-pinene (**1**), (-)-α-pinene (**2**), β-pinene (**3**), camphene (**4**), limonene (**5**), γ-terpinene (**6**), β-phellandrene (**7**), terpinolene (**8**), myrcene (**9**), phyllocladane (**10**), sclarene (**11**), abietatriene (**12**), humulene (**13**), (-)-α-selinene (**14**), (+)-β-selinene (**15**), (-)-alloaromadendrene (**16**), (+)-rimuene (**17**), (+)-phyllocladene (**18**), isophyllocladene (**19**), and laurene-1-ene (**20**).[21,22]

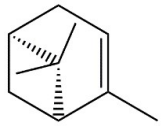

1

2

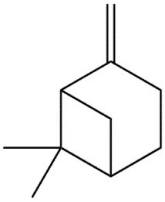

3

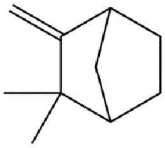

4

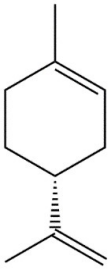

5

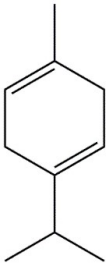

6

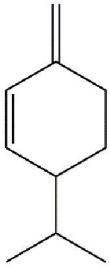

7

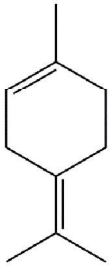

8

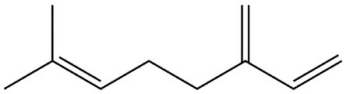

9

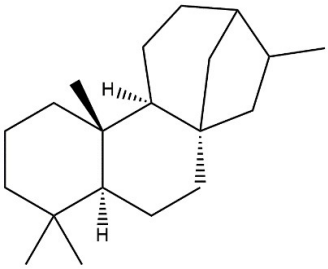

10

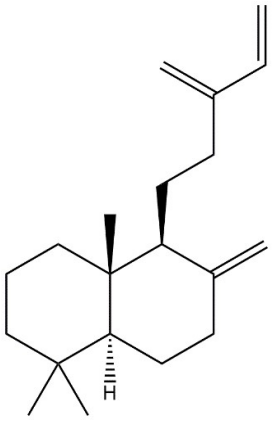

11

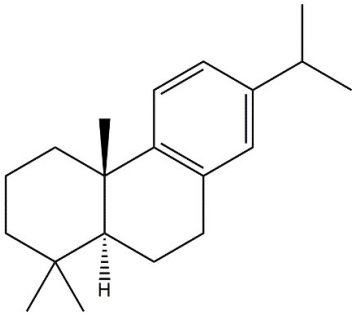

12

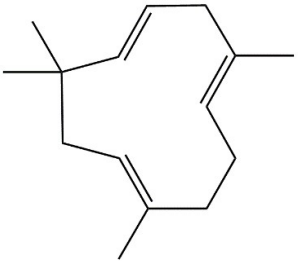

13

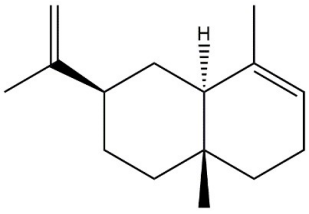

14

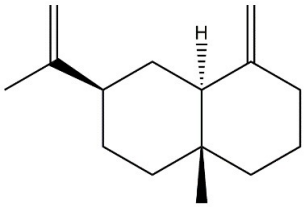

15

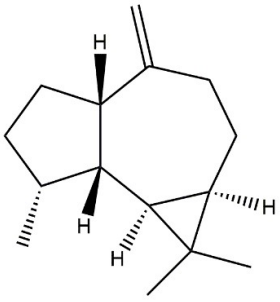

16

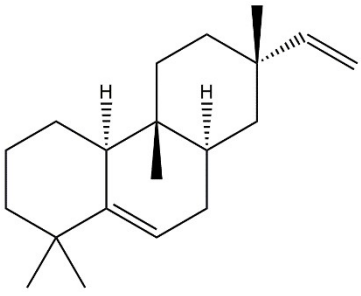

17

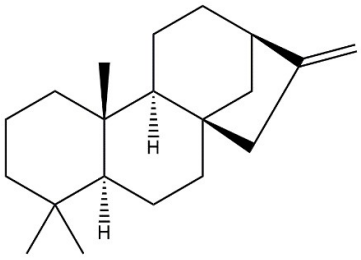

18

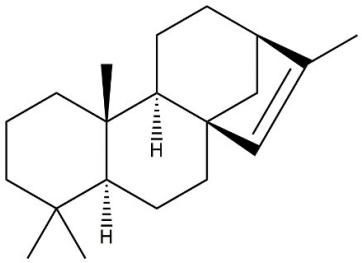

19

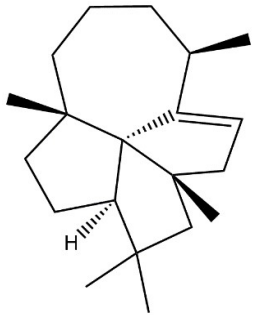

20

Additional foliage sesquiterpenes have also been reported including (+)-α-longipinene (**21**), (+)-longifolene (**22**), (-)-caryophyllene (**23**), (-)-caryophyllene oxide (**24**), δ-elemene (**25**), and (+)-longibornyl acetate (**26**).[23]

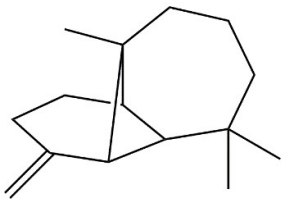

21

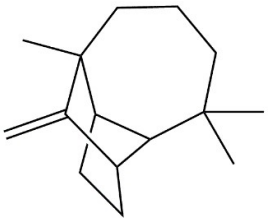

22

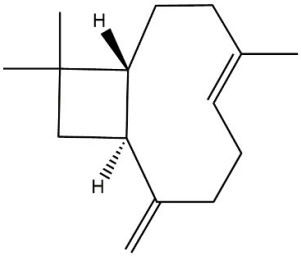

23

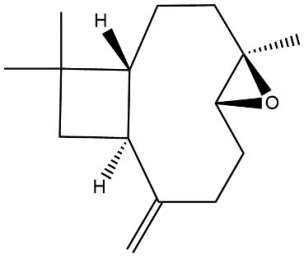

24

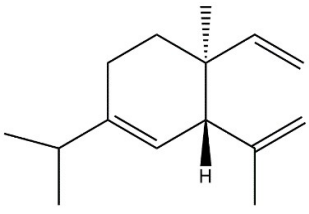

25

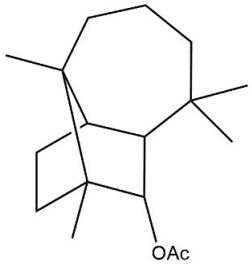

26

The heartwood is known to contain podocarpic acid (**27**), ferruginol (**28**), and xanthroperol (**29**), and the bark has been reported to contain the ecdysteroids dacrysterone (**30**) and ponasterone (**31**).[21,22] The bioflavonoids amentoflavone (**32**) and hinokiflavone (**33**) have been isolated from the leaves and branchlets.[21,22]

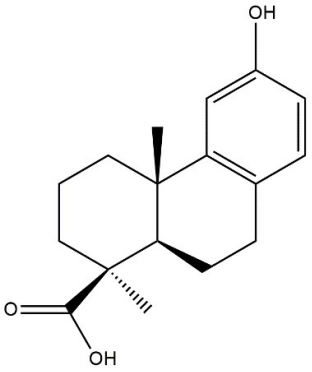

27

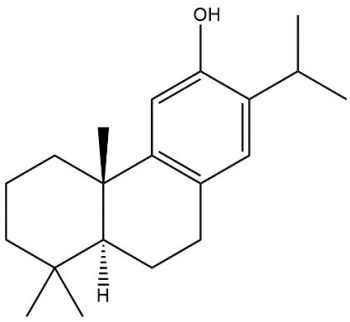

28

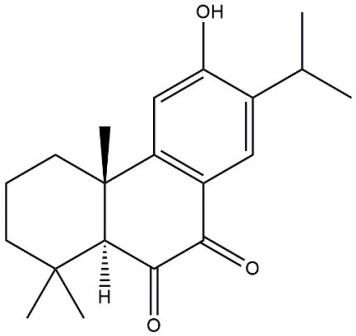

29

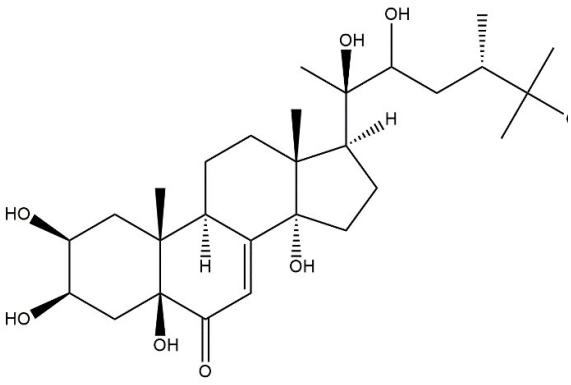

30

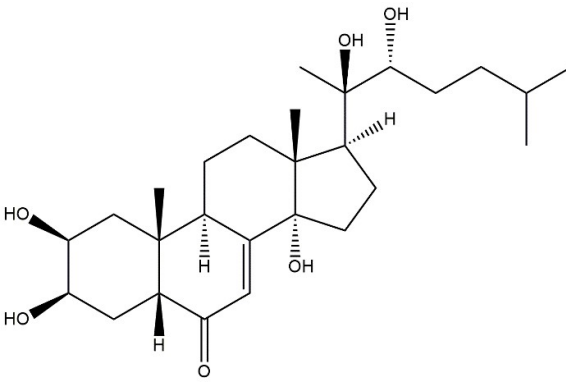

31

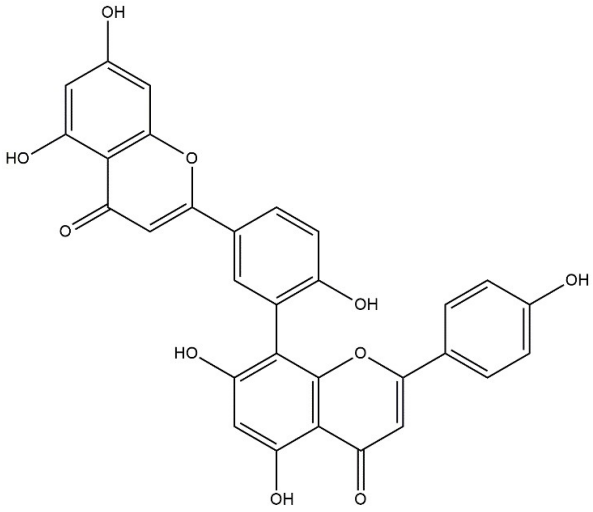

32

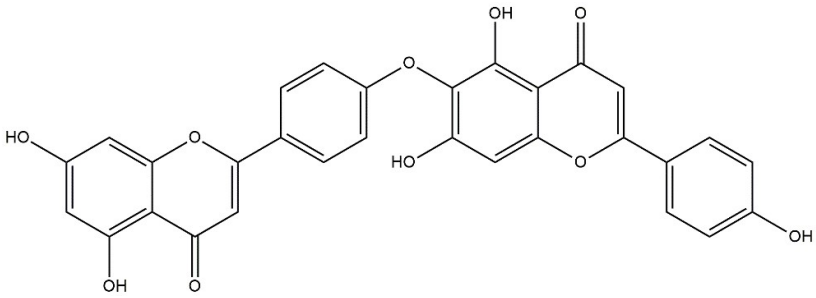

33

1.3 Rimu Berry Nutrition

The dietary composition of foods eaten by kākāpō, such as rimu berries, may influence their fecundity. The mast seeding of rimu or supplementary feeding supplying a nutritional pulse may help kākāpō surpass a nutritional threshold that

permits breeding.[15] The nutritional profile of rimu fruit makes it an ideal food for breeding and nesting birds.[10]

Rimu berries have been found to contain 7.2% crude protein with glutamic acid, aspartic acid, leucine, and arginine being present in the highest concentrations; 10.9% fatty acids with palmitic, oleic, linoleic, and linolenic acid having the highest concentrations; and 78% carbohydrate with 75% of this consisting of cellulose, hemicellulose, and lignin; fructose, glucose, and sucrose made up 6.5% of the dry matter content of the fruit.[12]

Calcium and vitamin D are known to be essential for eggshell production and the growing skeleton of the chick. Vitamin D acquired through the diet is of greater importance to kākāpō due to their nocturnal nature. Ripe rimu berries have a high calcium content (8.4 mg/g dry matter), very-high concentrations of vitamin D2 (70 µg/100g) and moderate amounts of vitamin D3 (11 µg/100g).[10]

Trace elements and minerals play important roles in the growth and development of the avian embryo.[24] Trace elements and minerals include aluminium, arsenic, boron, cadmium, cobalt, chromium, molybdenum, nickel, lead, selenium, copper, iron, potassium, magnesium, manganese, sodium, phosphorus, sulfur, and zinc. Trace mineral concentrations of rimu fruit are not fully documented in the literature. The concentrations of some trace elements and minerals of ripe rimu fruit collected from Whenua Hou and Anchor Island in 2019 are outlined in the following table (**Table 1**) from data provided from personal communication with Dr. Andrew Digby, the scientific advisor of the Department of Conservation kākāpō recovery team. The concentration of trace elements and minerals were determined by inductively coupled plasma mass spectrometry (ICP-MS) and inductively coupled plasma optical emission spectrometry (ICP-OES).

Table 1. The concentrations of trace minerals of ripe rimu fruit from Whenua Hou and Anchor Island. Reproduced from personal communication with kākāpō science advisor Andrew Digby from the Department of Conservation.

Trace Element / Mineral	Result (mg/kg)	Method Reference
Aluminium	15	AsureQuality Method ICP-MS
Arsenic	< 0.02	AsureQuality Method ICP-MS
Boron	24	AsureQuality Method ICP-MS
Cadmium	0.09	AsureQuality Method ICP-MS
Cobalt	0.08	AsureQuality Method ICP-MS
Chromium	0.16	AsureQuality Method ICP-MS
Molybdenum	0.055	AsureQuality Method ICP-MS
Nickel	0.65	AsureQuality Method ICP-MS
Lead	< 0.01	AsureQuality Method ICP-MS
Selenium	< 0.1	AsureQuality Method ICP-MS
Copper	5.8	AsureQuality Method ICP-OES
Iron	43	AsureQuality Method ICP-OES
Potassium	6200	AsureQuality Method ICP-OES
Magnesium	910	AsureQuality Method ICP-OES
Manganese	260	AsureQuality Method ICP-OES
Sodium	1100	AsureQuality Method ICP-OES
Phosphorus	1400	AsureQuality Method ICP-OES
Sulfur	1300	AsureQuality Method ICP-OES
Zinc	22	AsureQuality Method ICP-OES

There is currently no data reported in the literature on iodine levels in rimu fruit. Iodine is a critical mineral for thyroid health. Iodine deficiencies have been linked to avian thyroid hyperplasia (goitre) which can be reversed upon supplementation with iodine.[25,26] Thyroid hormones also have a significant effect on the reproductive function of birds. Hyperthyroid chickens have been shown to have decreased egg production, smaller eggs, thinner eggshells, smaller ovaries, small testes, low sperm count, or a complete stop of spermatogenesis.[26] Iodine deficiency was implicated in the low hatchability of critically endangered captive kaki (black stilt). Kaki are a wading bird found in rivers and wetlands of New Zealand. Similarly to kākāpō, kaki suffer threats from introduced predators, habitat loss, and anthropogenic forces. Populations have been intensively managed since 1981 when the wild population numbered around 23 adult birds. Iodine supplementation resulted in increased thyroxine hormone levels and increased survival rate of subadult kaki that were released into the wild.[27]

Conversely, excess iodine can also have deleterious effects on avian reproductive ability. Excess iodine in the diets of domestic fowl can prevent sexual maturation in both males and females, inhibit ovulation, result in low hatchability, and decrease male spermatogenesis.[28] Evidently, reproduction is deleteriously affected when iodine levels are either too low or too high, and thus, the management of iodine levels in kākāpō and in supplementary feed formulations would be beneficial for kākāpō conservation.

Better understanding the nutritional profile of the fruit of the rimu may offer insight into producing a supplementary feed for kākāpō which better mimics the nutritional status of their natural environment, especially during times of breeding and fledgling development. Previous studies analysing the rimu berry has provided data on the dry matter, total polyphenolic content, antioxidant activity, crude protein, lipid, amino acids, fatty acids, minerals, ash, energy, fibres, and simple sugars.[10,29] No data currently exists in the literature on the monomer compositions of complex sugars found in rimu berries.

Some complex carbohydrates such as water-soluble fibres, non-digestible oligosaccharides, and polysaccharides can be considered as 'functional foods', defined as any food component that provides health benefits beyond basic nutrition. Functional foods can be used to improve the texture, sensory characteristics, hydration, oil-holding capacity, and structural properties of food.[30] Understanding of the complex carbohydrates present in rimu berries, and the changes that take place during fruit ripening could offer insight into digestibility, effects on the gut microbiome, and possible breeding triggers which could help develop higher quality supplementary feeds. In addition, the absorption of phytoestrogens (refer to **Section 1.8**) may be affected by the degree of glycosylation which can affect their solubility and intermolecular recognition.[31,32]

1.4 Carbohydrates

Carbohydrates consist of four major groups; monosaccharides consisting of a single monomer unit; disaccharides which are homodimers or heterodimers of monosaccharides; oligosaccharides which are polymers of monosaccharides with a degree of polymerisation (DP) between 3 – 9; and polysaccharides which have a DP of 10 or greater.[33]

Carbohydrates are incredibly diverse and numerous classifications exist. One way of classifying carbohydrates in plants is based upon their location either within the cell or as a part of the cell wall (**Scheme 1**). In simplified terms, carbohydrates within the cell are usually forms of energy storage for the plant to metabolise when required, while the cell wall carbohydrates have more of a structural role. Cell wall carbohydrates also serve as an extracellular matrix and have important roles in microbial defence, signalling, and growth.[34] Carbohydrates within the cell include simple sugars (such as glucose, fructose, and sucrose) low DP oligosaccharides (such as fructooligosaccharides), fructan polysaccharides, and starch polymers.

Cell wall carbohydrates can be divided into primary and secondary cell walls. Polysaccharides make up about 90 – 95% of the dry weight of primary cell walls, and 60% in secondary cell walls. The primary cell walls of plants contain interdependent networks of polysaccharide classes including cellulose (*ca.* 30%), hemicelluloses (cross-linking glycans) (*ca*. 30%), and pectins (*ca.* 35%), with proteins, and in some cases phenolic compounds, making up the majority of the remainder (*ca.* 5%).[35] Secondary plant cell walls are formed after the cell has stopped expanding and the primary cell wall is complete. They offer additional mechanical strength and protection *via* the incorporation of hydrophobic polymers, such as lignin and suberin, and feature linear unsubstituted or lightly substituted polysaccharides including cellulose and heteroxylans. In secondary cell walls, the pectin and protein components are in low abundance or are absent.[36]

Cell wall architecture varies between the different groups of Kingdom Plantae due to evolutionary changes and specialisation. Changes in cell wall composition occurred as plants evolved to shift from aquatic to terrestrial habitats, grow to great heights by producing tissue with high tensile strength, avoid predation from microbes and herbivores by producing indigestible cell walls, and distribute their seeds by protecting them from the digestive tract of animals. In addition, the cell wall composition in plants is constantly remodelled during growth and reproduction and as a response to environmental conditions and biotic attacks.[37]

Gymnosperms, such as rimu, have cell walls containing high quantities of cellulose, hemicelluloses, and pectin and they can be differentiated by their high levels of homogalacturonans, rhamnogalacturonans I & II, and fucose containing xyloglucans. Compared to ‘less-evolved’ groups of plants, the xyloglucans of gymnosperms are reported to have a higher number of fucose side chains, and rhamnogalacturonan-II has a lower number of methylated side chains. The cell wall composition of gymnosperms is similar to non-grass angiosperms but possess a higher amount of glucomannans and have high amounts of homogeneous guaiacyl lignin in the secondary cell walls.[37]

Scheme 1. Overview of carbohydrate types found in higher plants organised by cell contents and cell walls.

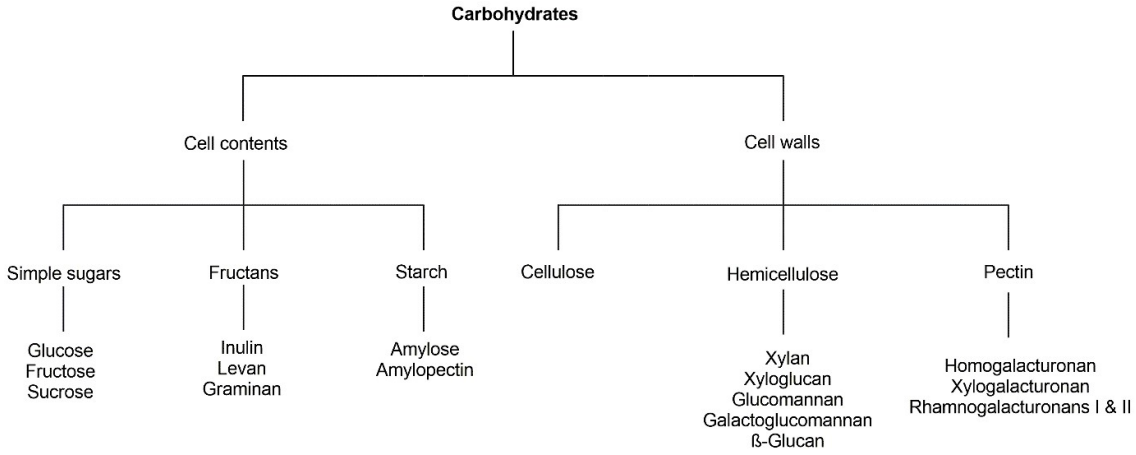

Fructans are polymers of fructose residues linked to a sucrose unit and function as an alternative energy storage to starch. Fructans are classified by the chain length, position of the sucrose moiety, and the type of linkage between the fructose residues. Types of fructans include inulin, levan, and graminan. Fructans vary from oligomers to polymers consisting of a few hundred residues.[38]

Starch is a non-structural storage polysaccharide that consists of the two glucose polymers amylopectin and amylose, which differ in their structure in terms of length and degree of branching. Both polymers consist of α-(1,4)-linked glucan chains connected *via* α-(1,6)-branch points. The two polymers together form insoluble, semi-crystalline starch granules. Amylopectin forms the structure of a semi-crystalline matrix, and amylose fills the voids, increasing the density of the granule.[39]

Cellulose is a long (7,000 – 15,000 residues in plants), linear polysaccharide consisting of β-(1,4)-linked glucose residues alternatively rotated 180° which forms a crystalline microfibre stabilised by extensive hydrogen bonding between individual cellulose fibres. Cellulose serves as the major structural component providing tensile strength to plant primary cell walls.[40]

Hemicelluloses are similar to cellulose in that they are formed by β-(1-4)-linked glucose residues, but hemicelluloses feature substitutions with other sugars, shorter chains (500 – 3000 residues), and an amorphous structure.[41] Types of hemicelluloses include xylans, xyloglucans, glucomannans, and galactoglucomannans. Hemicelluloses function to coat and cross-link cellulose fibres into a robust network.[40]

Pectins are complex acidic polysaccharides featuring high proportions of α-(1,4)-linked D-galacturonic acid residues with some residues featuring methyl esterification.[42] The percentage of methyl esterified residues plays a key role in the physical properties of pectin.[43] Pectins are embedded within the network of cellulose and hemicellulose in primary cell walls are provide additional strength and hydration. Types of pectin include homogalacturonan, xylogalacturonan, and rhamnogalacturonans I and II.[35]

During fruit ripening, the complex polysaccharides in fruit such as starch, cellulose, hemicellulose, and pectin begin to depolymerise. The depolymerisation of polysaccharides to oligosaccharides and eventually monosaccharides is dependent on enzyme-mediated degradation. In plant tissue, this process is a genetically co-ordinated phenomenon in which a number of biochemical changes take place including the increased activity of endogenous polysaccharide degrading enzymes.[44] Exogenous microbial enzymes can also contribute to the degradation of polysaccharides.[45] The degradation of the structural and storage polysaccharides leads to changes in fruit texture, taste, and nutrition as a result of the solubilisation, deesterification, and depolymerisation of polysaccharides.[44] The chemical degradation of polysaccharides is continued during digestion but not all glycosidic linkages are capable of being digested. Certain oligosaccharide products from polysaccharide degradation are transported through the stomach and small intestine unaffected, where they are then fermented in the colon by resident bacteria. Fermentation products of nonstarch oligosaccharides are healthy short-chain fatty acids such as acetate, propionate, and butyrate.[30] Foods which promote the growth and activity of resident bacterial species that produce a health benefit to the host are

known as prebiotics. The most commonly used prebiotics used in animal nutrition are fructooligosaccharides derived from the hydrolysis of inulin; galactooligosaccharides which are often found in the seeds and fruit of plants; and xylooligosaccharides from the degradation of hemicellulosic xylan.[46,47]

Prior to analysis, carbohydrates must be extracted and separated from other plant components. Extraction techniques include alcohol extraction, hot water extraction, ultrasonic-assisted extraction, enzyme-assisted extraction, ultrasonic-enzyme assisted extraction,[48] liquid-liquid extraction, solid-phase extraction,[49] supercritical fluid extraction,[50] pressurised liquid extraction,[51] and field flow fractionation.[52] The removal of other plant constituents from the extract commonly utilises techniques such as defatting in a hydrophobic solvent such as hexane.[53] Filtration commonly utilises membrane technologies such as dialysis or size-exclusion chromatography.[54]

For structural analysis, polysaccharides are generally hydrolysed to obtain the smaller constituent mono-, di-, or oligosaccharides. Complete hydrolysis to monomers is often desired in order to be able to identify the various monomer species present and to determine the ratios between them.[54] Glycosidic bonds can be hydrolysed enzymatically or using acidic, alkaline, and thermal conditions. Polysaccharides have differing susceptibility to hydrolysis allowing for partial degradation and selectivity in the substrate to be hydrolysed.[55] Carbohydrate susceptibility to hydrolysis depends on the position and configuration of the glycosidic linkage (α or β), the identity of the atom involved in the glycosidic linkage (O-, C-, S-, or N-), the identity of the residues at and near the site of hydrolysis, and the reaction conditions including pH, temperature, duration, and the structure and strength of the acid/base.[56] Due to the diversity of natural polysaccharides, the conditions of the hydrolysis reaction need to be carefully controlled and optimised to ensure complete hydrolysis of the polysaccharides while avoiding degradation of the liberated monosaccharides. Several procedures are often required in which different reagents or reaction conditions are used to hydrolyse certain glycosidic linkages more favourably. Strong and weak hydrolysis conditions are often employed and the data is combined to give a more accurate analysis of the monomer species

present.[57] Derivatisation can also be used to protect sites, manipulate the hydrolysis procedure, or aid detection.[54]

1.5 Detection Methodology for Hydrolysates

Carbohydrates present a number of challenges for analysis as they possess a wide range of structural diversity due to monomer composition, anomeric configuration, linkage type, and side chains, with complexity increasing in polymers with a higher DP.[58] Also, carbohydrates have low volatility, possess similar polarities, and lack a chromophore which complicates their analysis by gas chromatography (GC), chromatographic separation based on polarity, and ultraviolet (UV) detection, respectively.[55] Multiple analytical techniques are generally required to obtain complete structural information.

High-performance anion-exchange chromatography with pulsed amperometric detection (HPAEC-PAD) is one of the major technologies used for carbohydrate analysis due to featuring highly specific and sensitive detection without the need for derivatisation and displaying high resolution of underivatized oligosaccharides. HPAEC-PAD is run at highly alkaline conditions which partially or completely transforms the hydroxy groups on saccharides into oxyanions. Neutral and acidic monosaccharides can be quantified simultaneously in one run.[59] The oxyanions differentially interact with the anion exchange column and can be successively eluted using an increasing gradient of a pushing ion (such as sodium hydroxide or sodium salts of acetate, nitrate, and sulfate) which displaces the saccharide binding to the column. Retention rates are influenced by the molecular size and structure, degree of polymerisation, isomerism, anomerism, and the number of hydroxyl groups.[58]

Detection of analytes involves measuring the electrical current generated by the selective oxidation of hydroxyl groups which occurs on the surface of an electrode made from a noble metal (usually gold). The electrode is subjected to a series of potentials which are applied for defined time periods; this is referred to as the

waveform. The repeated application of a waveform forms the basis of pulsed amperometry. In the first stage of the waveform, the oxidation reaction results in the formation of substances which cumulatively block the surface of the electrode which results in electrode wear and decreased sensitivity of detection. This is remedied by a secondary phase in which the potential of the waveform is reversed to a reducing potential allowing for the substances blocking the electrode to be released. The third phase of the waveform briefly raises the potential to oxidise the electrode back to gold oxide, followed by the final phase in which the gold oxide is reduced to regenerate the electrode back to its native state, ready for the waveform to repeat.[58]

One of the major drawbacks of HPAEC-PAD is the loss of detection sensitivity resulting from electrode fouling which can require frequent cleaning or replacement and can make quantification difficult due to non-stable responses throughout a run. Therefore, hydrolysates should be free of sulfates, proteins, lipids, carbonates, salts, and borates to avoid electrode fouling. Another limitation of HPAEC-PAD is that alkaline conditions are required for oxyanion detection by PAD.[58] In addition, the run times are long making HPAEC-PAD not suitable for high-throughput experiments, and response factors between carbohydrate species can vary dramatically so quantitation requires pure standards for each species of interest.

1.6 The Hypothesis Linking Kākāpō Breeding to Mast Fruiting

The mechanism by which kākāpō synchronise breeding with mast fruiting of plant species such as rimu is not fully understood. It is thought that the abundance of unripe fruit preceding seed fall may provide kākāpō information about the future which influences their reproductive ability. An abundant food supply is potentially of great importance to kākāpō as they exhibit uniparental chick-raising associated with the lek breeding system. Fidler, Lawrence, and McNatty propose a hypothesis in which dietary phytochemicals (DPCs) present in the kākāpō's winter/spring diet may

produce oestrogenic effects which facilitate successful breeding in times of food abundance.[60]

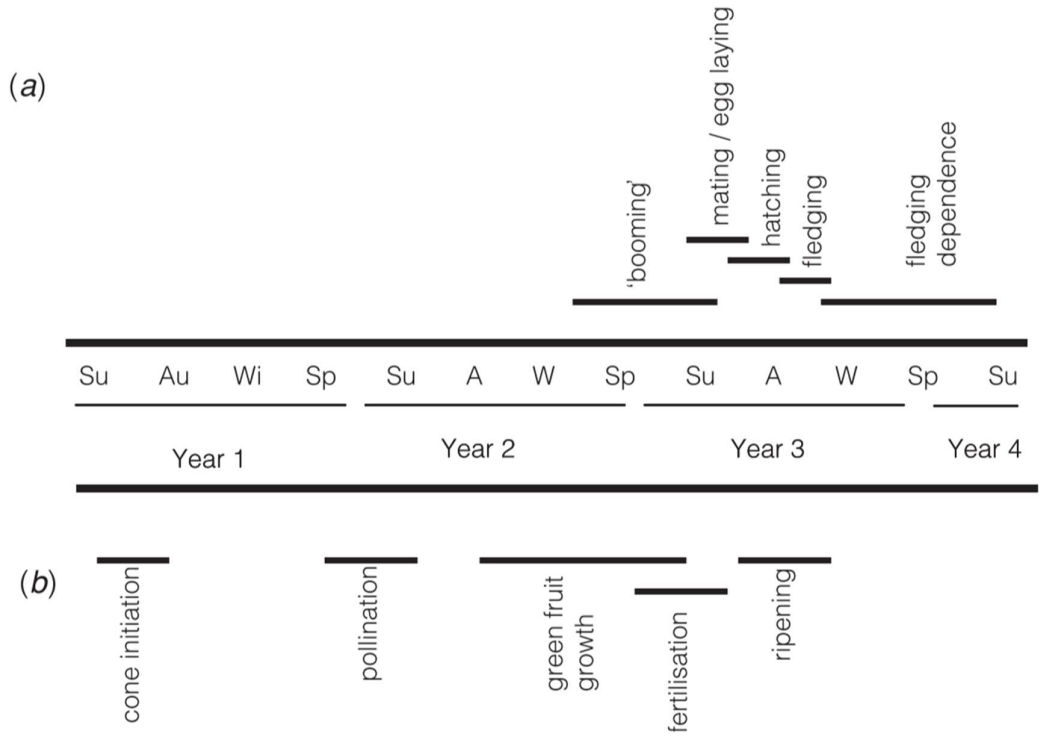

Figure 5. Relative timing of kākāpō reproductive events. **(A)** Male kākāpō preform their booming courtship display in spring through to late summer. Mating and egg-laying occur in mid to late summer, and egg hatching occurs from late summer to early autumn. Fledging occurs in late autumn and early winter. **(B)** Relative timing of rimu fruit development occurring over three summers with final fruit ripening occurring in late summer/autumn slightly two years after cone growth initiation. Reproduced from "An Hypothesis to Explain the Linkage Between Kākāpō (*Strigops habroptilus*) Breeding and the Mast Fruiting of their Food Trees" by Fidler *et al*., 2008, Wildlife Research, vol 35. (© CSIRO 2008).[60]

According to the hypothesis by Fidler *et al.*,[60] kākāpō are responsive to the amount of daylight hours which is measured by a 'circadian clock' (CC), allowing for reproductive efforts to coincide with the times of year in which food is most abundant.[61] The CC influences the secretion of gonadotropin releasing hormones from the hypothalamus (H) which acts on the pituitary (P) to control the production and release of follicle-stimulating hormone (FSH) and luteinising hormone (LH). FSH and LH promote the growth of small ovarian follicles (SOF). As SOF develop, they release increasing amounts of steroidal hormones, such as oestrogens (O), which activate egg yolk protein genes (EYPG) in the liver. The expression of EYPG leads to production of the egg yolk precursor vitellogenin which is responsible for transporting fatty acids (FA) to the follicle to prepare it to support a growing oocyte. As the follicle develops, increasing amounts of oestrogens are produced which creates a positive feedback loop with the EYPG in the liver supported by a hepatic gene memory mechanism.[62] The sensitised EYPG are therefore more responsive to oestrogen-mediated induction. DPCs such as phytoestrogens (refer to **Section 1.8**), could act on sensitised EYPG leading to greater concentrations of egg yolk protein being transported from the liver to the growing ovarian follicles, promoting their maturation to yolk-filled follicles (YF), and increasing the chance of successful egg laying.[60] This model is summarised below (**Figure 6**).

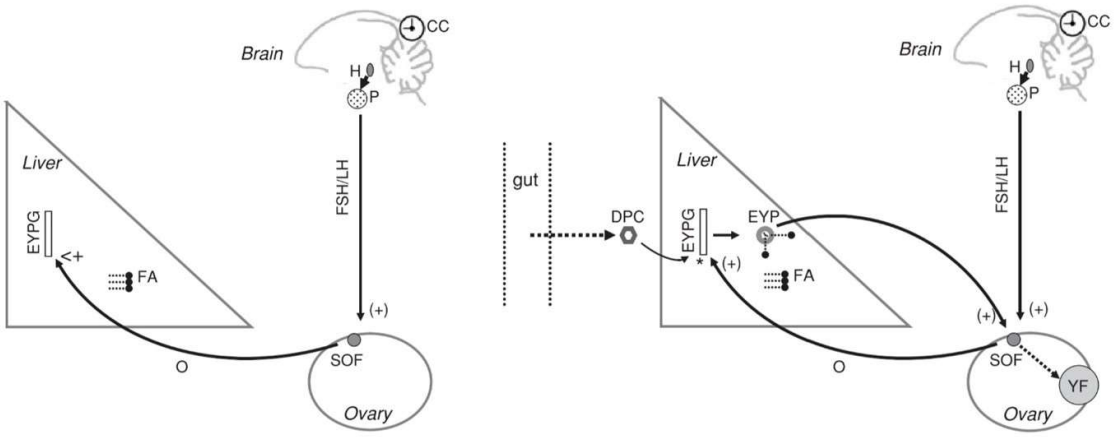

Figure 6. Model summarising the hypothetical mechanism of the linkage between kākāpō breeding and the mast fruiting of their food trees. Adapted from "An Hypothesis to Explain the Linkage Between Kākāpō (*Strigops habroptilus*) Breeding and the Mast Fruiting of their Food Trees" by Fidler, *et al*., 2008, Wildlife Research, vol 35. (© CSIRO 2008).[60]

It is currently unknown if rimu contains oestrogenic DPCs that could affect kākāpō fecundity. Podocarpic acid (**27**), which is found in the heartwood of rimu, is known to be weakly oestrogenic,[60,63] while the alcohol derivative podocarpinol (**34**) is much stronger and was found to have comparable oestrogenic activity with the known phytoestrogen genistein (**38**) (refer to **Section 1.8**) (*circa* 10^4-fold less than E2).[63]

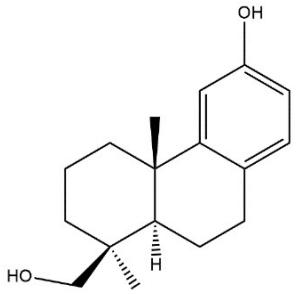

34

Podocarpic acid was not detected in a preliminary analysis of rimu embryos and fruit, and there exists no data on podocarpic acid levels in the twigs and foliage of rimu.[29,64] Bioassay experiments previously used to analyse estrogenic activity of extracts of rimu fruit have been conducted using recombinant human oestrogen receptors (hER) and have not detected the presence of phytoestrogens, but it has been noted that an assay utilising a hER cannot be accurately extrapolated to kākāpō as there are structural differences between human and kākāpō oestrogen receptors (ER) (refer to **Section 1.7**).[64] A deeper understanding about the chemical composition of rimu fruit would be advantageous for understanding if the natural diet of kākāpō has significant hormonal effects.[60]

1.7 Oestrogens

In vertebrates, oestrogens such as oestrone (E1) (**35**), 17β-oestradiol (E2) (**36**), and oestriol (E3) (**37**), serve primarily to regulate sexual growth and reproduction. Reproductive functions involving oestrogen include oogenesis, vitellogenesis, gonadotrophin regulation, and testicular growth. They also influence other physiological systems including immunity, development, and metabolism. Estrogens restrict bone resorption which serves to maintain bone mass. They also control the effect of parathormone which controls calcium levels in the blood. Other functions of estrogens include raising salt and water retention, increasing blood coagulation, promoting vasodilation, and causing increases in sex hormone binding globulin (SHBG), thyroxine binding globulin, and cortisol binding globulin.[65]

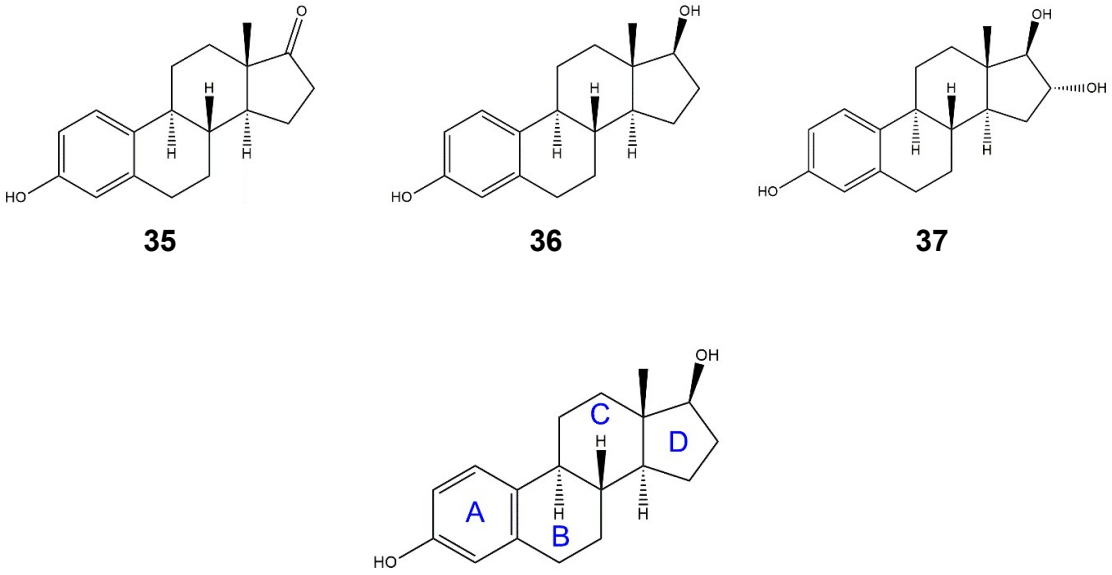

Figure 7. Oestrogens. **(Top)** E1 (**35**), E2 (**36**), and E3 (**37**). **(Bottom)** Oestrogen ring labelling convention using E2.

Three main functional domains make up the primary structure of an ER: the ligand binding domain (LBD), the area responsible for interaction with deoxyribonucleic acid (DNA), and a region that regulates transcription.[66] Oestrogen receptor isoforms (ER-α or ER-β) have differing affinity for ligands and distribution throughout organs and tissues. Crystallographic studies of human ER-α have determined that high ligand binding affinity requires the following structural features:

1. Hydroxyl groups that anchor the ligand *via* hydrogen bonds with polar amino acids Glu353, Arg394, and His524 (**Figure 8**).
2. A hydrophobic core structure, usually a phenyl group, similar the A-ring of E1, E2, and E3 (**Figure 7**).
3. A substituent equivalent to the C and D rings of E2 which can occupy the remaining space in the ligand binding pocket.[67]

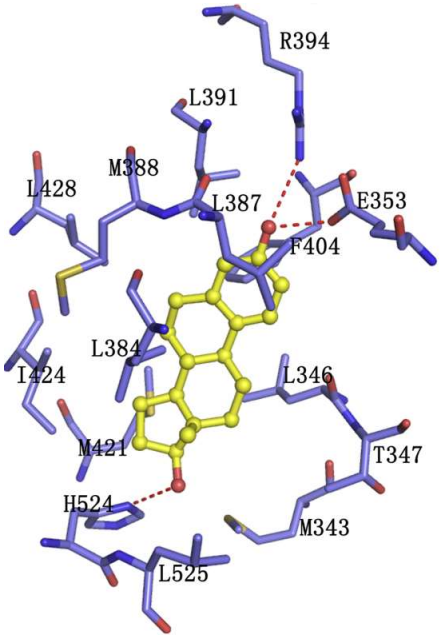

Figure 8. A binding configuration of E2 in hER-α. Hydrogen bonding of hydroxyl substituents to amino acids His524, Arg394, and Glu353 is indicated by the dashed red line. Reproduced from "The Molecular Mechanism of Bisphenol A (BPA) as an Endocrine Disruptor by Interacting with Nuclear Receptors: Insights from Molecular Dynamics (MD) Simulations", by Li *et al.*, 2015, PLOS One, vol 10(3). (CC BY 4.0).[67]

The ER-α binding domains of humans and kākāpō only differ by 14 amino acids, but a number of these exist in the region around the bound E2 molecule. The ER-β binding domain is more conserved between humans and kākāpō with 5 amino acid differences, 3 of which are in proximity to the bound E2 molecule.[68]

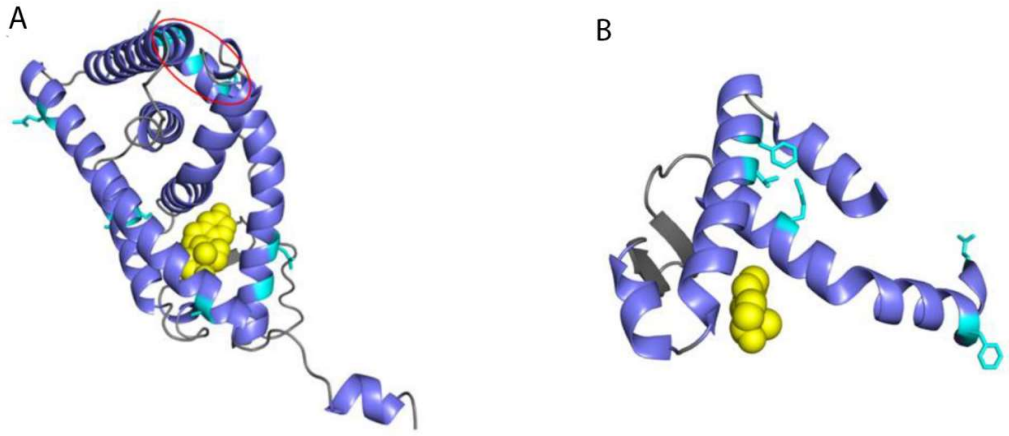

Figure 9. Representations of hER-α ligand binding domains. **(A)** Representation of hER-α LBD with native ligand (E2) in yellow, α-helices in blue, β-sheets and loops in grey, and the 14 amino acids that differ from kākāpō ER-α are displayed in light blue with their side chains. **(B)** Representation of hER-β LBD with native ligand (E2) in yellow, α-helices in blues, β-sheets and loops in grey, and the five amino acids that differ from kākāpō ER-β are displayed in light blue with their side chains. Adapted from "Kākāpō Reproduction: Identification of Steroid Receptors and Oestrogenic Activity in Native Flora" by Davis, 2013. (© Davis 2013).[68]

In-silico computational modelling of E2 docking in the kākāpō ER-α ligand binding domain found that the hydrogen bonding interactions of Arg394 and His524 and the hydrophobic interactions with Met388, Phe404, Ile424 present in the human model were not observed in the kākāpō receptor. Interactions of E2 unique to the kākāpō receptor were found in resides Met421 and Met528. The results of the *in-silico* computational studies concluded that the unique amino acids in the kākāpō ER-α result in a different three-dimensional arrangement of the receptor backbone and also alters the binding position of E2.[68]

1.8 Phytoestrogens

Phytoestrogens are nonsteroidal phytochemicals which mimic or modulate the action of endogenous estrogens.[66] There are many potential mechanisms by which this can occur, including direct binding to ERs in cell membranes, cytoplasm, and cell nuclei where they can act as agonists or antagonists with effects differing depending on dose, tissue type, estrogen receptor subtype (ER-α or ER-β), and levels of endogenous hormones.[69] Phytoestrogens may also have no affinity for the ER and may cause an oestrogenic response by activating or inhibiting specific enzymes (such as aromatase which converts free androgens to estrogens), altering the concentration of free estrogens in the body, or promoting the synthesis of proteins which may affect free oestrogen levels in circulation such as SHBG.[66] Phytoestrogens can therefore be considered as selective oestrogen receptor modulators (SERMs) that can trigger oestrogenic, antiestrogenic, or mixed responses.[69]

Phytoestrogens have been found in a variety of plants with concentrations varying depending on plant growth, soil, weather conditions, and plant age. Phytoestrogens are classified as phenolic phytochemicals or polyphenols which are the largest category of phytochemicals. Polyphenols are widely distributed in the plant kingdom serving as antioxidants, pollinator attractors, feed-repellents, and protectants from insects, fungi, viruses, and bacteria. Phytoestrogens exhibit a range of structurally diverse compounds and can be divided into four main classes: flavonoids, lignans, coumestans, and stilbenes.[70]

Flavonoids are a class of low molecular weight (MW) plant secondary metabolites with a polyphenolic structure which may possess antioxidant, anti-inflammatory, anti-mutagenic, anti-carcinogenic properties, and may also modulate cellular enzyme functions.[71] In plants, flavonoids are partly responsible for the colour, taste, and aroma of flowers and fruit which helps to attract pollinators and promote seed dispersion.[72] Flavonoids also serve to protect plants from UV radiation, frost, drought, heat and biotic/abiotic stresses. They may also act as signalling molecules, phytoalexins, and antimicrobial defensive agents.[71]

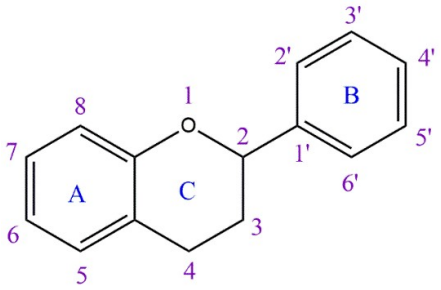

Figure 10. Basic flavonoid skeleton illustrating conventional ring lettering and carbon numbering.

Flavonoids can be divided into a number of different subgroups depending on the degree of oxidation and unsaturation on the C ring, and by what carbon on the C ring that the B ring is attached (Figure 10). Isoflavones feature the B ring attached to C-3 on the C ring. Neoflavonoids have the B ring linked through C-4 of the C ring. Where the B ring is linked through C-2 of the C ring, further subgroups are defined by the structural features of the C ring and include flavones, flavonols, flavanones, flavanols or catechins, anthocyanins, and chalcones.[71]

Flavones possess a double bond between C-2 and C-3 and a ketone on C-4 of the C ring. Many flavones also possess hydroxyl groups in positions 5 and/or 7 of the A ring, and/or 3' and/or 4' of the B ring. Flavonols are similar to flavones in that they possess a ketone on C-4 of the C ring and a double bond across C-2 and C-3 of the C ring. Their defining feature is a hydroxy substituent on C-3 of the C ring which may also be glycosylated. Flavonols may also display a diverse range of methylation and hydroxylation patterns. Flavanones (also known as dihydroflavones) are defined by a saturated C ring and so lack the double bond between C-2 and C-3 on the C ring present in flavones and flavonols but retain the ketone at C-4 on the C ring. Flavanols (also known as catechins or flavan-3-ols) possess a hydroxyl group bound to position 3 of the C ring and lack a double bond between C-2 and C-3 on the C

ring. Anthocyanins are pigments that a responsible for colours in plants which is influenced by the oxonium ion on the C ring. The colour of anthocyanins depends on the pH and any methylation or acylation at hydroxy groups on the A and B rings. Chalcones lack the C ring are referred to as open-chain flavonoids.[71]

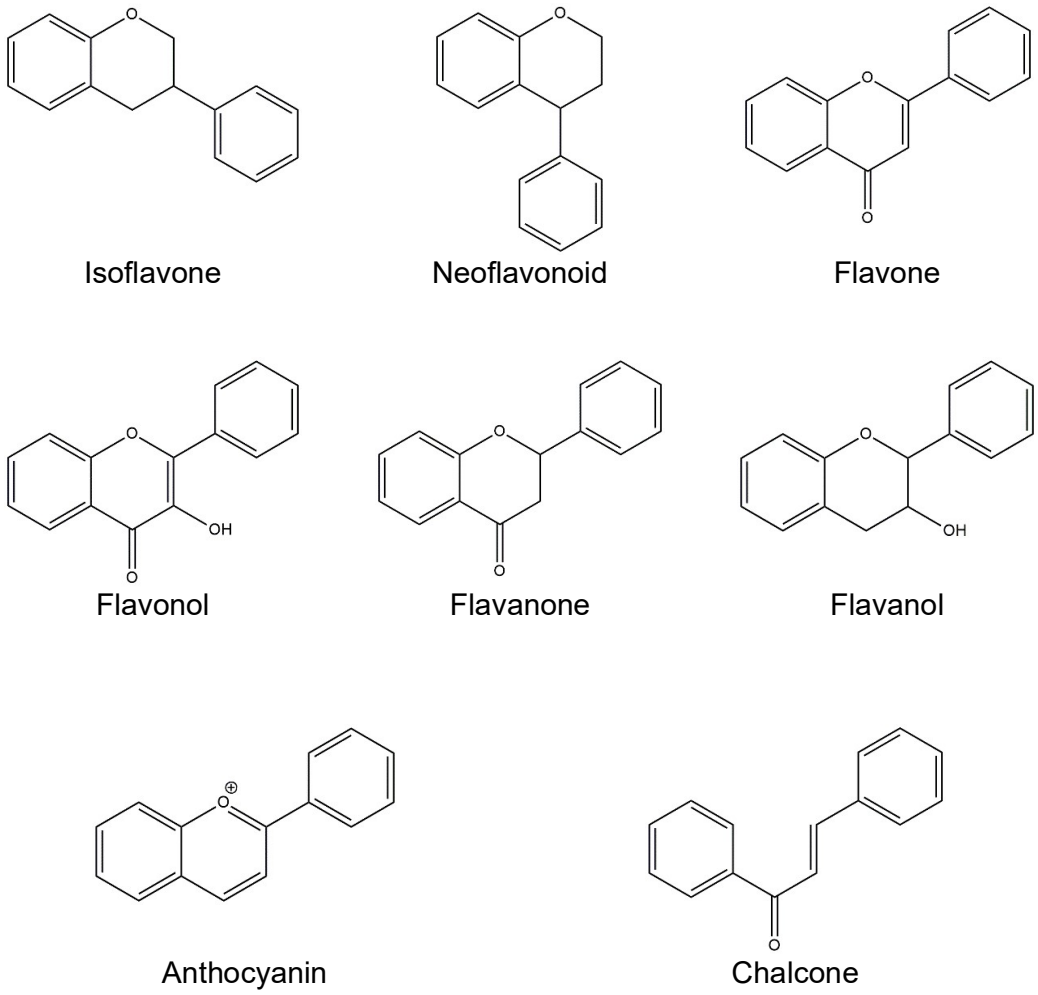

Figure 11. Basic structures of flavonoid subgroups.

Flavonoids have been demonstrated to have effects on hormone levels and reproductive success. A study on captive pandas revealed that bamboo from the Sichuan region in China had higher concentrations of total flavonoids than bamboo from Shaanxi and Beijing. This resulted in the pandas from Sichuan having higher levels of the reproductive hormones E2, FSH, LH, testosterone, progestin, and prolactin, along with a significantly higher birthrate.[73] In another study, supplementary genistein (**38**) (an isoflavone phytoestrogen) given to quails resulted in increased egg production and quality.[74] Genistein and the flavanone 8-prenylnaringenin (**39**) have been reported to increase the fertilising ability of mouse sperm *in vitro via* a mechanism that is independent of ER.[75]

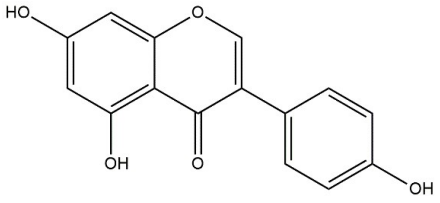

38

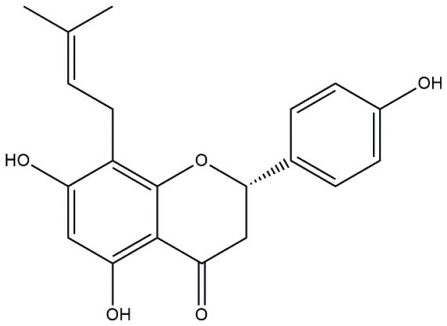

39

Lignans are a large group of phytochemicals primarily found as glycosides stored in vacuoles in the outer layers of grains, vegetables, and fruits.[75] Lignans are plant secondary metabolites derived from the shikimic acid biosynthetic pathway from oxidative coupling of phenylpropanoids. Lignans offer plants protection against herbivores and microorganisms along with antioxidant activity. Lignans can be divided into five subgroups based on their carbon skeletons and cyclisation patterns: lignans, cyclolignans, neolignans, cycloneolignans, and oxyneolignans.[76]

Lignans have a characteristic dimeric structure formed by a β,β'-linkage (8,8'-linkage) between two phenylpropanoid units which can exhibit different degrees of

oxidation in the side chains and substitution patterns on the aromatic rings. Standard nomenclature conventions number one of the six membered rings starting from the propyl group from 1 – 6, and the propyl group is numbered from 7 – 9 starting from the benzene ring. The second phenylpropanoid unit is numbered in the same fashion, with the numbers primed. In the case where the two phenylpropanoid units are not joined by a C-8 – C-8' bond, the dimer is termed a neolignan. In an oxyneolignan, the linkage between the two phenylpropanoid units occurs through an ether oxygen atom. Cyclolignans consist of phenylpropanoid units joined together through two carbon-carbon bonds forming a ring, including an 8,8'-linkage and another carbon-carbon bond linkage. Cycloneolignans also have two carbon-carbon bonds linking the dimers through a ring, but do not possess the 8,8'-linkage.[77]

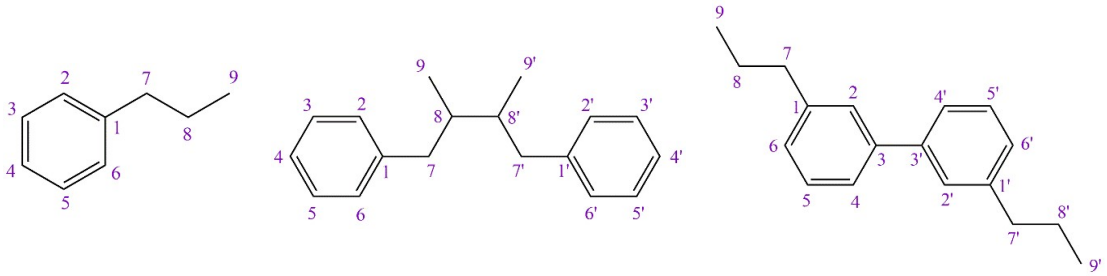

Phenylpropanoid unit | Lignan skeleton with 8,8' linkage | Neolignan skeleton with 3,3' linkage

Figure 12. Illustration of lignan numbering convention.

Lignans themselves are not oestrogenic or are only weakly oestrogenic. However, after ingestion they can be converted by intestinal bacteria to biologically active oestrogenic metabolites. For example, secoisolariciresinol diglucoside (SDG) is a phytoestrogen that is present in flax, sunflower, sesame and pumpkin seeds which is converted by gut microflora to produce the biologically active oestrogenic metabolites secoisolariciresinol (**40**), enterolactone (**41**), and enterodiol (**42**).[69] Diets supplemented with flaxseed and SDG has been shown to affect pregnancy outcome and reproductive development in rats.[78] In chickens, flaxseed supplementation

resulted in a significant reduction in circulating oestradiol levels, and SDG was shown to be converted to lignan compounds by pullet caecal microflora.[79]

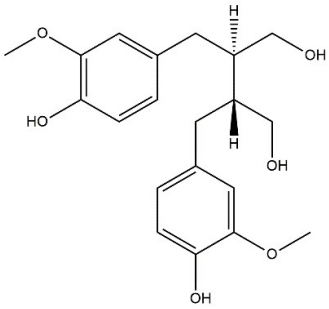

40

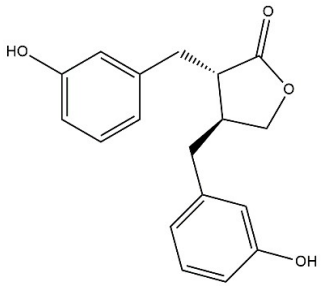

41

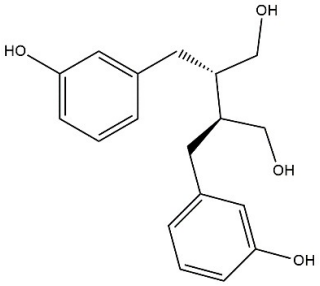

42

Coumestan (**43**) is a heterocyclic organic compound which forms the core of a variety of natural compounds known as coumestans. Coumestans are oxidation products of pterocarpanes, which are derivatives of isoflavonoids found in the Fabaceae (legume) family. Coumestans have been reported to have the most pronounced oestrogenic effect of all the phytoestrogens.[80] Coumestrol (**44**) is a well-known coumestan originally isolated from clover which possesses an oestrogenic activity 30 to 100 times greater than isoflavones.[81] This is due to the chemical structure of coumestrol having a strong resemblance to E2 in which the position of the two hydroxyl groups serves to inhibit the action of aromatase and 3β-hydroxysteroid dehydrogenase enzymes which interferes with metabolism of endogenous hormones.[82] Coumestrol has a similar binding affinity for the ER-β receptor as E2, and binds to ER-α with an affinity 3-fold less than E2.[83] Administration of coumestrol to ovariectomised rats resulted in uterotrophic effects typical of natural oestradiol including increased weights of the uterus, cervix, and vagina, and a doubling of total uterine DNA.[84]

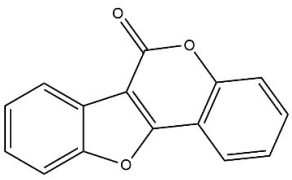

43

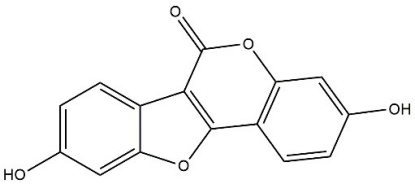

44

Stilbenes are natural phenolic defence compounds which can be found in a number of different plant species and have been reported to possess antimicrobial and antioxidant properties. They have also been reported to protect against ozone and UV stress.[85] Stilbene (1,2-diphenylethylene) (**45**) is the parent structure for this class of phytochemicals and exists as either the E or Z isomer. The Z isomer is unstable due to steric interactions which force the two aromatic rings out of plane preventing conjugation,[86] and will readily photoisomerise.[54] Stilbene derivatives (especially the E isomers) have oestrogenic activity and have found use in the production of non-steroidal synthetic estrogens.[88]

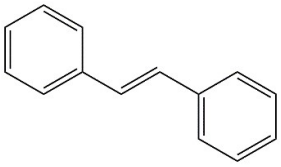

(E)-45

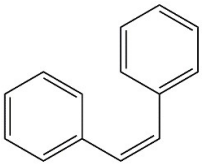

(Z)-45

Resveratrol is a stilbene derivative found in the skin of red grapes and other fruits and acts as a phytoalexin to protect plants from attack by pathogens such as bacteria and fungi.[88] (E)-resveratrol (**46**) can bind to ERs and evoke mixed antagonistic and agonistic effects in differing tissue types. Female rat offspring that were exposed to (E)-resveratrol during nursing exhibited reduced body weight and increased ovarian weight, while male rat offspring exposed to (E)-resveratrol

exhibited decreased body weight, plasma testosterone concentration, and sociosexual behaviour.[89] Pterostilbene (**47**) is a stilbenoid that is chemically related to resveratrol and is found in blueberries and grapes with studies suggesting that pterostilbene helps in lowering blood lipid and cholesterol levels.[88]

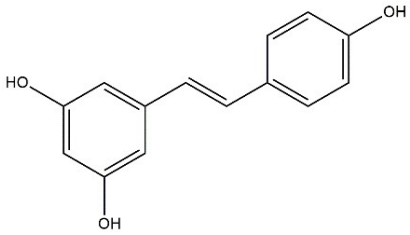

46

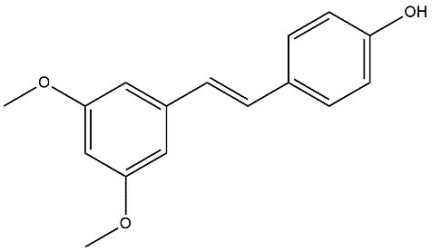

47

Chapter 2. Carbohydrate Analysis

2.1 Proposed Research

Characterisation of the carbohydrates present in rimu berries was undertaken, with a focus on the identity of cell wall carbohydrates which may have prebiotic properties.

The goals of this portion of the research project were:

- Extraction and fractionation of rimu berries for carbohydrate analysis.
- Analyse the fraction containing simple sugars for sucrose, D-fructose, and D-glucose by enzymatic assay.
- Quantify starch content in selected fractions using Association of Official Agricultural Chemists (AOAC) Official Method 996.11.
- Separation and quantitation of monomer constituents of potentially prebiotic oligosaccharides present in rimu berries using methanolic hydrochloric acid/ trifluoroacetic acid (MeHCl/TFA) hydrolysis and two-stage sulfuric acid (H_2SO_4) hydrolysis of selected fractions analysed by HPAEC-PAD.
- Quantify monomer composition of selected fractions and identify likely polysaccharide species present.

2.2 Rimu Berry Carbohydrate Composition

The following tables (**Table 2** and **Table 3**) reproduce data from the paper by Cottam, Merton, and Hendrix on the nutrient composition of the diet of parent-raised

kākāpō nestlings,[12] and from the thesis by Cottam which examines the characteristics of green rimu fruit that might trigger breeding in kākāpō.[29] In these studies, simple sugars were analysed by a combination of gas chromatography and spectrophotometry according to the method of Englyst (1994),[90] and cellulose, hemicellulose and lignin were calculated from neutral detergent fibre (NDF), acid detergent fibre (ADF), and acid detergent lignin analyses conducted using methodology described by Van Soest (1991).[91]

Table 2. Carbohydrate composition (g/100g) of entire rimu fruit as determined by a combination of gas chromatography and spectrophotometry. Reproduced from "Nutrient Composition of the Diet of Parent-Raised Kākāpō Nestlings" by Cottam *et al.*, in Notornis, 2006, vol. 53, pages 90-99. (© The Ornithological Society of New Zealand, Inc. 2006).[12]

Component	Entire fruit
Carbohydrates	77.69
Starch	4.47
Cellulose	17.34
Hemicellulose	10.59
Lignin	30.63
Total Sugars	6.45
Fructose	4.06
Glucose	1.98
Sucrose	0.42
Maltose	0.00

Table 3. Gross nutrient content of rimu fruit. Reproduced from "Characteristics of Green Rimu Fruit that Might Trigger Breeding in Kākāpō" by Cottam, 2010. (© Cottam, 2010).[29]

Sample	**May-07**	**Aug-07**	**Nov-07**	9 Jan	21 Jan	6 Feb	**Feb-08**
Fresh sample (%):							
Dry Matter	39.7	40.1	35.7	32.5	33.7	35.1	35.6
Dry matter basis (%):							
Ash	5.4	5.4	6.1	6.2	6.0	6.0	5.5
Crude protein	6.0	5.5	6.7	6.6	6.6	7.0	6.6
Amino acids	5.9	5.5	6.0	6.2	6.6	5.7	6.5
Crude fat	2.3	2.4	2.2	1.8	1.6	2.0	2.7
Fatty acids	1.0	1.1	1.1	1.0	1.0	1.3	1.7
Fatty acids:crude fat	0.44	0.44	0.48	0.60	0.63	0.67	0.65
Sugars	3.5	4.9	4.6	5.5	1.0	2.7	4.1
Crude fibre	36.6	37.0	34.3	35.5	39.0	40.6	42.0
NDF	48.7	48.2	47.6	48.6	53.4	53.3	54.6
ADF	39.5	39.4	40.2	41.6	44.8	44.4	45.5
Ca (mg/g)	11.6	11.5	12.2	12.7	12.1	12.7	11.2
P (mg/g)	1.1	1.1	1.3	1.4	1.3	1.4	1.4
Ca:P	10.1	10.4	9.4	8.8	9.2	9.3	8.2
CP+CF+CFibre+ ash+sugars[a]	53.7	55.3	54.0	55.6	54.1	58.3	60.9

[a] crude protein + crude fat+ fibre + ash + sugars

The inclusion of lignin (**Table 2**) as a portion of the total carbohydrate content of rimu berries is not technically correct as lignin is not a class of carbohydrate, but it is commonly included as a carbohydrate in neutral detergent fibre methodologies. This lignin is likely associated with the protective coating of the seed and with the vascular tissues of the modified bracts of the fruit.[92] Most of the lignin would not be expected to be nutritionally available to the kākāpō.[93]

2.3 Extraction and Fractionation of Rimu Berries

The approach taken for extraction and fractionation of the different carbohydrate contents of rimu berries relies upon differential solubility of carbohydrates in ethanol and water at various temperatures, and the difference in size between carbohydrate types. Polysaccharides are both polymolecular and polydisperse, and therefore, are heterogeneous with respect to their chemical structures, molecular weights, and solubilities. The molecular weight, molecular weight distribution, charge, degree of branching, presence of substituents, and conformation all have an impact on the solubility of polysaccharides.[94]

Rimu berries (**Figure 13**) were sourced from a collection from Anchor Island in May 2016 and stored at -80 °C (refer to **Table 11**).[*] The berries appeared to be overripened with a faint smell of fermentation and are identified herein as berries (overripe). Upon close inspection, it appeared that a small number of berries showed signs of microbial decomposition, and these were removed from the sample. The berries contained seeds which were retained and included in this analysis.

Figure 13. Rimu berry sample for carbohydrate analysis. **(Left)** Rimu berries (overripe) from Anchor Island collected May 2016. **(Right)** Grinding to a fine powder prior to 70% EtOH extraction.

[*] Acknowledgement to A. Prof. Janet Pitman who supplied the rimu berries used for this study.

Fresh rimu berries were used for the extraction as drying procedures can affect the non-structural carbohydrates and other nutritive attributes of the fruit.[95] The decision to extract the berries in a wet state along with their seeds was to approximate how they are consumed by kākāpō in the wild, and was proposed to better represent the native state of the fruit.

Scheme 2. Overview of extraction and fractionation of rimu berries illustrating the expected locations of carbohydrate types in fractions.

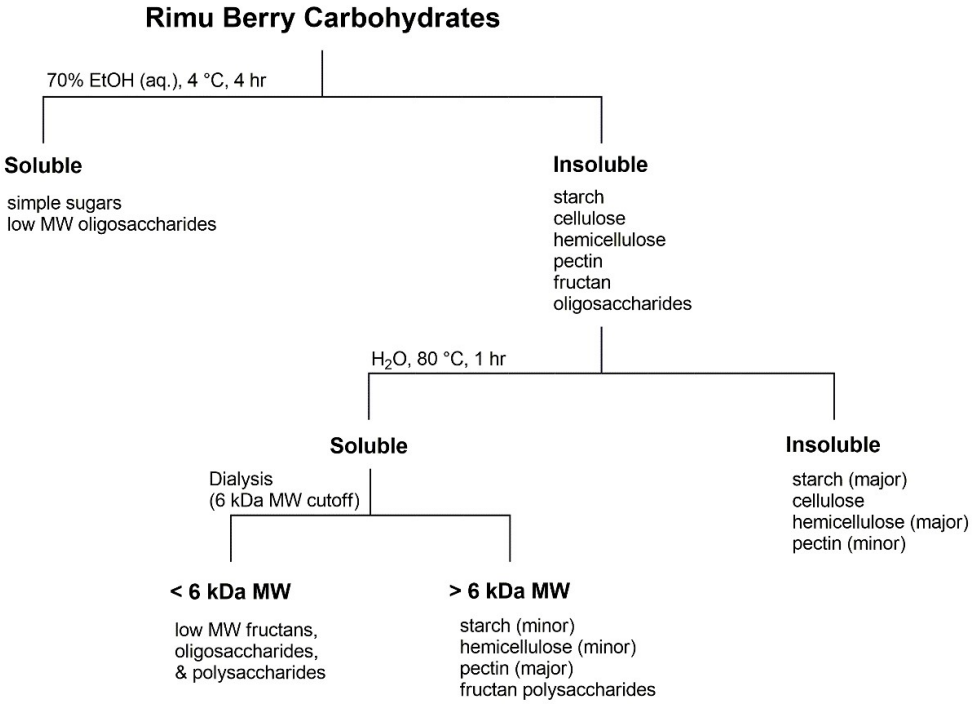

The berries were frozen with liquid nitrogen and ground to a fine powder (**Figure 13**), liberating starch and cell wall polysaccharides that will contribute to the sugar compositional data. The carbohydrate content of the seeds is not likely to be nutritionally available for kākāpō but were included in this analysis to get a representation of the complete carbohydrate content of the mature fruit.

Ground material was extracted into 70% aqueous ethanol (4 °C, 4 hours) and centrifuged to produce an alcohol insoluble residue (AIR) and an alcohol soluble solution (SS) (**Figure 14**). The methodology was addition of 100% ethanol to the powdered fruit (32.71 g) approximating the water content at 70%.

Figure 14. Soluble and insoluble components of 70% ethanol extraction of rimu berries. **(Left)** AIR of 70% EtOH extraction of rimu berries. **(Right)** Dried SS of 70% EtOH extraction.

The wet AIR was further extracted (warm water, 80 °C, 1 hour) then centrifuged producing a water insoluble residue (WWE_Insol) and a water soluble solution (WWE_Sol) (**Figure 15**).

Figure 15. Soluble and insoluble components of warm water extraction of rimu berries. **(Left)** Insoluble residue of the warm water extract (WWE_Insol). **(Right)** Dried soluble fraction from the warm water extract (WWE_Sol).

The water soluble solution was dialysed with a 6 kDa MW cut-off to exclude low MW saccharides. The low MW saccharide fraction was discarded due to it being impractical to remove the volume of water used for dialysis. This was a drawback for the dialysis method as the low MW saccharide fraction may contain potentially prebiotic fructooligosaccharides that would be of interest to this study, but in order to apply continued osmotic pressure, water must be continually refreshed in the dialysis vessel resulting in a fraction of low MW carbohydrates dissolved in a large volume of water. Size exclusion chromatography would have been a reasonable alternative to dialysis for the separation of fructans and other low MW saccharides from the warm water extract.[96] The retained solution from the dialysis tubing (> 6 kDa) is expected to contain fructan polysaccharides, and water soluble hemicelluloses and pectin.

2.3.1 Mass Recovery and Partitioning

In order to compare the results of this study to the values presented in the literature, an estimate was made for the dry weight of the berry and of the AIR. The dry weight of the berry was based upon the results from a separate experiment in which rimu berries were lyophilised and weighed to determine their water content which was found to be 72.1%. The approximate dry weight of the AIR was calculated by subtracting the dry mass of the alcohol soluble solution (SS) from the approximate dry mass of the berries. These approximate dry masses were then used to calculate the dry berry recoveries.

Table 4. Mass recovery of fractions generated from rimu berry extracts for carbohydrate analysis.

	Mass (g)	Approx. dry mass (g)	Wet berry recovery (%)	Dry berry recovery (%)
Berries (wet)	32.71	9.126		
AIR	22.473	8.407	68.70	92.12
SS	0.7187		2.20	7.88
WWE_Insol	5.1089		15.62	55.98
WWE_Sol	0.0911		0.28	1.00

The quantity of rimu berries available for extraction was limited which restricted parallel studies using dry rimu berries which would have allowed for comparisons between the wet and dry states, and for more accurate comparisons with the values previously reported in the literature.

Low molecular weight mono-, di-, and oligosaccharides, along with cytoplasmic contents and other small molecules, are soluble in alcohol solutions, whereas proteins, polysaccharides, and dietary fibre are insoluble.[97] The SS carbohydrates will primarily be comprised of simple sugars (mono- and di-saccharides) and

potentially low MW fructans from the extracted rimu berries, with the low temperature of the extraction helping to exclude more polydisperse species. The AIR carbohydrates are expected to consist of the storage polysaccharides such as starch and fructan, along with the cell wall components such as cellulose, hemicellulose, and pectin.

Cellulose is insoluble in water excepting forcing conditions, therefore, the majority of cellulose from rimu berries will be present in the water insoluble residue.[98,99]

Hemicellulose chain lengths (500 – 3,000 residues) are much shorter than cellulose (7,000 – 15,000) and also exhibit branching.[40] The amorphous structure of hemicellulose leads to fewer intermolecular hydrogen bonds compared to cellulose which makes hemicellulose easier to solubilise in water and hydrolyse with acid. The majority of hemicellulose from rimu berries is likely to remain insoluble during the warm water extract, but glucomannan and galactoglucomannan hemicelluloses may be found in the water soluble fraction.

Pectic polysaccharides display variable solubility in water depending on the chain length, pH, and degree of methyl esterification. Water solubility is facilitated by the uronic acid carboxylate groups which exist as charged species at neutral pH. This creates an electrostatic repulsive force between residues promoting a linear conformation and a higher degree of hydration. At low pH, the degree of hydration is reduced allowing for more inter- and intra-molecular hydrogen bonds which leads to formation of a less soluble, crystalline structure. A higher degree of methyl esterification is expected to increase solubility due to a lower number of free carboxyl groups in the pectin molecule, but this can be offset in the presence of multivalent metal ions (such as Ca^{2+}), where pectin with a lower degree of methyl esterification is more susceptible to cross-linking and gel formation.[100] Warm water extraction is considered an efficient and green method for extracting pectin.[101] The majority of extracted pectin from rimu berries is expected to be contained in the soluble fraction of the warm water extract, but portions of pectin may be associated with cross-linking agents such as cellulose which cause them to remain insoluble in warm water.[102]

Fructans are soluble in water and degradation at neutral pH is not expected at the 80 °C temperature used for the water extract.[103,104] The majority of fructan polysaccharides should be present in the soluble fraction of the warm water extract.

Starch is insoluble in water at room temperature owing to its dense crystalline structure. Upon heating with water, the intermolecular bonds of starch molecules break down allowing the water to penetrate the crystalline structure and occupy the hydrogen bonding sites causing gelatinisation. The gelatinisation endotherms and enthalpy are related to the source of starch, water content, and ratio of amylose/amylopectin.[105] The 80 °C temperature used for the warm water extraction of rimu berries should be insufficient to solubilise starch granules and ensure the majority of starch is remains in the insoluble fraction, but a portion of low DP or highly branched starch may also be present in the soluble fraction.

2.4 D-Glucose, D-Fructose, and Sucrose Assay

The 70% ethanol soluble solution was assayed for free D-glucose, D-fructose, and sucrose using Megazyme assay kit K-SUFRG.[106] The method implemented from this assay kit is outlined in the following (**Scheme 3**).

Scheme 3. Overview of Megazyme sucrose, D-glucose, D-fructose assay reactions.

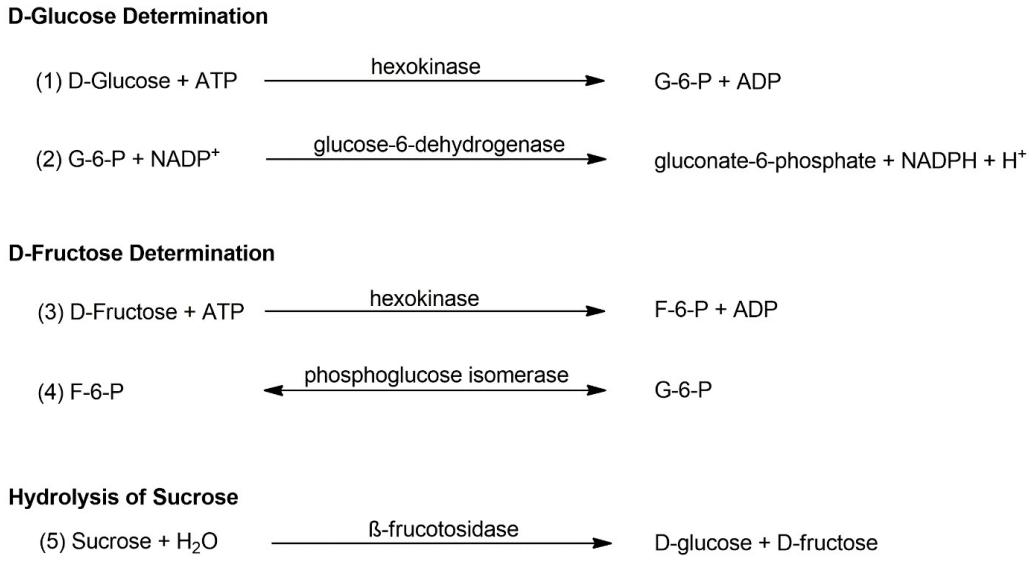

(1) Hexokinase catalyses the transfer of a phosphate group from adenosine-5'-triphosphate (ATP) to D-glucose resulting in the formation of glucose-6-phosphate (G-6-P) and adenosine-5'-diphosphate (ADP).

(2) Glucose-6-dehydrogenase catalyses the oxidation of G-6-P by nicotinamide-adenine dinucleotide phosphate ($NADP^+$) to gluconate-6-phosphate with the formation of reduced nicotinamide-adenine dinucleotide phosphate (NADPH). The formation of NADPH is stoichiometric with the amount of D-glucose. The amount of NADPH produced in this reaction is measured by the increase in UV absorbance at 340 nm.

(3) Hexokinase also catalyses the phosphorylation of D-fructose from ATP producing fructose-6-phosphate (F-6-P) and ADP.

(4) Phosphoglucose isomerase converts F-6-P to G-6-P which in turn reacts with $NADP^+$ producing NADPH, which can be measured by a further rise in

absorbance which is stoichiometric with the amount of D-fructose.

(5) Sucrose is hydrolysed by β-fructosidase in acidic conditions forming D-glucose and D-fructose.

2.4.1 Rimu Berry Sugar Components

D-glucose is the most abundant free sugar in the rimu berry sample, followed by sucrose then D-fructose. D-glucose is roughly twice as abundant than sucrose and D-fructose. The total free sugar results based on the mass of wet berries and approximate mass of dry berries were 5.19% and 1.45%, respectively. These values are similar to the values reported by Cottam *et al.*,[12,29] in which total sugars were determined to range from 1.0 – 6.5% of the dry matter of the fruit in samples collected between May 2007 to February 2008.

Table 5. D-glucose, D-fructose, and sucrose in the 70% EtOH soluble fraction as determined by Megazyme K-SUFRG assay.

	Analyte	Result (g/L)	Result (g/100 g)	Wet berry (%)	Dry berry (%)
70% EtOH soluble (SS)	D-glucose	0.0803	8.0272	2.63	0.73
	D-fructose	0.0363	3.6386	1.19	0.33
	Sucrose	0.0421	4.2105	1.38	0.38
	Total	**0.1587**	**15.876**	**5.19**	**1.45**

Interestingly, the ratios of the free sugars differs in these results compared to Cottam *et al.* In their study, fructose was reported as the most abundant free sugar with a concentration roughly twice that of glucose, and almost ten times that of sucrose. A possible explanation for the change in free sugar ratios is that this occurs as a result

of fruit ripening. As fruits ripen, the sugar content increases with a subsequent decrease in acidity, which often makes ripened fruit taste sweeter. The depletion of starch and an increase in the concentration of sucrose and reducing sugars is observed during fruit ripening.[107]

2.5 Total Starch Assay

The 70% ethanol insoluble residue (AIR), and the insoluble and soluble fractions from the warm water extract (WWE_Insol and WWE_Sol, respectively) were assayed for total starch content using a Megazyme assay kit following the AOAC Official Method 996.11.[108] The method implemented from this assay kit is outlined in the following (**Scheme 4**).

Scheme 4. Megazyme total starch assay kit reactions.

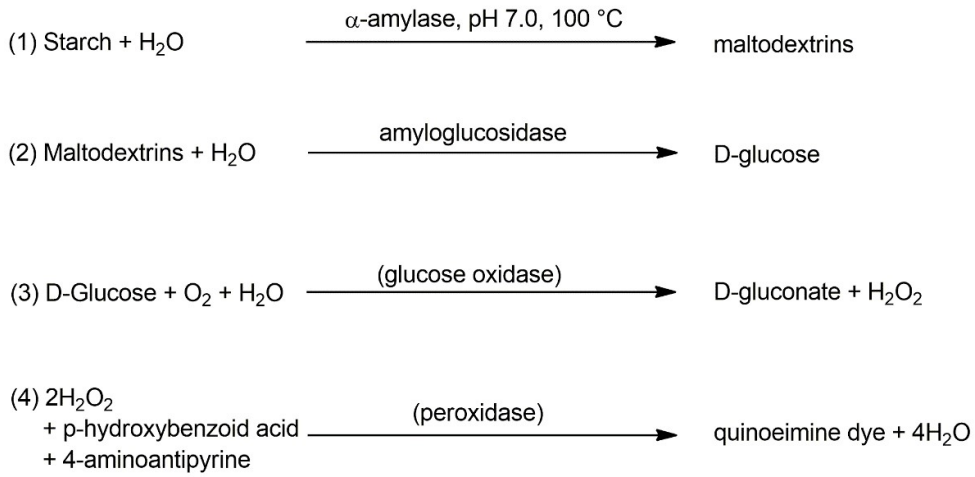

(1) Thermostable α-amylase catalyses the hydrolysis of starch into soluble branched and unbranched maltodextrins.

(2) Amyloglucosidase catalyses the hydrolysis of maltodextrins to D-glucose.

(3) D-glucose is oxidised to D-gluconate releasing equimolar amounts of hydrogen peroxide.

(4) Hydrogen peroxide is quantitatively measured in a colourimetric reaction using peroxidase to produce a quinonimine dye.

2.5.1 Rimu Berry Starch Components

The result for the starch content of the dry berry was measured and calculated to be 15.43%. This value is much higher than the 4.47% reported by Cottam *et al.*

Table 6. Starch content of insoluble residue from 70% EtOH extraction and insoluble and soluble fractions from warm water extract as determined by Megazyme total starch assay kit.

	Free glucose (g/100g)	Glucose post hydrolysis (g/100 g)	Total starch (g/100 g)	Starch content dry berry (%)
AIR	8.409	25.154	16.746	15.43
WWE_Insol	11.544	23.088	11.544	6.46
WWE_Sol	0.292	26.715	26.423	0.26

The unexpectedly high results for free glucose measurements of the AIR and WWE_Insol fractions were concerning as free glucose was expected to be extracted into the soluble fraction of the 70% EtOH extraction (SS). The free glucose measured in the AIR was 8.409 g/100 g which exceeds the value for free glucose in the SS fraction 8.0272 g/100 g.

The possibility that the majority of free sugars might not have been extracted into the SS fraction was investigated. This possibility was supported by the results from the Megazyme Glu/Fru/Suc assay, in which the total free sugar results for the dry content of the berry (1.45%) were determined to be at the low end of the range of values reported by Cottam *et al.* (1.0 – 6.5% dry content of the berry).

The solubility of glucose in 70% EtOH at 4 °C is roughly 5%.[109] The extraction used 70 mL of 100% EtOH which was diluted by the approximate water content of the berry sample (~30 mL) to produce 100 mL of 70% EtOH solution used for extraction. This volume may not have been sufficient to ensure complete extraction of free glucose given the low solubility. In retrospect, doubling the solvent volume from 100 mL to 200 mL would have been advantageous to account for the low solubility of glucose in 70% EtOH at 4 °C and ensure a more complete extraction of free sugars.

The high free glucose result for WWE_Insol of 11.544 g/100 g indicates that low solubility of free sugars in 70% EtOH may not have been responsible for the high free glucose measurement in the AIR. This aberrant result led to the conclusion that colourimetric interference was likely responsible for the high free glucose measurements in the AIR and WWE_Insol. Unfortunately, due to limited time and material, this experiment was unable to be repeated to test this hypothesis. Therefore, the total starch results presented here are not considered to be robust enough to give an accurate value for the total starch content of rimu berries.

2.6 Hydrolysis of Fractions

Two hydrolysis methods were implemented for carbohydrate analysis of rimu berries. The first method is in two stages and combines an initial hydrolysis in 3N methanolic hydrochloric acid (MeHCl) (80 °C, 18 hours) with a secondary hydrolysis using 2.5M trifluoroacetic acid (TFA) (aq., 120 °C, 1 hour). The second method implements a two-stage hydrolysis process, with both steps using aqueous H_2SO_4. The second method is tailored to achieve total hydrolysis of cellulose:[110] Primary hydrolysis using

72% H_2SO_4 (aq., 30 °C, 3 hours) is followed by secondary hydrolysis in 6% H_2SO_4 (aq., 100 °C, 3 hours). Samples AIR and WWE_Insol were subjected to MeHCl/TFA and H_2SO_4 hydrolysis. WWE_Sol was subjected to MeHCl/TFA hydrolysis only (having minimal dissolved cellulosic material).

Acidic methanolysis is a relatively mild hydrolysis method compared to sulfuric acid but is less suited to hydrolysis of crystalline material or chemically stabilised glycosidic bonds. The main advantages of methanolysis compared to sulfuric acid hydrolysis is minimising side reactions and that it can readily be removed by evaporation. Methanolysis converts the released monosaccharides to their corresponding methyl-glycosides and converts carboxylic acid moieties to methyl esters. The formation of multiple isomers for each monosaccharide complicates chromatograms and can impair analyte sensitivity due to overlapping peaks. The conversion of carboxylic acid moieties to methyl esters makes methanolysis more suitable for analysis of uronic acids compared to sulfuric acid hydrolysis.[111]

TFA hydrolysis alone is considered mild compared to sulfuric acid and is not sufficient for hydrolysis of uronic acids. Methanolysis followed by TFA hydrolysis can be a useful method as it can hydrolyse uronic acids and converts the methyl glycosides resulting from methanolysis back to their respective monosaccharide which overcomes the issue of overlapping peaks in the chromatogram. Combined MeHCl/TFA hydrolysis was determined to be superior to four other methods (including H_2SO_4 and acidic methanolysis) for carbohydrate analysis of water soluble uronic-acid containing polysaccharides.[56]

Sulfuric acid hydrolysis results in high conversion of polysaccharides to monomers and is especially suited to substrates that are relatively resistant to hydrolysis due to structural features such as the high crystallinity exhibited in starch and cellulose, or from chemical influences that stabilise the glycosidic linkage such as with the carboxylic acid moiety in uronic acids.[112,111] In the two-stage hydrolysis, the initial hydrolysis with strong acid breaks cellulose down to glucose. Some of the liberated glucose will be subjected to derivatisation or degradation *via* oxidation or polymerisation reactions.[113] The function of the secondary hydrolysis with dilute acid

is to hydrolyse the glucose reversion products (such as disaccharides) resulting from the primary hydrolysis.[110] The major drawbacks associated with sulfuric acid hydrolysis are unwanted side reactions and the difficulty of removal of the residual sulfuric acid. Side reactions include the decarboxylation of uronic acids, introduction of sulfuric acid groups, and acid-catalysed dehydration of 5-carbon sugars.[111]

2.7 Determination of Monomer Composition of Hydrolysates by HPAEC-PAD

The hydrolysates were analysed by HPAEC-PAD (refer to **Appendix A** for chromatographic traces and data tables, and **Experimental Section 6.4** and **6.5** for chromatographic methods).

The hydrolysates were analysed against a standard solution containing a mixture of 12 monosaccharides including arabinose, ribose, xylose, glucose, galactose, fucose, glucuronic acid, galacturonic acid, galactosamine, glucosamine, rhamnose, and mannose (**Figure 16**). Fructose was not included in the 12-sugar mix due to being incompatible with the chromatographic method. Standard curves were produced for quantitation in the range of 1.25 μg mL^{-1} to 20 μg mL^{-1} for neutral sugars, and from 2.5 μg mL^{-1} to 40 μg mL^{-1} for acidic sugars (refer to **Appendix A** for examples).

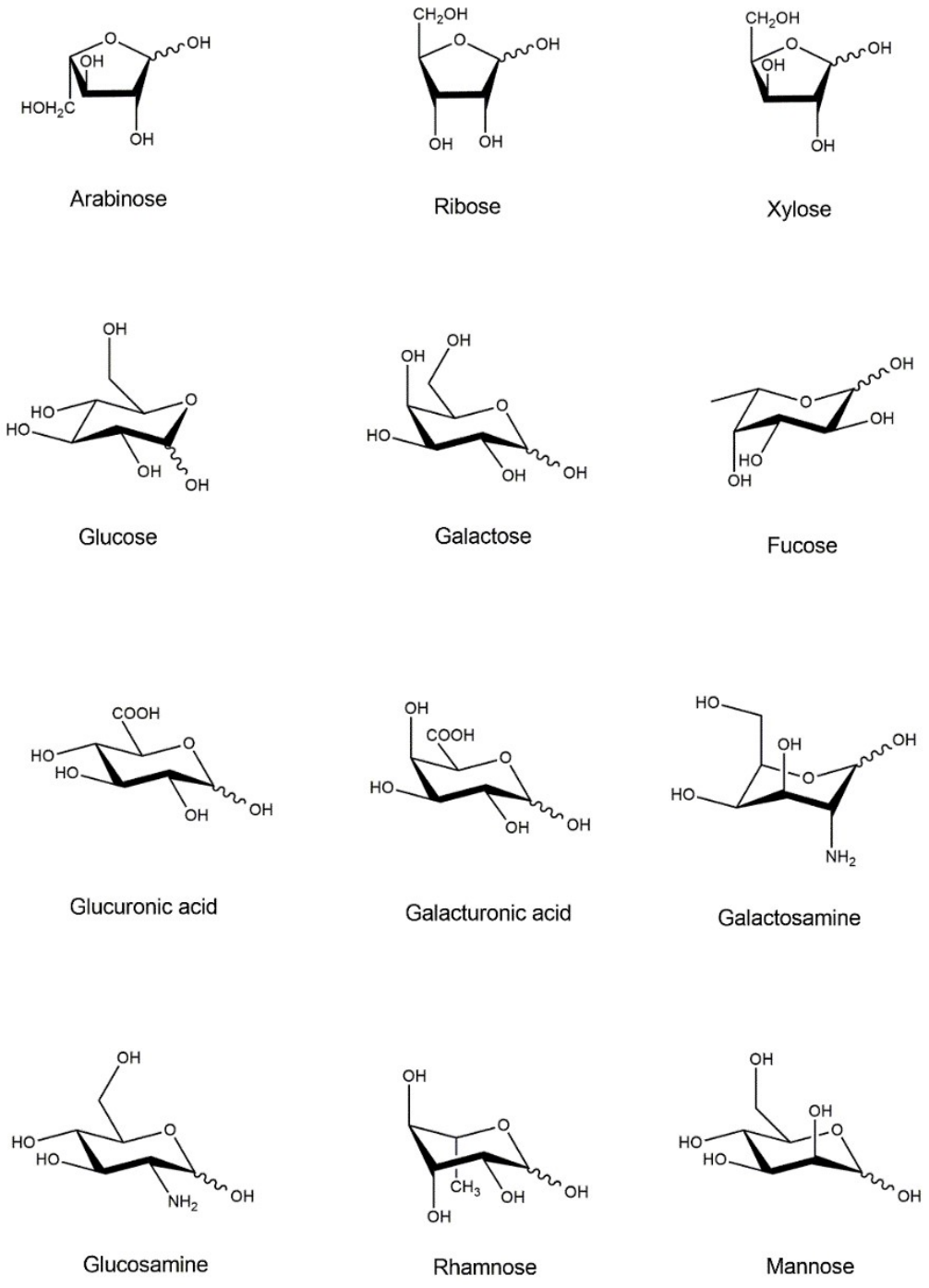

Figure 16. Monosaccharides included in 12 sugar mix as standards for HPAEC-PAD analysis of hydrolysates.

2.7.1 AIR Sugar Composition

The monomers were detected based on their retention time compared to that recorded for the 12-sugar mix standards. Quantitation was completed on the Dionex through peak integration and comparison of peak areas to values derived with individual monosaccharide standard curve response factors. The molar percentages of the detected monosaccharides for each of the analysed hydrolysates was calculated as the average of duplicate analysis (**Figure 17**).

Not all of the monosaccharides in the 12-sugar mix are constituents of plant storage and cell wall polysaccharides. Ribose and galactosamine were not detected in any of the samples. Glucosamine was detected in minor amounts in the AIR (0.3%) and WWE_Insol (0.4%) H_2SO_4 hydrolysates, and at an unusually high level in the WWE_Insol (3.4%) MeHCl/TFA hydrolysate.

Glucosamine is not a major component of plant storage or cell wall carbohydrates. Glucosamine in a minor component of arabinogalactan proteins (AGPs) which exist in cell walls, but the backbone of the glycan portion of AGPs consists of arabinose and galactose residues with glucosamine only making up a small portion of AGP side chains.[114] As the detected level of glucosamine in all samples exceeded the detected level of galactose, it is speculated that the glucosamine likely originated from inadequately cleaned Kimax tubes.

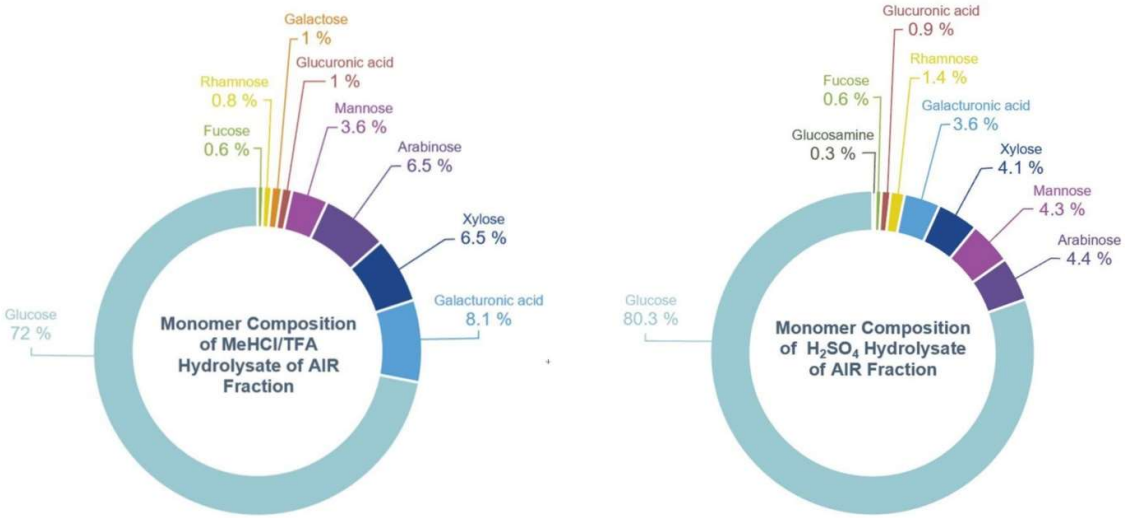

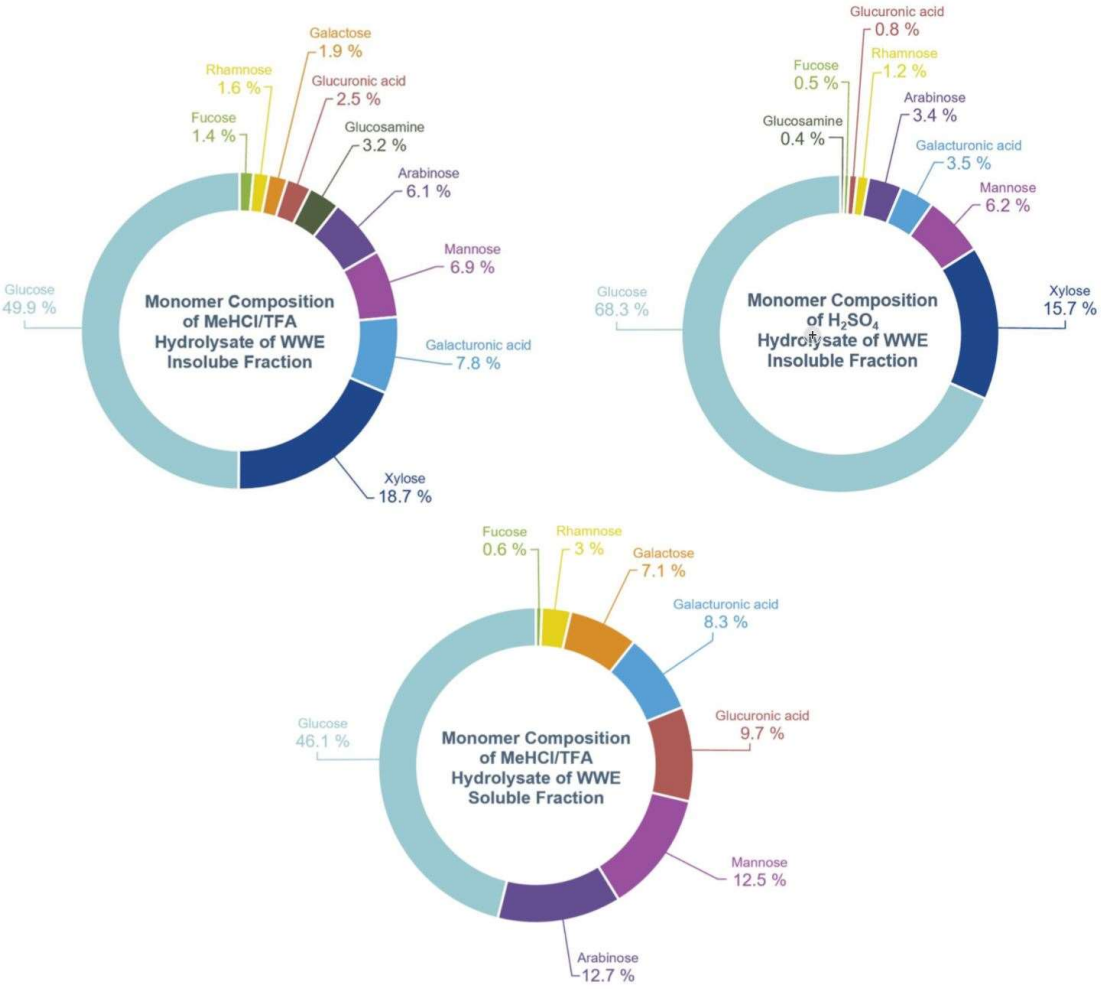

Figure 17. Monomer composition of extracts expressed as molar percentage.

The majority of cellulose is expected to be contained in the WWE_Insol fraction. Cellulose is expected to be mostly resistant to hydrolysis by MeHCl/TFA, but not to hydrolysis by H_2SO_4. The glucose molar percentage in the WWE_Insol sample increased by 18.4% between the MeHCl/TFA and H_2SO_4 results. The hydrolysis of cellulose is likely to represent the majority of this increase in glucose molar percentage as the starch content would have been mostly hydrolysed by MeHCl/TFA. This figure can be used to approximate the cellulose content as 10.3% of the dry weight of the berry which is less than 17.34% as reported by Cottam *et al.* The low result for the approximation of cellulose potentially indicates that cellulose

was partially hydrolysed by MeHCl/TFA hydrolysis, or that H_2SO_4 treatment resulted in incomplete hydrolysis of cellulosic material. Another explanation is that degradation of cellulose by bacterial and fungal species has occurred which is possible given the observed decomposition of the berry sample prior to extraction.[115]

The glucose molar percentage in the WWE_Sol fraction was measured to be 46.1% after MeHCl/TFA hydrolysis. The majority of the detected glucose was liberated as a result of the hydrolysis procedure as the free glucose concentration of WWE_Sol measured during the starch assay prior to hydrolysis was determined to be 0.29%. The starch content of WWE_Sol was found to be around 26%, but this was calculated to represent only 0.26% of the dry weight of the berry. This indicates that the majority of starch was successfully fractionated into the WWE_Insol fraction, but a small percentage of the total starch was warm water soluble. The small quantity of starch in the WWE_Sol sample is likely responsible for the large value for the molar percentage of glucose.

Xylans are a type of hemicellulose and were expected to be fractionated into WWE_Insol. Xylans consist of β-(1,4)-linked xylose residues with side branches of α-arabinose and/or α-glucuronic acid. No xylose was detected in WWE_Sol. WWE_Insol had a xylose molar percentage of 15.7 – 18.7% in the two hydrolysates, with sufficient molar percentages of arabinose and glucuronic acid to represent the side chains. From this it can be concluded that xylans present in rimu berries have been extracted into WWE_Insol.

Xyloglucans are a potentially prebiotic hemicellulosic polysaccharide that are exclusively present in the WWE_Insol fraction. Xyloglucans have a backbone consisting of β-(1,4)-linked glucose residues. The majority of glucose residues are substituted with (1,6)-linked xylose sidechains which generally feature a terminal galactose residue or a galactose-fucose moiety.[116] Small molar percentages of both galactose and fucose were detected in WWE_Insol which could represent these terminal moieties on the side chains of xyloglucans.

Mannose and galactose are present in higher concentrations in the WWE_Sol fraction compared to WWE_Insol. Glucomannan and galactoglucomannan species are typically water soluble,[117] and are likely more abundant in the WWE_Sol fraction.

Pectin is primary composed of galacturonic acid residues and can be split into covalently linked domains depending on their structure. These domains include homogalacturonan which consists of a linear chain of α-(1-4)-linked galacturonic acid residues; xylogalacturonan which feature xylose branching from the galacturonic acid backbone; rhamnogalacturonan-I which feature alternating rhamnose and galacturonic acid residues in the backbone with sidechains that feature glucuronic acid and arabinose; and rhamnogalacturonan-II which possess a backbone made up of galacturonic acid residues featuring adipose, fucose, arabinose, galactose, and xylose residues in the side chains.[41] The molar percentage of galacturonic acid ranged from 3.5 – 7.8% in the WWE_Insol hydrolysates, and 8.3% in the WWE_Sol hydrolysate. From the results of the monomer composition of the hydrolysates, it cannot be determined which fraction contains the majority of pectinaceous domains. In addition, pectin features both water soluble and water insoluble domains. The presence of xylogalacturonans can be excluded from WWE_Sol as no xylose was detected. This is also the case for rhamnogalacturonan-II species as these feature xylose in the side chains. The higher molar percentage of rhamnose in WWE_Sol makes this fraction a more likely candidate for the isolation of rhamnogalacturonan I.

2.8 Summary

These results represent the initial stages of carbohydrate analysis that can serve to guide future work in which specific polysaccharides can be isolated, characterised, and tested for their fermentability by resident bacterial species in the digestive tract of kākāpō.

Naturally present xylans in animal feed have been determined to act as an antinutrient, which reduces the ability of the animal to absorb essential nutrients.

Whereas xylooligosaccharides derived from hydrolysis of xylans (either in the intestine or by chemical methods) have been identified to possess prebiotic properties. It has yet to be determined if supplementation of xylanase or xylooligosaccharides to animal feed can result in improved intestinal health and performance.[118] Further investigation into the xylan polysaccharides present in the WWE_Insol fraction could lead to a better understanding of the antinutrient and prebiotic properties of these polysaccharide species in rimu berries.

Glucomannans and galactoglucomannans are hemicelluloses which have been shown to have prebiotic, antidiabetic, and immuno-stimulatory effects and can effectively prevent gastrointestinal disorders.[119] Glucomannans have been identified as useful additives for treating obesity,[117] making them attractive candidates for improving supplementary feed formulations for kākāpō who have been reported to have lower fecundity due to obesity when given supplementary food *ad libitum*.[120] Further information on these polysaccharides could be obtained through investigation into the WWE_Sol fraction of rimu berries.

Pectin oligosaccharides have been identified as potent prebiotics and would be worthy of further investigation as additions to supplementary feed formulations for kākāpō.[121] These oligosaccharides could be identified through further investigations into both WWE_Insol and WWE_Sol fractions of rimu berries.

Future work would also entail determining linkage sites, anomeric configurations, absolute configurations, locations of non-carbohydrate substituents, and the ring forms (pyranose or furanose) of residues in polysaccharides.

Chapter 3. Iodine Assay

3.1 Proposed Research

The main objective of this portion of the research project was to determine the iodine content of rimu berries, seeds, and foliage.

Specifically, the objectives were:

- Extract iodine from rimu berries, seeds, and foliage in duplicate using 25% tetramethylammonium hydroxide (TMAH).

- Submit to collaborators for assay by ICP-MS to determine iodine content.

3.2 Iodine in New Zealand

New Zealand soils have very low levels of iodine in certain areas. The iodine content of plants is reflective of the iodine levels in the soil which they grow in. The iodine content of plants is a nutritional component for the animals which eat them.[122]

Goitre was endemic in many parts of New Zealand during the earlier years of the previous century which led to the introduction of iodine supplementation in foods such as salt and bread.[123] Re-emergence of iodine deficiency in New Zealand human populations were reported following a dietary survey conducted from 1987 – 1998.[124] Iodine is predominantly deposited into soils by sea spray with iodine levels being elevated in soils that are close to the sea. The concentration of iodine in soils is also affected by its mobility in soil which is related to pH, redox potential, organic carbon, and clay content.[122]

As kākāpō populations are managed on offshore islands, the proximity to the sea may affect the iodine levels in the rimu that grow there, but without analysis of the soil and plants on these islands, this currently remains speculative. Given the lack of

data on the iodine content of rimu and the important role that iodine plays in avian reproduction, the following data should be informative for nutritional characterisation of iodine in rimu collected from these sites.

3.3 Method

Rimu berries, seeds, and foliage were extracted in duplicate using 25% aqueous TMAH according to the method by Tagami *et al.*[125] TMAH is a quaternary ammonium salt with the molecular formula $N(CH_3)_4^+$ which undergoes acid-base reactions to produce tetramethylammonium salts with anions derived from the acid.

The extraction was conducted in falcon tubes overnight at 60 °C. The lids for the tubes were sealed with electrical tape to prevent loss of material to evaporation. This was measured by weighing the vessels before and after extraction which revealed a very minor reduction in mass for all samples (0.01 – 0.1%). Following extraction, the samples were centrifuged, and the supernatant (1.00 mL) was pipetted into vials which were subsequently shipped to our collaborators at Otago University who analysed the samples by ICP-MS.

ICP-MS is a widely used for the determination of trace elements in various materials owing to its high sensitivity with an iodine detection limit of 0.013 μg L^{-1}, and quantitation limit of 0.045 μg L^{-1}.[125,126]

3.4 Results

Prior to analysis, the samples were diluted by our collaborators as the TMAH concentration in the supplied extracts was too high and the samples were of inadequate volume for their ICP-MS method. Dilution duplicate precision checks were carried out and the dilution was determined to have only a very minor effect on

the precision with percentage coefficients of variation between diluted and non-diluted samples ranging from 0.59 – 3.5%. Matrix spiking was conducted by our collaborators and post-extraction spiked recoveries ranged from 103 – 115% which is within the bounds of the analytical technique (where spiked recoveries of < 75% or > 125% would indicate significant interference from matrix effects). The blank had an iodine concentration of 0.41 ng mL^{-1} which is expected as the TMAH will contain background levels of iodine. The detection limit of this technique was reported at 0.2 ng mL^{-1}, which was suitably below the lowest reading of rimu plant material.

The following (**Table 7**) displays the average results of the iodine concentration of the duplicate samples with blank subtraction to remove background signal.

Table 7. Average iodine detected in duplicate samples of rimu plant material as determined by ICP-MS.

	Average [I] (ng/mL)	[I] dry berry (ng/g)
Rimu berry - ripe	5.9	150
Rimu berry - overripe	12	300
Rimu seed	8.3	210
Rimu foliage	34	840

The iodine content of rimu berries is 150 ng g^{-1} for the ripe berries, and 300 ng g^{-1} for the overripe berries. The average iodine content of a variety of fresh fruit and vegetables has been reported between 18 – 70 ng g^{-1}.[127,128] The iodine content of dry rimu seeds is 210 ng g^{-1} which is similar to the average value of nuts at 218 ng g^{-1} as reported by Haldimann *et al.* The iodine content of rimu foliage is 840 ng g^{-1} which is much higher than the average value for most food groups in the study by Haldimann *et al.*, including fresh fruit, vegetables, nuts, cereals, and grains.

3.5 Summary

The quantity of plant materials used for this study were limited and represent only a tiny portion of the geographical area of the island sanctuaries where kākāpō currently reside. No strong conclusions can be drawn from such a small data set, but these preliminary results indicate that iodine levels in rimu plant material sampled from these locations are high compared to other food groups. One explanation for these comparatively high results is that the island sanctuaries' proximity to the sea is resulting in iodine accumulation in rimu beyond what may occur on the mainland.

Future work could examine the iodine and thyroid hormone levels in kākāpō to determine if iodine supplementation or restriction may be beneficial to their fecundity. More samples of both soil and rimu berries from a large range of geographical areas could be tested for iodine content to produce a more robust data set.

Chapter 4. Search for Phytoestrogens

4.1 Proposed Research

Samples of rimu berries, foliage, seeds, and unfertilised ovules were investigated for the presence of phytoestrogens using spectroscopic techniques and a bioassay provided by collaborators at the Victoria University of Wellington School of Biological Sciences utilising recombinant yeast strains expressing human or kākāpō oestrogen receptors.

Specifically, the goals for the search for phytoestrogens included:

- Exhaustive extraction of rimu berries, foliage, seeds, and unfertilised ovules in water, methanol, then chloroform.

- Standardised fractionation of the methanol extracts based on a cyclic loading procedure.

- Selected fractions undergo further fractionation based on an oestrogenic response detected by bioassay or spectroscopic evidence from 1D and 2D NMR analysis of fractions displaying potential phytoestrogen motifs.

- Isolation and structure characterisation of potential phytoestrogens.

4.2 Sequential Double Extractions in Water, Methanol, and Chloroform

Phytoestrogens produced by plants are considered as secondary metabolites and therefore are metabolically expensive to the producing organism and are generally

only present in low amounts. Given the low quantity of rimu material available for extraction, the goal was to exhaustively extract the plant material across a range of polarities while avoiding degradation of thermolabile compounds by the application of heat. The maceration extraction technique was applied which involves soaking pulverised plant material in a closed container at room temperature with gentle stirring overnight. Exhaustive extraction is ensured by filtering the solvent after 24 hours and then adding additional fresh solvent for a second extraction and combining the filtrates together.[129]

Rimu foliage, berries (ripe), berries (overripe), seeds, and unfertilised ovules (refer to **Table 11**) had been stored at -80 °C to prevent degradation before extraction. The plant samples were ground to a fine consistency with a mortar and pestle to increase the surface area for solvent penetration. The plant material was submerged in liquid nitrogen prior to grinding to ensure the material remained frozen to minimise any changes to the metabolite profile and assist with grinding. Grinding the material by hand in a mortar and pestle, rather than with mechanical assistance, serves to minimise excess heat which may degrade thermolabile metabolites. It also helps to prevent over-grinding the material resulting in particle sizes that are too small for efficient solvent penetration.[129]

Rimu foliage, berries (ripe), berries (overripe), seeds, and unfertilised ovules were doubly and sequentially extracted in water, methanol, then chloroform (2 × 300 mL) at room temperature overnight with gentle agitation. Water, methanol, and chloroform are common solvents used for natural products extraction and represent a range of polarities with relative polarity indices of 9.0, 5.1, and 4.1, respectively.[130]

Oestrogen and other steroid receptors exist in discrete cellular locations including the nucleus and extra-nuclear compartments in cells. In addition to the nucleus, ER-α and ER-β are present in the plasma membrane, mitochondria, and the endoplasmic reticulum of cells.[131] Phytoestrogens would therefore be expected to display similar characteristics to other drug-like molecules such that they can survive first pass metabolism in which they are absorbed into the blood circulatory system by passing through the gut wall, and access the interior of cells by possessing suitable

chemical characteristics in order to cross the plasma membrane to gain access to ERs. Lipinski's rule of five is a heuristic for determining drug-likeness of chemical compounds based on molecular properties that are important for pharmacokinetics and is based upon the observation that most orally administered drugs have MW > 500 and have moderate lipophilicity such that they are at least partially soluble in hydrophilic and hydrophobic media.[132] Whilst this heuristic has been criticised based on its low accuracy at predicting drug-like compounds,[133] it offers a useful starting point for deciding which extracts and fractions are most worthy of spectroscopic investigation in the search for phytoestrogens. Phytoestrogenic compounds are postulated to exist in an intermediate 'mass window' of low relative mass and intermediate polarity between highly polar and high mass compounds such as carbohydrates and low polarity and high mass compounds such as lipids. A hydrophobic core structure, usually a phenyl group, similar the A-ring of E1, E2, and E3 (**Figure 7**) is a key moiety for ER binding, and thus the mass window for phytoestrogens is postulated to be offset slightly towards low polarity (**Figure 18**).

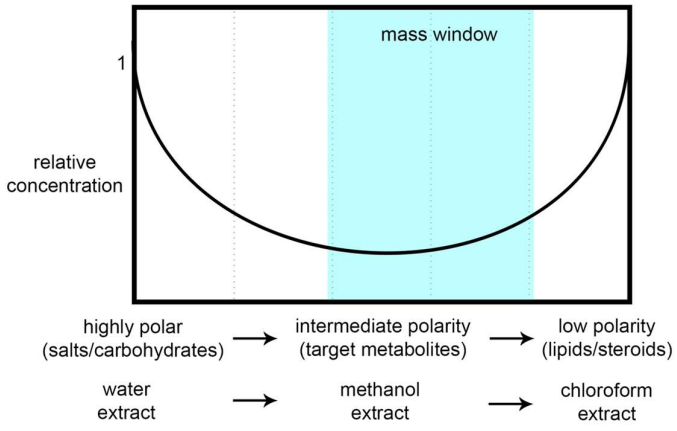

Figure 18. Schematic of mass and polarity distribution of extracts. Phytoestrogens are postulated to exist as low mass compounds with intermediate to low polarity as indicated by the mass window. Adapted from "Secondary Metabolites from the New Zealand Marine Sponge *Mycale hentschelí*" by Singh, 2007. (© Singh 2007).[134]

4.3 Cyclic Loading

The methanol extracts of all the plant materials were subjected to fractionation using the cyclic loading procedure (**Scheme 5**), developed by Northcote and West at Victoria University of Wellington.[135] This technique uses poly(styrene-divinylbenzene) (PSDVB) (reversed-phase solid support) as the stationary phase and water/acetone mixtures for the mobile phase. Extracts can be loaded directly onto the column without preconcentration negating the issue of precipitation of polar compounds in a non-polar solvent and *vice versa*. Extracts were redissolved in methanol and passed through the PSDVB column. The non-polar compounds present in the extract will be retained by the stationary phase. The eluent is then slowly diluted with water (typically 100% v/v), ensuring that no precipitation is observed during dilution, and passed through the column again. The water serves to increase the polarity of the eluent and promote the retention of compounds of slightly higher polarity than those previously adsorbed on the stationary phase. This process was repeated twice for a three-fold dilution of the extract. The column can then be eluted with organic modifier/water mixtures of decreasing polarity. The extracts of all plant materials were eluted using the same acetone/water mixtures, with acetone concentrations of 20, 40, 60, 80, and 100% producing five fractions for each extract.

The presence of water in the eluents is undesirable as they tend to foam when concentrating under reduced pressure. To prepare the five fractions in 100% organic solvent for simple concentration, a modified cyclic loading process termed ‘back-loading’ was employed. The back-loading process involves dilution of the fraction with water and passing the fraction through a column with a PSDVB stationary phase. Similarly to the cyclic loading procedure, these eluents are then further diluted with water increasing their polarity and passed through the column again promoting greater retention on the non-polar stationary phase. The column can then be eluted with 100% organic modifier and easily concentrated under reduced pressure.

Scheme 5. Cyclic loading procedure. Reproduced from "The Isolation of Secondary Metabolites from New Zealand Marine Sponges" by West, 2001. (© West 2001).[135]

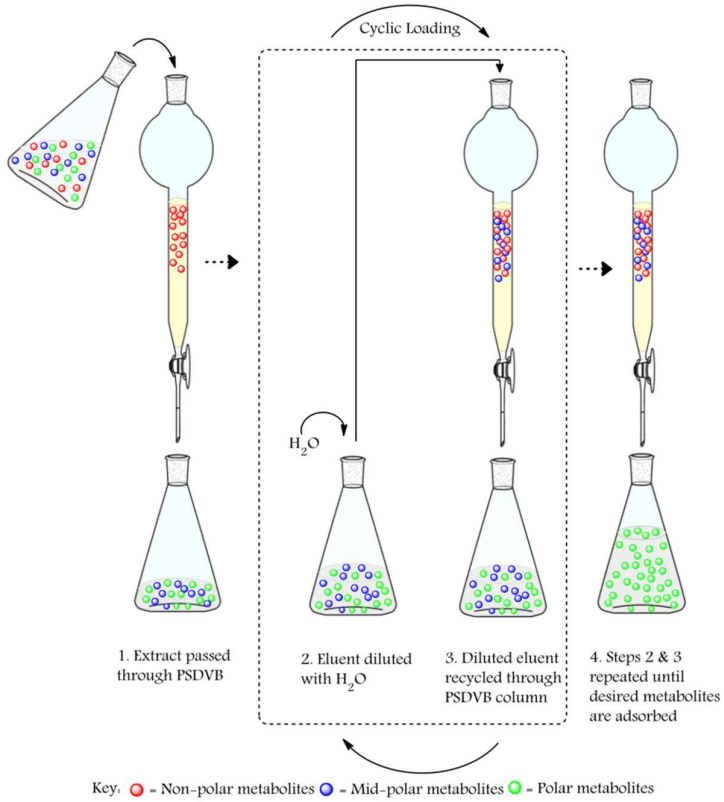

By using this method, the extracts of the different rimu materials could be separated into five standardised fractions based on polarity. These five fractions could then be analysed by ^{1}H NMR and/or 2D NMR spectroscopy to search for structural motifs that would inform further fractionation efforts.

Analysis of the ^{1}H NMR spectra of the five fractions produced by the backloading procedure of rimu berries (overripe), foliage, seeds, and unfertilised ovules revealed the presence of a common contaminant in high abundance in most of the fractions. It was postulated that this contaminant must have originated from one of the solvents. Acetone and methanol were separately concentrated under reduced pressure and

analysed by ^{1}H NMR spectroscopy which revealed that the contaminant was a phthalate ester that had originated from the “analytical-grade” acetone used in the cyclic-loading procedure. The identity of the phthalate contaminant was determined by ^{1}H NMR,[136] and gas chromatography-mass spectrometry (GC-MS) to likely be bis(2-ethylhexyl) phthalate (refer to **Appendix E**). Full characterisation was not undertaken as this phthalate ester was not of great importance to this study. The presence of this phthalate contaminant was particularly concerning due to the oestrogenic activity of many phthalates,[137] which could produce an artificial positive in the oestrogenic bioassay.

At this stage of the research project the bioassay provided by our collaborators was not operational. Unfortunately, the bioassay was not able to be utilised in this study until just before the end of this project timeline, so fractionation was solely driven by spectroscopic evidence. This also resulted in uncertainty over how the bioassay would react to phthalate contamination. It was unknown if the phthalate contamination would produce positive results, or if minor amounts of phthalate contamination could be tolerated.

Only a small portion of rimu berries were available to repeat the extraction and cyclic loading procedures. To save time, a double methanol extraction (rather than sequential double extractions in water, methanol, and chloroform) was carried out using rimu berries (ripe). Liquid chromatography-mass spectrometry (LC-MS) grade acetone was obtained and tested for impurities prior to cyclic loading by ^{1}H NMR spectroscopy. No contaminants were detected in the LC-MS grade acetone and the cyclic loading procedure produced five fractions of rimu berries which could be utilised in the bioassay with confidence that artificial positives would not arise from phthalate contamination.

4.4 Structural Features of Podocarpic Acid and Phytoestrogens to Guide Spectroscopic Analysis

Podocarpic acid (**27**) is a known phytoestrogen found the heartwood of rimu. While podocarpic acid has not been detected in other rimu plant structures, the structure of this compound can serve to inform what structural motifs may be important for oestrogenic activity, and by which biosynthetic pathway these may be produced in rimu.

Podocarpic acid possesses structural features that confer high binding affinity to hER-α *(*refer to **Section 1.7***)*, namely, the presence of the phenol moiety which has the aromatic core structure required for interaction, and the hydroxyl group to form hydrogen bonds with Glu353 and Arg394 in the hER-α binding pocket. The *trans*-decalin and carboxylic acid moieties are postulated to occupy the remaining space in the ligand binding pocket and orient the hydroxyl group on the carboxylic acid into a favourable position to hydrogen bond with the His524 residue. As it has been reported that podocarpinol (**34**) has greater oestrogenic activity compared to podocarpic acid,[63] the carbonyl moiety is possibly hindering the interaction of podocarpic acid with hER.

Podocarpic acid, the structures of common phytoestrogens (refer to **Section 1.8**), and the structural features required for ligand binding to hER-α were used to guide analysis of ^{1}H NMR spectra of crude extract and fractions. Experimental podocarpic acid for reference spectra was obtained by extraction from rimu hardwood.[*]

[*] Thanks to A. Prof. Peter Northcote for the preparation and exhaustive purification of this material.

Table 8. NMR Data for podocarpic acid (**27**)[a]

position	^{13}C		^{1}H		COSY	HMBC
	δC	mult.	δH	mult. (J, Hz)		
1a	39.4	CH_2	1.37		1b, 2a, 2b	2, 9, 10, 17
1b			2.15[b]	m	1a, 2a, 2b	1, 2, 3, 5, 17
2a	20.0	CH_2	1.60	dquin (14.1, 3.5)	1a, 1b, 2b, 3a, 3b	-
2b			2.00[b]	m	1a, 2b, 2a, 3a, 3b	1, 3
3a	37.5	CH_2	1.08	m	2a, 2b, 3b	2, 4, 15, 16
3b			2.25	br d (13.2)	2a, 2b, 3a	-
4	44.0	-	-	-	-	-
5	52.9	CH	1.54	br d (12.3)	6a, 6b	4, 6, 7, 10,15, 16, 17
6a	21.1	CH_2	2.00[b]	m	5, 6b, 7a, 7b	5, 7
6b			2.15[b]	m	5, 6a, 7a, 7b	4, 5, 7, 8, 10
7a	31.3	CH_2	2.71	ddd (18.5, 12.7, 6.2)	6a, 6b, 7b	5, 6, 8, 9
7b			2.83	dd (16.0, 4.9)	6a, 6b, 7a, 14	5, 6, 8, 9, 14
8	127.5	-	-	-	-	-
9	149.6	-	-	-	-	-
10	38.8	-	-	-	-	-
11	112.1	CH	6.73	d (2.6)	13	8, 10, 12, 13
12	153.8	-	-	-	-	-
13	113.2	CH	6.59	dd (8.2, 2.6)	11, 14	8, 11, 12
14	130.2	CH	6.89	d (8.2)	7b, 13	7, 9, 12
15	183.8	-	-	-	-	-
16	28.8	CH_3	1.32	s	-	2, 3, 4, 5, 15
17	23.2	CH_3	1.09	s	-	1, 5, 9, 10

[a] Data recorded in $CDCl_3$ (25 °C, referenced to solvent signals, ^{1}H: 7.26 ppm, ^{13}C 77.16 ppm)
[b] Signals unresolved, these assignments are correlations are interchangeable.

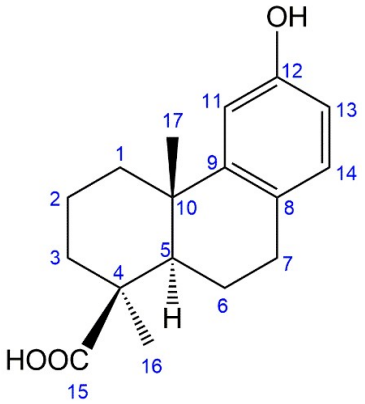

The ^{1}H NMR spectra of extracts and fractions can be difficult to interpret due to the large number of peaks, overlapping signals, and difficulty in analysing the true multiplicity and integration of signals. Therefore, the ^{1}H NMR spectra of the fractions from cyclic loading were analysed for the following features:

- The presence of aromatic signals between 6.00 – 8.50 ppm. Podocarpic acid and all the phytoestrogen types analysed in Section 1.8 possess aromatic rings. E2 (**36**) and podocarpic acid share a 3,4-disubstituted phenol moiety with two aromatic protons *ortho* and one *meta* to the hydroxyl group. Protons on the other *meta* position and *para* position are not observed due to the presence of a cyclohexane ring at these positions. Therefore, compounds with aromatic moieties similar to podocarpic acid or E2 would display three aromatic signals each integrating to one proton (**Figure 19**). This arrangement includes a doublet of 8 Hz indicating an *ortho* coupling, a doublet of doublets (8 and 2 Hz) indicating *ortho* and *meta* coupling, and a 2 Hz doublet indicating *meta* coupling.

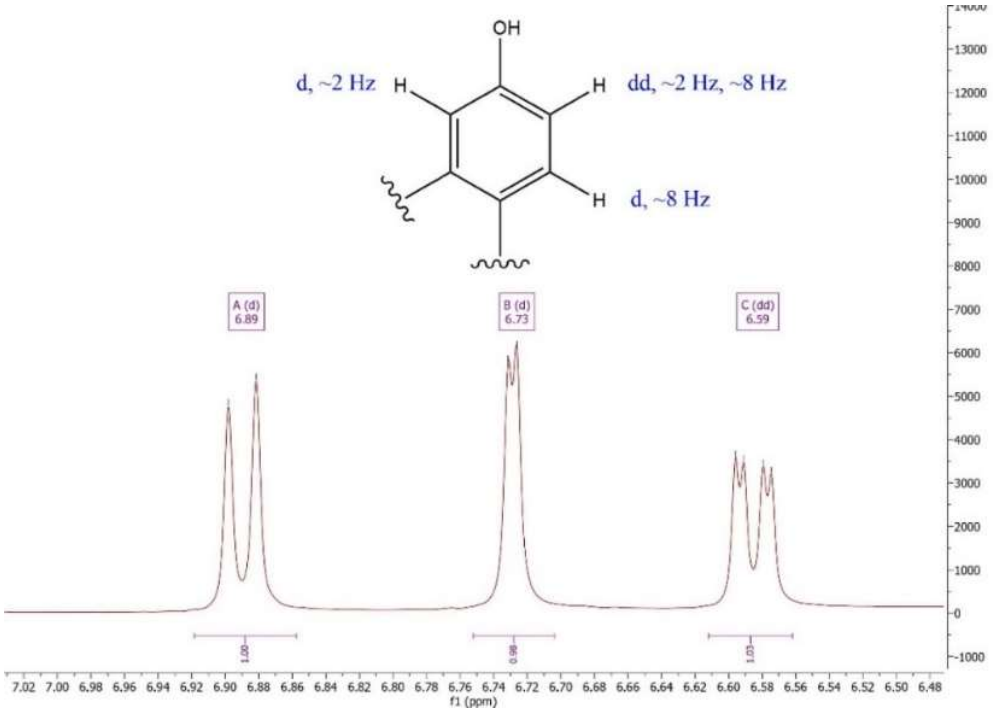

Figure 19. The aromatic moiety of podocarpic acid with characteristic ^{1}H NMR signals.

- The presence of methyl singlets would be observed in ^{1}H NMR spectra of both E2 and podocarpic acid. In the case of E2, only one methyl group is present in the molecule at the junction of the C and D rings. Podocarpic acid possesses two methyl groups in the molecule, one of which shares C-4 with the carboxylic acid moiety and would be shifted slightly downfield, while the other is bonded to the C-10 decalin junction in a *trans* relationship to H-5. This moiety could be recognised by heteronuclear multiple bond correlation (HMBC) spectra in which the methyl protons share a correlation to C-5 on the decalin ring junction and show separate correlations to carboxylic acid C-15 and aromatic C-9.

- The presence of hydroxyl protons from a carboxylic acid moiety between 10.00 to 13.00 ppm (in $CDCl_3$), in conjunction with the presence of aromatic

and methyl signals could possibly indicate a podocarpic acid derivative or similar diterpenoid structure. It was postulated that similar diterpenoid acid structures could share some degree of oestrogenic activity, although this moiety was not considered vital due to the increased oestrogenic activity of podocarpinol compared to podocarpic acid.

- The presence of methine and methylene dispersed resonances between 1.00 to 3.50 ppm as an indication of cyclisation which is a feature of many terpenoids, and which may indicate the decalin moiety of podocarpic acid. Chemical shifts between 2.00 – 4.00 ppm were also considered as these may provide evidence of heteroaromatic functionality as present in flavonoids, lignans, and coumestans.

4.5 Extract Fractionation

The ^{1}H NMR spectra of all of the fractions produced by cyclic loading of the methanol extracts were examined for spectroscopic features which may indicate the presence of phytoestrogens. Further fractionation efforts were conducted by flash chromatography using silica gel (refer to **Experimental Section 6.11**) Eluents of chromatography were combined to produce fractions based upon isolating peaks from instrument response signals from the evaporative light scattering detector (ELSD) and UV detection at 254, 265, 280, and 320 nm.

4.5.1 Analysis of Rimu Foliage Extracts

Examination of the ^{1}H NMR spectra combined with thin layer chromatography (TLC) of the five fractions produced by cyclic loading of the methanol extract of rimu foliage led to interest in the 80% acetone/water fraction (See **Appendix B** for the ^{1}H NMR

spectrum). This fraction possessed many of the spectroscopic features that would indicate the presence of a compound with similarity to podocarpic acid or a related diterpenoid compound. This included the presence of hydroxyl protons from a carboxylic acid moiety, the presence of a number of aromatic signals with well-defined doublets and singlets, multiple methyl singlets, and unresolvable methine and methylene signals. In addition, the signals associated with the phthalate impurity were in low abundance. Analysis by silica TLC (visualised by H_2SO_4/vanillin stain and heating) revealed non-UV active (254 nm and 365 nm) purple spots with a retention factor (R_f) value of ~0.4 (100% DCM), primarily in the 80% acetone/water fraction, but also present in the 100% acetone fraction. The purple spots indicated the possible presence of a terpenoid/steroidal compound.[138]

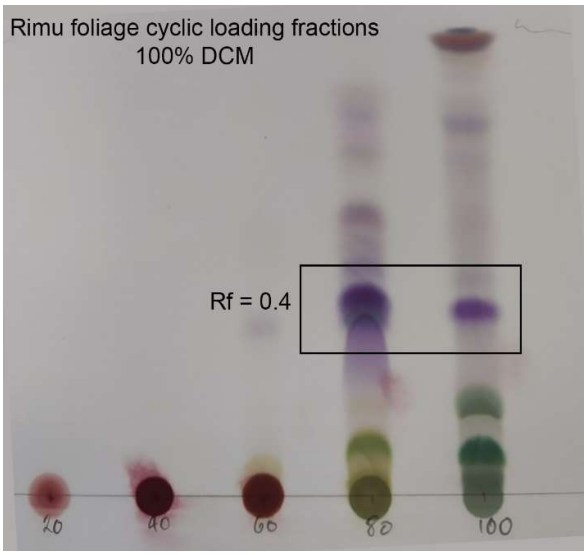

Figure 20. TLC of cyclic loading fractions of rimu foliage. The purple spots of interest indicated in the 80% and 100% acetone/water fractions may indicate the presence of a terpenoid/steroidal compound.

Further spectroscopic evidence for a podocarpic acid-like compounds were observed in the HMBC of the 80% acetone/water fraction (**Figure 21**).

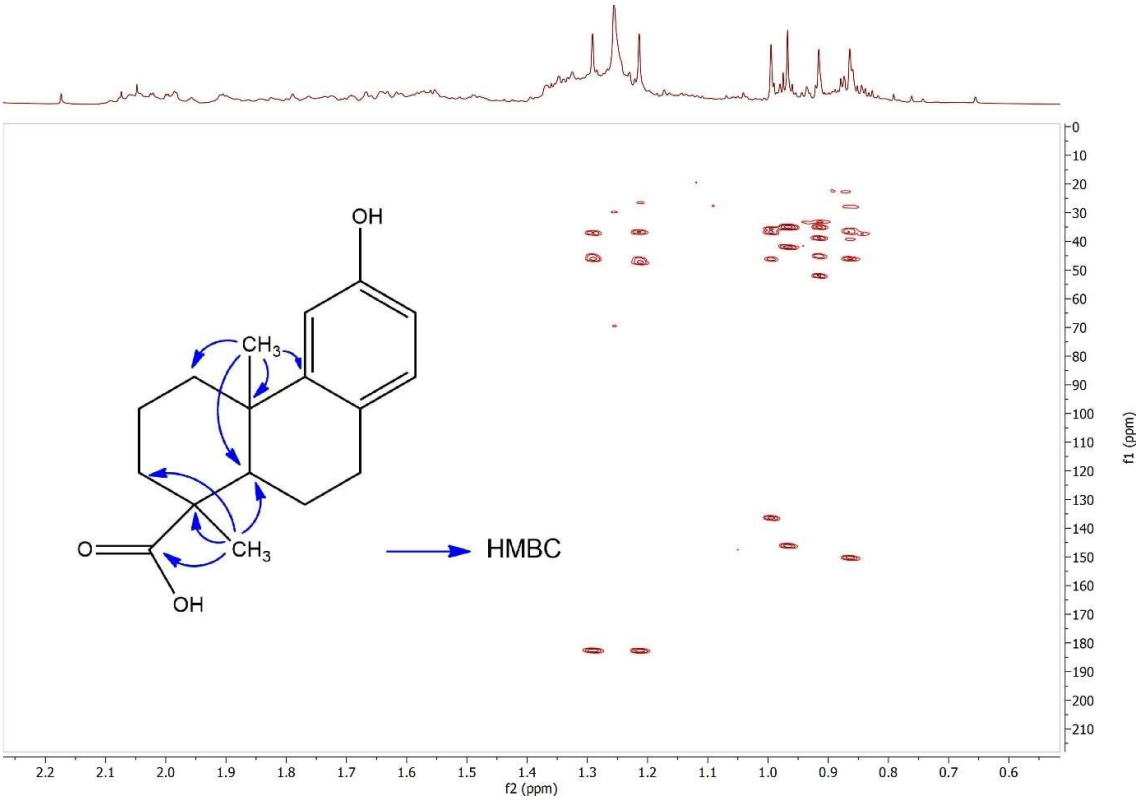

Figure 21. HMBC NMR spectrum of the 80% acetone/water fraction of the methanol extract of rimu foliage displaying evidence of podocarpic acid-like methyl group correlations.

The methyl signals in the HMBC spectra of crude extracts and fractions provided a quick way to determine if podocarpic acid-like compounds are present. The methyl signals in an HMBC experiment are generally more intense due to possessing three protons and display 2 – 3 bond correlations. The proton signal of the methyl group at the decalin junction would be seen to correlate strongly with carbon atoms three bonds away. In this case, we would expect to see one correlation to a substituted

aromatic carbon meta to phenolic hydroxyl (130 – 145 ppm), one correlation to a methylene ring carbon between 35 – 40 ppm, and one to the methine carbon on the opposite side of the decalin ring junction at 45 – 55 ppm. The correlation to the methine carbon would be shared with the other methyl group in proximity to the carboxylic acid. This methyl group would also display correlations to the carboxylic acid carbon at around 180 ppm, along with a correlation to a methylene carbon belonging to the cyclohexane ring at around 35 – 40 ppm.

The 80% acetone/water fraction was fractionated by flash silica chromatography producing five fractions. TLC of the five fractions visualised by H_2SO_4/vanillin stain revealed the presence of multiple purple spots in fractions 2, 3, and 4. Two of these five fractions (**Scheme 6.** DSH1_20_F2 and DSH1_20_F3) were selected for further fractionation.

Scheme 6. Fractionation diagram of rimu foliage. Displaying the fractions, sample codes, mass recoveries, and chromatographic method and solvent systems used for each stage.

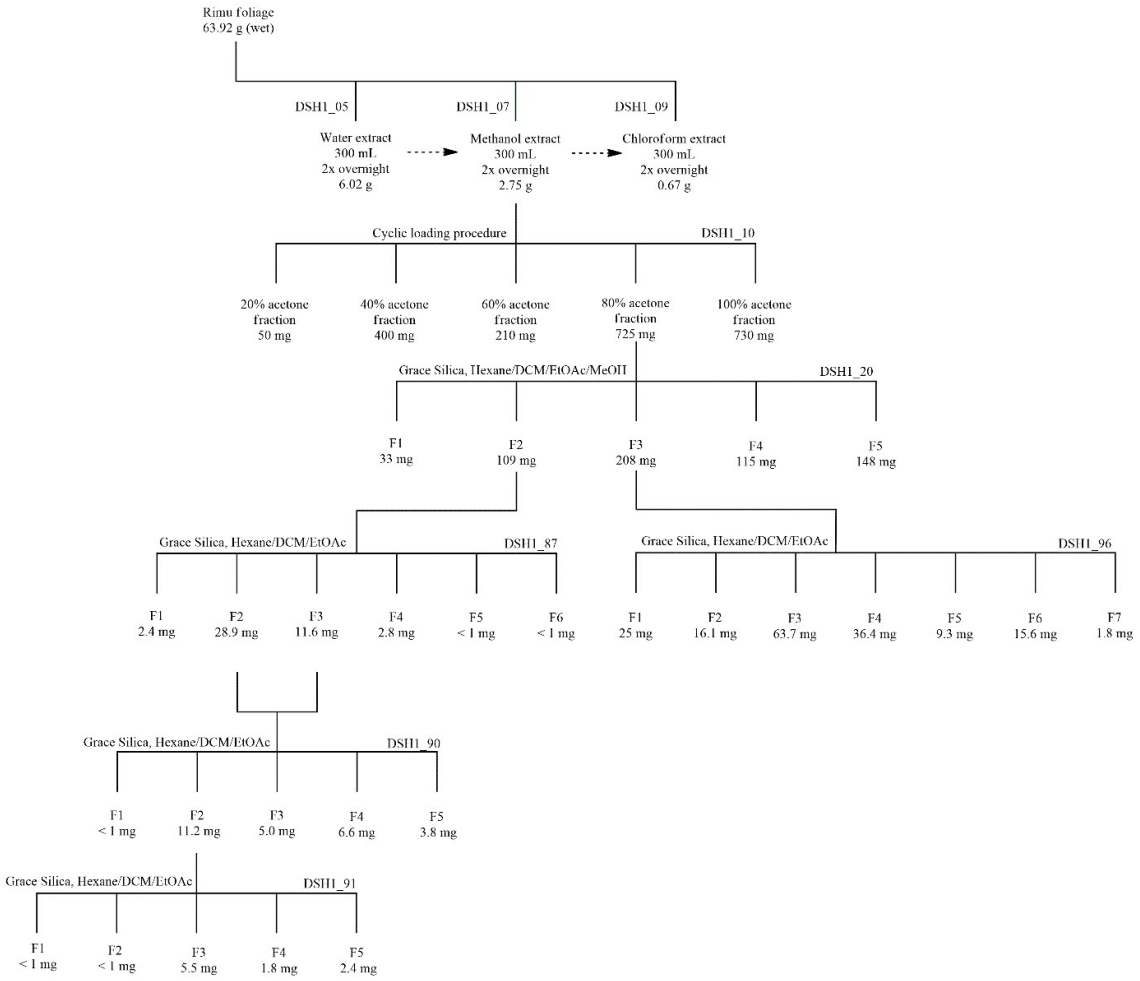

The ^{1}H NMR of DSH1_20_F2 (**Scheme 6**) showed the presence of six methyl singlets between 0.85 – 1.27 ppm along with a strong signal at 5.77 ppm with a multiplicity pattern of two overlaid doublet of doublets with coupling constants of 17 and 10 Hz possibly representing two similar compounds featuring a conjugated olefinic system. Additionally, a strong set of signals around 4.89 ppm were observed which displayed multiple doublet, triplet, and doublet of doublet signals. It was postulated that the true multiplicity of these signals was four independent doublet of doublets. Two of the doublet of doublets displayed coupling constants of around 17/1.5 Hz and 10/1.5 Hz which was indicative of a terminal olefin related to the conjugated olefinic system at 5.77 ppm. Multiple singlets were observed at 3.80 ppm indicating the possibility of methyl ether/ester groups. The methyl singlet signals were integrated and compared with the integrals of these signals which resulted in comparable ratios of whole numbers of hydrogens possibly indicating that these signals belong to the same compound or two similar compounds. There was also a significant number of unresolvable signals with comparable intensity between 0.85 – 2.00 ppm indicating the presence of primary and secondary alkyl groups. Low levels of discrete aromatic or polarised alkene signals were also observed but integration of these signals determined that these are not related to higher intensity signals. There was also the presence of weak singlet signals between 9.50 to 13.00 ppm indicating the presence of aldehyde and carboxylic acid groups. The HMBC spectrum of fraction 2 displayed the podocarpic acid-like pattern of methyl protons correlating with carboxylic acid and aromatic carbons and sharing a correlation to alkyl group carbons around 37 – 45 ppm. The HMBC of the overlaid doublet of doublets at 5.77 ppm showed two sets of correlations to alkyl regions between 21 – 45 ppm. The signals at 4.89 ppm showed correlations to both the alkyl region between 35 – 37 ppm and the aromatic or polarised olefin region between 146 – 150 ppm. The singlet signals at 3.80 ppm correlated into several regions including the alkyl region between 25 – 40 ppm, aromatic or polarised alkene region between 130 – 150 ppm, and the ester or amide region between 160 – 170 ppm. The ^{1}H-^{1}H correlation spectroscopy (COSY) spectrum of fraction 2 displayed correlations between the signals at 5.77 and 4.89 ppm, while the remaining signals did not correlate to each

other, indicating that these signals may be from different compounds or that these functionalities are distant to each other or are linked through regions lacking in protons.

Comparing the spectroscopic evidence to the known compounds in rimu (refer to **Section 1.2**) led to postulating that the signals at 5.88 and 4.89 ppm may be indicative of the conjugated olefin system observed in myrcene (**9**) or sclarene (**11**).

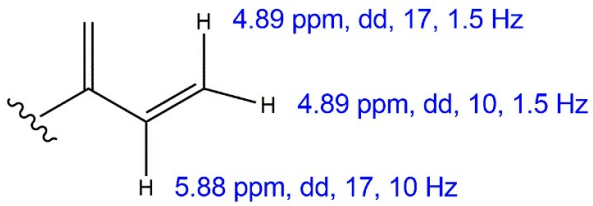

Figure 22. Postulated conjugated olefinic system from observed 2D NMR signals in DSH1_20_F2.

The ^{1}H NMR spectrum of fraction 3 showed several aromatic doublets and other resonances with unresolved multiplicities. The signals observed in fraction 2 at 5.77 ppm and 4.89 ppm were also present but with much lower intensity. The signal at 3.80 ppm observed in fraction 2 was also present in fraction 3, but with greater intensity. Fraction 3 also displayed reduced intensity in the alkyl signals between 0.85 – 2.00 ppm, and reduced intensity of the methyl singlet signals.

Fractions 2 and 3 were selected for further fractionation. For fraction 2 the goal was to follow the previously described podocarpic acid-like methyl signals and to deconvolute the spectrum so that a better idea of the structure could be ascertained to see if this fraction should be subjected to isolation efforts to characterise the compound producing the observed signals. For fraction 3, further fractionation was carried out with the goal of producing additional samples for analysis by bioassay given the indications in the TLC of a terpenoid/steroidal compound. The

chromatographic methods were informed by the R_f of the purple spots observed by TLC and utilised similar solvent systems as the previous chromatographic steps but were adjusted to have longer gradients of the less polar solvents. These fractionation steps also served to remove or reduce the concentration of the phthalate impurity from the fractions of interest which made them suitable for analysis by bioassay.

Further fractionation of DSH1_20_F2 produced six new fractions (**Scheme 6**. DSH1_87). Analysis by ^{1}H NMR led to the combination of fractions 2 and 3 as the previously described signals at 5.77, 4.89, 3.80, and six methyl singlets between 0.85 – 1.27 ppm were present in both. Further fractionation (**Scheme 6**. DSH1_90 and DSH1_91) was carried out on these combined samples to further isolate these signals. Ultimately, the flash chromatography methods used were not able to isolate any discrete compounds. The 2D NMR spectra showed evidence of multiple similar compounds coeluting in the fraction with the signals of interest.

The foliage fractions were stored until the bioassay was operational and could be further investigated/isolated if they produced positive results in the bioassay.

4.5.2 Detailed Fractionation Focused on Rimu Berries (Overripe), Seeds, and Unfertilised Ovules

The rimu berries (overripe), seeds, and unfertilised ovules that had been sequentially extracted and fractionated by cyclic loading were fractionated by flash chromatography using a standardised solvent gradient (see **Experimental Section 6.11.3**). The main objective of this fractionation step was to remove the phthalate contamination and produce samples for analysis by bioassay. Phthalate removal was generally observed in the early eluting fractions having been eluted during the hexane portion of the solvent gradient.

The ^{1}H NMR spectra of all these fractions were examined for evidence of a podocarpic acid-like compound or spectral similarities. No evidence of a podocarpic

acid-like aromatic moiety was detected. Several fractions showed evidence of carboxylic acid moieties, methyl singlets, and methylene signals which may be indicative of diterpene compounds with some structural similarity to podocarpic acid.

Berry (overripe) fraction DSH1_139_F5 (**Scheme 7**) and unfertilised ovules fraction DSH1_137_F2 (**Scheme 9**) shared signals with one of the foliage samples of interest (**Scheme 6**. DSH1_20_F2). The shared signals included the overlaid doublet of doublets at 5.77 and 4.89 ppm, and methyl singlets at 0.96 and 0.98 ppm (refer to **Appendix Section B** for ^{1}H NMR comparison), indicating some structural similarity with the postulated diene unit from the foliage fractions.

Due to time constraints, it was decided to store these samples and await the results from the bioassay before undergoing further fractionation or isolation efforts.

Scheme 7. Fractionation diagram of rimu berries (overripe).

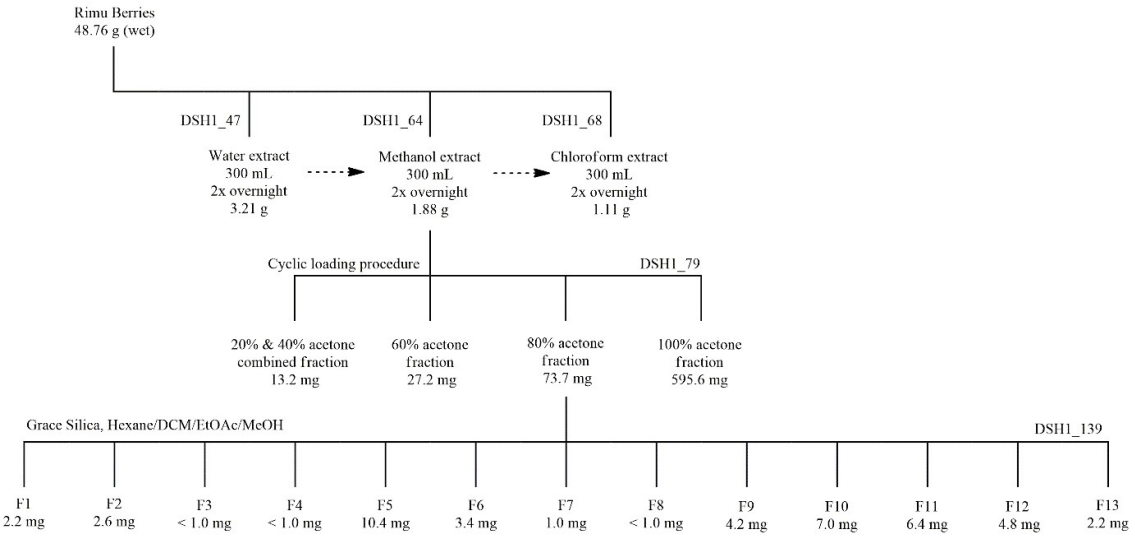

Scheme 8. Fractionation diagram of rimu seeds.

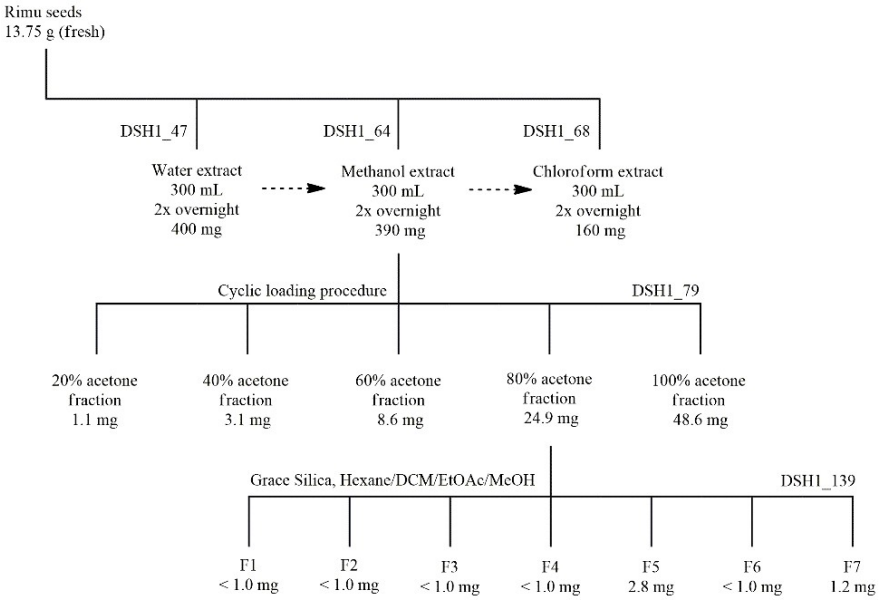

Scheme 9. Fractionation diagram of rimu unfertilised ovules.

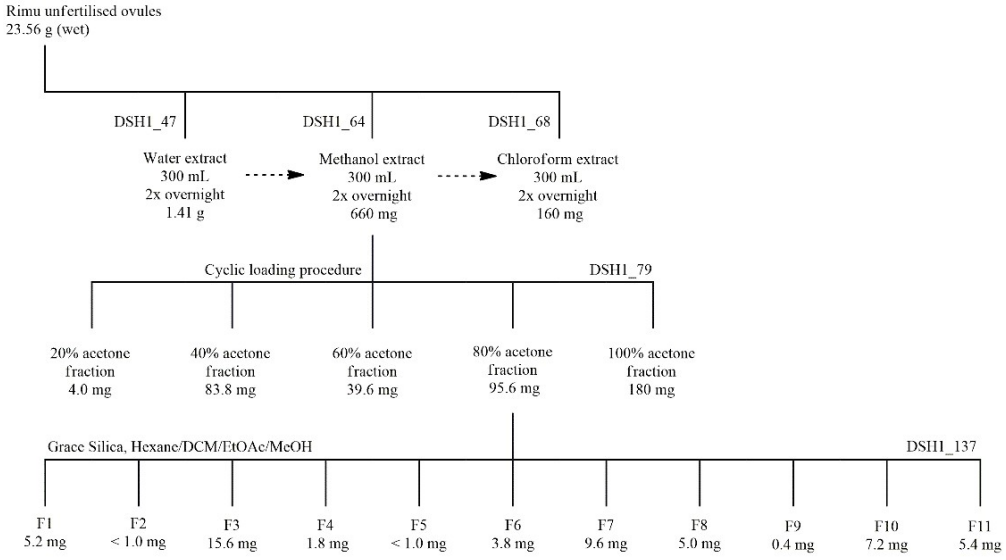

4.5.3 Rimu Berries (Ripe) Constituents

The sample of rimu berry (ripe) was extracted twice in methanol and fractionated by cyclic loading utilising LC-MS grade acetone that was confirmed to be free of phthalates.

Examination of the ^{1}H NMR spectrum of the 80% acetone/water fraction from cyclic loading showed the presence of two aromatic singlets along with methyl singlets which when analysed by HMBC gave evidence of a podocarpic acid-like compound which had an additional aromatic substituent. The 80% acetone/water fraction was further fractionated by flash chromatography producing eight fractions (**Scheme 10**. DSH1_111). The previously observed aromatic and methyl singlet signals were identified in fraction 3. Further flash chromatography of fraction 3 (**Scheme 10**. DSH1_128) produced fourteen fractions. The signals of interest were observed in the 2D NMR spectra of fraction 6 with sufficient purity and resolution to identify the compound (**48**) as either lambertic acid (**49**) or the isomer dehydroabietic acid (**50**). Fraction 6 was selected for purification by high-performance liquid chromatography (HPLC) followed by high-resolution MS and 2D NMR for full structural characterisation.

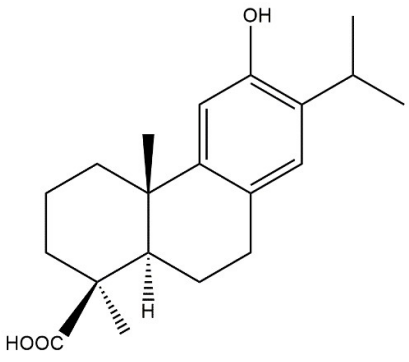

49

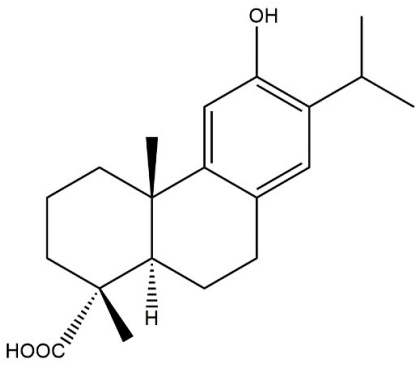

50

Scheme 10. Fractionation diagram of rimu berries (ripe) leading to the identification of compound **48**.

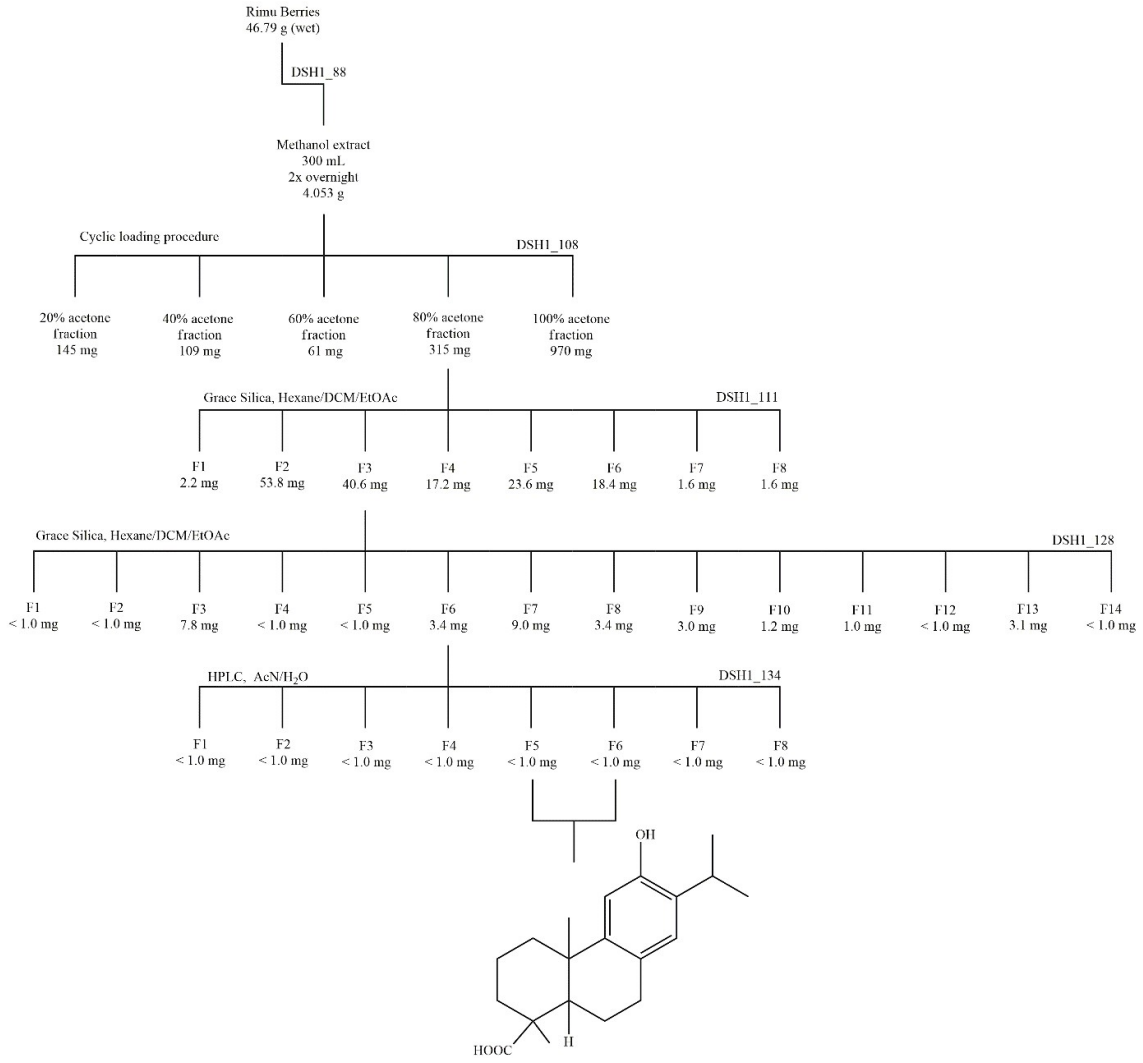

48

4.6 Isolation and Structural Characterisation of Compound 48

The purification of **48** from berry (ripe) fraction DSH1_135_F5&6 (**Scheme 10**) was achieved using HPLC with a reverse phase C18 column. Compound **48** was isolated with a 7.1 min retention time (refer to **Experimental Section 6.12** for method and **Appendix Section D** for HPLC trace). Structural characterisation was achieved through high-resolution MS and 2D NMR spectroscopy. Nuclear Overhauser effect spectroscopy (NOESY) was used for determination of stereochemical configurations.

The chemical formula of lambertic acid (**49**) or dehydroabietic acid (**50**) was confirmed using high-resolution MS (refer to **Appendix Section D**) which displayed a deprotonated molecule (*m/z* 315.1961) suitable for a molecular formula of $C_{20}H_{28}O_3$. The ^{13}C NMR spectrum accounted for all twenty carbons, and the ^{1}H and HSQC NMR experiments together account for 26 of the 28 hydrogens as being attached to carbon.

Additionally, the HSQC NMR spectrum confirmed that the ^{1}H signals at 2.16 and 2.01 ppm each had contributions from hydrogens on two independent carbon atoms.

Table 9. NMR Data for compound **48**[a]

position	^{13}C		^{1}H		COSY	HMBC
	δC	mult.	δH	mult. (J, Hz)		
1a	39.3	CH_2	1.39	td (13.5, 4.1)	1b, 2a, 2b	-
1b			2.16[b]	m	1a, 2a, 2b	-
2a	19.9	CH_2	1.61	dquin (14.0, 3.5)	1a, 1b, 2b, 3a, 3b	-
2b			2.01[b]	m	1a, 1b, 2a, 3a	10
3a	37.5	CH_2	1.07	m	2a, 2b, 3b, 5	-
3b			2.25	br d (13.4)	2a, 3a	-
4	43.7	-	-	-	-	-
5	52.7	CH	1.54	dd (12.2, 1.2)	6a, 6b	4, 6, 7, 9, 10, 18
6a	21.1	CH_2	2.01[b]	m	5, 6b, 7a, 7b	10
6b			2.16[b]	m	5, 6a, 7a, 7b	-
7a	31.2	CH_2	2.72	ddd (18.5, 12.7, 6.2)	6a, 6b, 7b, 14	8, 14
7b			2.84	dd (16.5, 5.8)	6a, 6b, 7a, 14	8, 14
8	127.4	-	-	-	-	-
9	146.4	-	-	-	-	-
10	38.3	-	-	-	-	-
11	111.9	CH	6.62	s	-	8, 9, 10, 12, 13, 15
12	150.8	-	-	-	-	-
13	131.8	-	-	-	-	-
14	126.7	CH	6.83	s	7a, 7b	7, 9, 10, 11, 12, 15
15	26.8	CH	3.12	sept (6.8)	16, 17	12, 13, 14, 16, 17
16	22.7	CH_3	1.22[b]	d (5.8)	15	13, 15, 17
17	22.5	CH_3	1.24[b]	d (5.8)	15	13, 15, 16
18	181.3	-	-	-	-	-
19	28.7	CH_3	1.32	s	-	2, 3, 4, 5, 18
20	23.1	CH_3	1.11	s	-	1, 5, 9, 10

[a] Data recorded in $CDCl_3$ (25 °C, referenced to solvent signals, ^{1}H: 7.26 ppm, ^{13}C 77.16 ppm)
[b] Signals unresolved, these assignments are correlations are interchangeable.

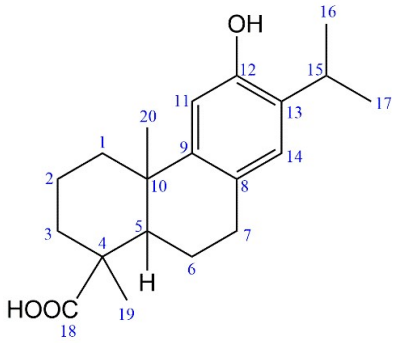

Connectivity was determined by COSY and HMBC NMR spectra. Assignment of the C-11 and C-14 aromatic signals was based on HMBC and COSY correlations, with the distinguishing HMBC correlation of the aromatic proton on C-14 to C-7 in the decalin system, along with the COSY correlation of the proton on C-14 to both protons on C-7. Despite the non-equivalence of isopropyl methyl NMR resonance signals,[139] assignment of the isopropyl methyl groups was arbitrary given their similarity in ^{1}H and ^{13}C signals and since their COSY and HMBC NMR spectra only displayed correlations to each other and C-15. The C-19 methyl group was distinguished by the downfield ^{1}H and ^{13}C NMR signals indicating proximity to the nearby electron-withdrawing carboxyl group. Both C-19 and C-20 possessed the previously described podocarpic acid-like HMBC correlations. Decalin ring signals were assigned based on COSY correlations which generally identified the protons on the immediate carbon neighbour(s), with the exceptions of the overlaid ^{1}H NMR multiplet signals at 2.01 and 2.16 ppm.

The relative configuration of the decalin ring junction and the carboxylic acid and methyl group on C-4 was unable to be determined by NOESY. The 2D NOSEY spectrum (see **Appendix D**) displayed insufficient correlation data from the methyl groups and from H-5 to unequivocally assign relative correlation around the decalin ring and C-4. The 2D NOSEY spectrum displayed a correlation between H-19 to one of either H-1b or H-6b. Under the assumption of a *trans* decalin ring, justified given the similarity in chemical shifts between **48** and podocarpic acid (**27**), this correlation could be interpreted as either a 1,3 diaxial interaction with H-6b or a 1,4 pseudo-diaxial interaction with H-1b. One possible explanation for the inconclusive NOSEY experiment is that the compound is dimerising in solution due to the presence of the phenol and carboxylic acid moieties. Further NOSEY experiments are required to establish the relative configuration of **48** and would benefit from a longer run time with a drier sample and rerunning the sample in deuterated methanol to prevent potential dimerisation.

4.7 Bioassay

The bioassay provided by our collaborators at the Victoria University of Wellington School of Biological Sciences only became available after the completion of the experimental component of this study, so the results were not available to direct fractionation and isolation efforts of potential phytoestrogens.

A small number of extracts and fractions were submitted for assessment: The water, methanol, and chloroform crude extracts of the foliage, seed, unfertilised ovules, and berries (overripe) along with the 80% acetone/water fractions of methanol extracts of foliage and seeds. In addition, isolated podocarpic acid and the phthalate contaminant from the acetone used in the cyclic loading procedure were also submitted. The yeast bioassay utilised yeast strain w303a transfected with hER1 and oestrogenic responses were measured colourimetrically against and E2 standard curve and classified as none, low, or high oestrogenic activity. Yeast strains expressing kER were not yet available for this study and at this stage the results are limited to hER oestrogenic responses only.

The optimum solvent for extract dissolution in order to complete bioassays was discussed with our collaborators and led to the consideration of ethanol, methanol, and dimethyl sulfoxide (DMSO). In general, ethanol was reported as the most well tolerated solvent in yeast of the three considered with maximal tolerance levels of ethanol ranging from 7 – 12%.[140] Methanol is not as well tolerated by yeast with maximal tolerance levels ranging from 5.5 – 8.0%.[141] DMSO is the least tolerated solvent of those considered with maximal tolerance levels ranging from 1 – 3%.[142] Solubility experiments on crude extracts and fractions utilising ethanol, methanol, and DMSO resulted in the observation that DMSO was the most effective solvent for full solubilisation of the greatest number of extracts and fractions. It was decided to utilise only one solvent for the first submission to the bioassay so that the results may be more readily compared. Completely dissolved extracts was preferred as it was postulated that this would generate the most reliable results, so long as the solvent concentration was tolerated by the yeast. The samples were submitted in DMSO at a concentration of 25 mg mL^{-1} (2.5%) of which all extracts and fractions

were solubilised upon gentle agitation or with the assistance of ultrasonication at low temperature (to 30 °C).

Table 10. Oestrogenic responses of all samples submitted for initial analysis by bioassay in DMSO (2.5%). Sample naming is cross-referenceable with fractionation schemes. Abbreviations: Fol – foliage, RS – rimu seed, RB – rimu berry (overripe), RUO – rimu unfertilised ovules, WE – water extract, ME – methanol extract, CE – chloroform extract, 80% – 80% acetone/water fraction of methanol extract.

Sample Number	Sample	Level of Oestrogenicity
1	DMSO blank	No
2	Podocarpic acid	Low
3	Phthalate impurity	No
4	DSH1_05 Fol_WE	High
5	DSH1_10_Fol_ME 80%	Low
6	DSH1_64_RS_ME	Low
7	DSH1_47 RS_WE	High
8	DSH1_68 RS_CE	No
9	DSH1_07_Fol_ME	High
10	DSH1_09 Fol_CE	No
11	DSH1_79_RS_ME_80% (1)	Low
12	DSH1_79_RS_ME_80% (2)	Low
13	DSH1_79_RS_ME_80% (3)	Low
14	DSH1_68_RB_CE	No
15	DSH1_64_RB_ME	No
16	DSH1_68_RUO_CE	No
17	DSH1_47_RUO_WE	High
18	DSH1_47_RB_WE	High
19	DSH1_64_RUO_ME	No

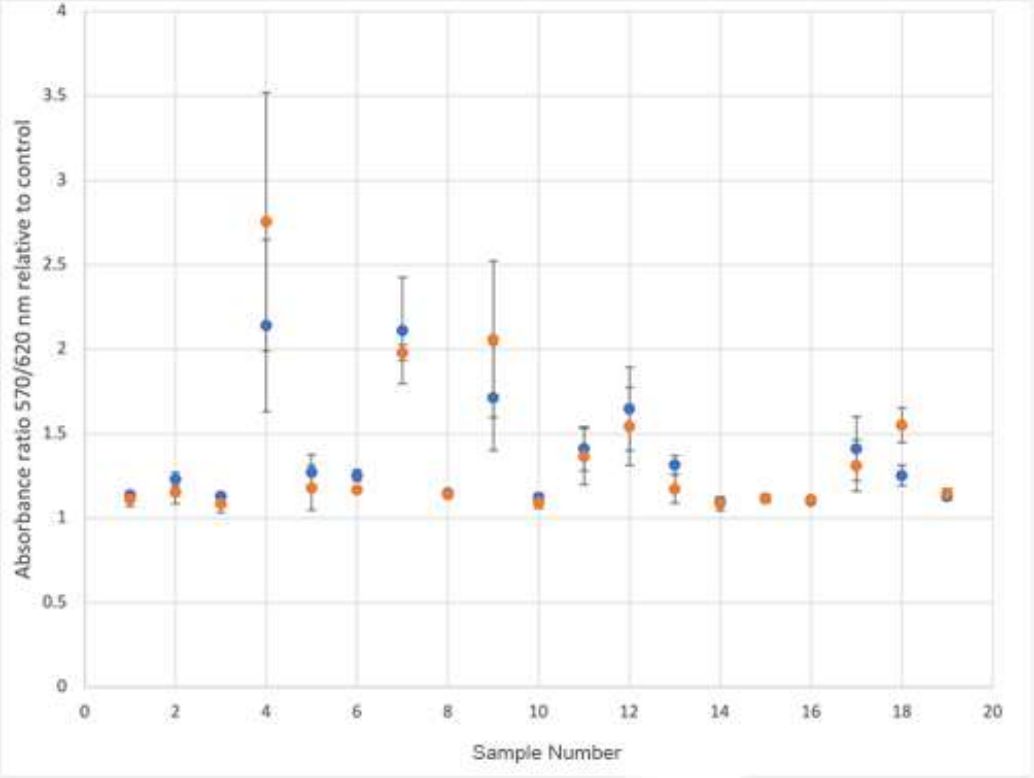

Figure 23. Oestrogenic response of the yeast bioassay to *D. cupressinum* extracts and fractions at 72 h (blue) and 96 h (orange). Sample number correlates to **Table 10**.*

All water extracts (foliage, seeds, berries (overripe), and unfertilised ovules) displayed a high level of oestrogenic activity. Oestrogenic activity was also detected in the foliage and seed methanol extracts, and the foliage 80% acetone/water fraction. Podocarpic acid was confirmed as a weak phytoestrogen in this assay. The phthalate impurity did not show oestrogenic activity which provides greater certainty that the results are not displaying artificial positives.

* Acknowledgments to A. Prof. Janet Pitman and Amey Hughes for bioassay results.

4.8 Summary

The extraction and fractionation of rimu foliage, seeds, berries (ripe), berries (overripe), and unfertilised ovules was conducted across a range of polarities in preparation for analysis by oestrogenic bioassay. In the absence of the bioassay to guide fractionation, spectroscopic evidence of phytoestrogenic motifs was used to guide fractionation efforts.

The presence of contaminants producing artificial positive results was not initially considered as the solvents used in the laboratory are generally of analytical grade or higher. It was thought that the phthalate contamination was a result of a “bad batch” of analytical grade acetone, but subsequent experiments on other bottles of analytical grade acetone from other laboratories on-site with different batch numbers revealed that the same phthalate impurity was present. This served as a vital lesson to always consider possible sources of contamination and to not blindly trust the purity of reagents from suppliers by first experimentally confirming their suitability before use.

Flash chromatography was used to separate compounds of interest based upon spectroscopic motifs. Analysis by TLC was used to identify possible steroidal terpenoids by staining with vanillin and to inform solvent selection and gradients for flash chromatography based on R_f values of spots of interest.

Isolation of **48** was driven by structural similarity to the known phytoestrogen podocarpic acid (**27**) and was purified by HPLC and structurally characterised by 2D NMR spectroscopy and high-resolution MS. Additional experiments are required in order to determine the relative configuration of **48** to identify the compound as either lambertic acid (**49**) or dehydroabietic acid (**50**).

Bioassay results have confirmed the presence of phytoestrogens which interact with hER in the water extracts of all analysed rimu plant materials, and in the methanol extracts of rimu foliage and seeds. Further work is required to isolate these oestrogenic compounds and a yeast bioassay expressing kER will help elucidate if these are relevant to kākāpō.

Chapter 5. Conclusion

The main objectives of this study were to analyse rimu plant materials consumed by kākāpō to assess if the constituents had a role in the birds fecundity. Work completed was to assess rimu extracts for carbohydrate content and composition, iodine content, and assess spectroscopically and by bioassay for phytoestrogens; all of which may affect kākāpō fecundity or inform supplementary feed formulations.

Novel data on the monomer compositions of the simple and complex carbohydrates present in rimu berries was produced. Of particular relevance was the composition of the warm water soluble fraction of the AIR where arabinose and mannose were detected as the major monomer species secondary to glucose with molar percentages of 12.7% and 12.5%, respectively. This result suggests the presence of prebiotic glucomannan and galactoglucomannan species. In addition, the composition of the warm water insoluble fraction of the AIR displayed xylose as the major monomer species present secondary to glucose, with molar percentages of 18.7% and 15.7% in the MeHCl/TFA and H_2SO_4 hydrolysates, respectively. The presence of xylans and xylooligosaccharides has nutritional relevance for the prebiotic properties of rimu berries. This data will assist in the characterisation of rimu berries in terms of their nutrition, prebiotic potential, and phylogenicity. This work represents the initial stages of an in-depth carbohydrate analysis. Future work could examine these complex carbohydrates for their structural identities, linkage configurations, and presence of substituents in order to better understand their nutritional impacts, including prebiotic potential and effects on digestion, or suitability for inclusion in supplementary feed formulations for kākāpō.

The iodine content of rimu plant structures was analysed due to the importance of iodine levels for thyroid function and reproductive ability. The analysed samples were found to have high iodine levels. Rimu berries were found to have iodine levels between 150 – 300 ng g^{-1} which is much higher than the average iodine levels found in fresh fruit and vegetables (18 – 70 ng g^{-1}). Rimu seeds had iodine levels (210 ng g^{-1}) similar to the average iodine levels found in nuts and seeds. Rimu foliage

displayed very high levels of iodine (840 ng g^{-1}) which exceeds the average iodine content of most food groups. Future work could examine larger geographical areas to analyse the iodine content of soil and rimu plant structures on the island sanctuaries where kākāpō currently reside. A better understanding of the iodine content in these environments and the thyroid health of kākāpō could be examined to help understand if controlling iodine intake could be beneficial to kākāpō health and reproduction.

The presence of phytoestrogens was detected in water and methanol extracts of rimu plant structures which are eaten by kākāpō. Although, the identity of these phytoestrogens remains unknown. Future work will be able to isolate these compounds using spectroscopic techniques guided by oestrogenic bioassay. The impact of the phytoestrogens present in rimu on kākāpō fecundity can be studied by examining the oestrogenicity of these compounds when interacting with the structurally distinct kākāpō oestrogen receptor. The known rimu phytoestrogen, podocarpic acid, was not detected in any of the plant structures that kākāpō consumes, but the structurally similar compound **48**, was isolated from ripe rimu berries. Spectroscopic evidence remains for other structurally similar compounds to podocarpic acid in various fractions of methanol extracts.

The presence of phytoestrogens in rimu berries has previously been hypothesised to act as a trigger for kākāpō to synchronise their reproductive efforts with the mast fruiting of their food trees. The evidence of phytoestrogenic activity produced by this study gives more credibility to this hypothesis. Future work is warranted to better understand what governs the reproductive cycle of kākāpō. The continuation of this work could have impacts on conservation efforts and perhaps even provide a way for conservationists to improve breeding success and survivability of kākāpō.

Ultimately, we need to do everything we can if we are to help save this remarkable species from extinction. No amount of research, supplementary feeding, or hormonal stimulation can substitute providing large areas of mature native forest that are free from predators available for kākāpō to make their homes. In the meantime, studies

such as this hope to improve our ability to care for the precious remaining individuals through better understanding of their needs, behaviour, and biology.

Chapter 6. Experimental

6.1 General

500 MHz NMR spectra were obtained using a Bruker spectrometer equipped with an Advance 500 probe. 400 MHz NMR spectra were obtained using a Bruker 400 MHz NEO spectrometer equipped with a Bruker 5 mm BBI probe. Chemical shifts δ (ppm) were referenced to the residual solvent peak. NMR samples were performed in $CDCl_3$.

Positive and negative ion high resolution mass spectrometry was carried out on a Waters Xevo G2-XS Q-TOF Tandem Mass Spectrometer.

Reverse phase column chromatography was carried out using Supelco Diaion HP-20 stationary phase.

Automated column chromatography was carried out on a Buchi Flash-Pure C-850 system using prepacked silica cartridges. Detection includes ELSD and UV at 254, 265, 280, and 320 nm.

TLC analysis was carried out with Merck normal-phase silica gel 60 matrix F254 plates using a mobile phase of 5% MeOH/CH_2Cl_2. The developed plates were analysed by UV 254 and 365 nm. TLC plates visualised by dipping in a solution of 5% (v/v) H_2SO_4 (conc.)/MeOH, then a solution of 0.1% vanillin/EtOH (% wt/vol) immediately prior to heating.

HPLC was preformed using an Agilent 1260 Infinity II preparative solvent delivery module with 50 mL pump heads and equipped with an Agilent 1290 Infinity II open-bed fraction collector. Solvents used were of LCMS grade.

Water was purified through a Pentair GRO-75EN and for dialysis or HPAEC further purified through a Sartorius Arium pro UV with a final 0,22um filtration giving filtered type-2 water.

HPAEC-PAD analysis was preformed using a Dionex ICS-5000$^+$.

GCMS analysis was preformed using an Agilent 6890N with Agilent 5973 Mass Selective Detector.

UV absorbances were read with a Molecular Devices SpectraMax M3.

6.2 Samples of Berries, Foliage, Seeds, and Unfertilised Ovules of *Dacrydium cupressinum*

Table 11. Overview of plant materials.

Plant Material Sample	Collection Date	Collection Location	Quantity Used for Extraction (g) (fresh)	For Use in Assay
Foliage	10/10/2016	Ōrongorongo Valley	63.92	Phytoestrogen
			19.55	Iodine
Berry (overripe)*	May-16	Anchor Island Western Loop	43.76	Phytoestrogen
			35.62	Carbohydrate
			24.67	Iodine
Seed	20/02/2016	Anchor Island Hutt	13.75	Phytoestrogen
			18.51	Iodine
Unfertilised ovules	06/12/2016	Anchor Island Hutt	23.56	Phytoestrogen
Berry (ripe)	15/03/2019	Anchor Island Southwest	46.79	Phytoestrogen
			29.3	Iodine

*Overripe Berries from Anchor Island displayed some evidence of decomposition. Non-decaying berries were selected for extraction.

6.3 Extraction of Berries of *Dacrydium cupressinum* for Carbohydrate Analysis

Berries (ripe) (32.71 g) from Anchor Island Southwest were frozen in $N_{2\,(l)}$ and ground to a fine consistency in a mortar and pestle and transferred to a Schott bottle. EtOH (70 mL) was added, and the Schott bottle was submerged in an ice bath at 4 °C and the contents gently stirred by magnetic flea for 4 hours. The solution was centrifuged at 3000 rpm for 11 minutes at 20 °C. The pellets were washed with 80% EtOH/H_2O (60 mL), vortexed, then centrifuged at 3000 rpm for 5 minutes at 20 °C. The alcohol insoluble residue (AIR) pellets produced a brown clumping powder/paste that weighed 22.4730 g (sample code: AIR).

The supernatant of the wash was added to the supernatant of the first centrifugation. The combined supernatants were filtered through celite into a round-bottomed flask. EtOH and H_2O were removed by rotary evaporation and lyophilisation, respectively. The dried sample was a yellow/brown coloured brittle solid. The dried supernatant was dissolved in H_2O (30 mL) then filtered through a Whatman glass microfibre filter GF/D 2.7 µm. The filtrate was collected and lyophilised producing a yellow/brown brittle solid with a recovered mass of 0.5187 g (sample code: SS). The AIR (19.552 g) was extracted in H_2O (200 mL) at 80 °C for 1 hour with gentle stirring. After cooling to room temperature, the solution was centrifuged twice at 5000 rpm for 20 minutes at 20 °C. The mass recovery of the pellets from the warm water extraction was 5.1089 g of a brown brittle solid (sample code: WWE_Insol). The supernatant of the warm water extraction was concentrated by rotary evaporation to a volume of approximately 40 mL, then poured into dialysis tubing (6–8 kDa cut-off, 45 cm). The dialysis tubing was sealed and placed in a large container with H_2O (4 L) and stirred gently at 5 °C for 4 days, replacing the H_2O in the container twice per day. The contents of the dialysis tubing were emptied and centrifuged at 5000 rpm for 30 minutes at 20 °C. The supernatant was decanted into a round-bottomed flask and lyophilised overnight to produce a fluffy white solid material with a mass recovery of 0.0911 g (sample code: WWE_Sol). The pellets were lyophilised to produce a white solid with a mass recovery of 0.0584 g.

6.4 Analysis of Monosaccharides in MeHCl/TFA Hydrolysates using HPAEC-PAD Chromatography

A 12 sugar mix standard including fucose, galactosamine.HCl, glucose, xylose, ribose, galacturonic acid.Na, rhamnose, arabinose, glucosamine.HCl, galactose, mannose, and glucuronic acid was prepared by first drying aliquots of sugars at 40 °C over P_2O_5. The dried neutral sugars were accurately weighted to generate 10 mg mL^{-1} solutions, and acidic sugars were prepared to make 20 mg mL^{-1} solutions in H_2O. A standard mix was prepared by combining each sugar solution (100 µL) lyophilising the mixture, then redissolution in H_2O (1 mL) resulting in a solution of neutral sugars (1 mg mL^{-1}), and acidic sugars (2 mg mL^{-1}).

Dried samples from previously described extraction of ripe rimu berries for carbohydrate analysis (SS, WWE_Sol, and WWE_Insol) (10 mg) were dissolved in H_2O (1 mL). The samples WWE_Sol and WWE_Insol required heating to 60 °C for 10 minutes to ensure complete solubility. Sample aliquots (100 µL), 12 sugar mix standard solution (100 µL), and a hydrolysis blank (H_2O 100 µL), were added to acid washed Kimax tubes in duplicate and lyophilised overnight. To each Kimax tube, Teflon tape was applied around the threads followed by addition of 3N MeHCl (500 µL). The Kimax tubes were capped tightly and incubated at 80°C for 18 hours in a dry block heater. Reagent was removed by evaporating in a gentle stream of air. Additional 3N MeHCl (500 µL) was added and evaporated to dryness. To each Kimax tube, 2.5M TFA (aq. 500 µL) was added, topped with $Ar_{(g)}$, capped tightly, and incubated at 120°C for 1 hour. The Kimax tubes were cooled to room temperature. Kimax tubes were then placed in a heating block at 40 °C and the TFA was removed under a gentle stream of air. Water (250 µL) was added to each tube and evaporated to dryness to ensure removal of residual acid. All samples were resuspended in H_2O (1 mL), vortexed, incubated at 30 °C for 30 minutes, followed by filtering through PTFE syringe filters (hydrophilic 0.20 µm). Sugar standards were diluted with H_2O to produce standard concentrations of (1) 1.25 µg mL^{-1}, (2) 2.5 µg mL^{-1}, (3) 5 µg mL^{-1}, (4) 10 µg mL^{-1}, and (5) 20 µg mL^{-1} samples for neutral sugars, and (1) 2.5 µg mL^{-1}, (2) 5 µg mL^{-1}, (3) 10 µg mL^{-1}, (4) 20 µg mL^{-1}, and (5) 40 µg mL^{-1} samples for acidic

sugars which were used to produce standard curves for monomer quantitation. All solutions for analysis were placed in HPLC vials with split septa. Aliquots (20 µL) are separated at 25 °C on a CarboPac PA-1 (4 x 250 mm) column equilibrated in 25 mM NaOH and eluted with simultaneous gradients of NaOH (25 – 10 mM from 0 – 10 minutes, then 10 – 100 mM from 10 – 30 minutes and held to 55 minutes) and sodium acetate (0 – 500 mM from 30 – 55 minutes) at a flow rate of 1 mL min^{-1} and monitored by pulsed amperometric detection using the Dionex standard carbohydrate waveform.

6.5 Analysis of Monosaccharides in Two-Stage H_2SO_4 Hydrolysates using HPAEC-PAD Chromatography

The same sugar mix and calibration data was used as in Section 6.4. A 12 sugar mix standard including fucose, galactosamine.HCl, glucose, xylose, ribose, galacturonic acid.Na, rhamnose, arabinose, glucosamine.HCl, galactose, mannose, and glucuronic acid was prepared by first drying aliquots of sugars at 40 °C over P_2O_5. Neutral sugars were prepared to make 10 mg mL^{-1} solutions, and acidic sugars were prepared to make 20 mg mL^{-1} solutions in H_2O. Each sugar solution (100 µL) was combined and lyophilised, then dissolved in H_2O (1 mL) resulting in a solution of neutral sugars (1 mg mL^{-1}), and acidic sugars (2 mg mL^{-1}).

Dried samples from material extracted from rimu berries (AIR, WWE_Insol) (2 mg) was added to acid-washed Kimax tubes (analysis completed in duplicate). Two Kimax tubes were prepared for duplicate hydrolysis blanks. 72% H_2SO_4 (125 µL) was added to the bottom of each Kimax tube. Teflon tape was added around the threads of all Kimax tubes, and the tubes were topped with $Ar_{(g)}$, sealed tightly, and incubated in a dry block heater at 30 °C for 3 hours with mixing every 30 minutes. H_2O (1.375 mL) was added to each Kimax tube. Tubes were topped with $Ar_{(g)}$, sealed tightly, and incubated in a dry block heater at 100 °C for 3 hours. Additional H_2O (500 µL) was added to each tube resulting in a 1 mg mL^{-1} solution. The samples were mixed thoroughly and filtered with PTFE filter (0.20 µm) into a new Eppendorf tube. Aliquots (50 µL) of each sample were added to HPLC vials with split septa and

H_2O (950 µL) was added. Sugar standards were diluted with H_2O to produce standard concentrations of (1) 1.25 µg mL^{-1}, (2) 2.5 µg mL^{-1}, (3) 5 µg mL^{-1}, (4) 10 µg mL^{-1}, and (5) 20 µg mL^{-1} samples for neutral sugars, and (1) 2.5 µg mL^{-1}, (2) 5 µg mL^{-1}, (3) 10 µg mL^{-1}, (4) 20 µg mL^{-1}, and (5) 40 µg mL^{-1} samples for acidic sugars which were used to produce standard curves for monomer quantitation. All solutions for analysis were placed in HPLC vials with split septa. Aliquots (20 µL) are separated at 30 °C on a CarboPac PA-1 (4 × 250 mm) column equilibrated in 25 mM NaOH and eluted with simultaneous gradients of NaOH (25 – 10 mM from 0 – 10 minutes, then 10 – 100 mM from 10 – 30 minutes and held to 55 minutes) and sodium acetate (0 – 500 mM from 30 – 55 minutes) at a flow rate of 1 mL min^{-1} and monitored by pulsed amperometric detection using the Dionex standard carbohydrate waveform.

6.6 Sucrose, D-Glucose, and D-Fructose Assay

Assay conducted using Megazyme Sucrose, D-Glucose, and D-Fructose assay kit containing buffer I (25 mL, pH 7.6) plus sodium azide (0.02% w/v) as a preservative, $NADP^+$ plus ATP, hexokinase plus glucose-6-phosphate dehydrogenase suspension, phosphoglucose isomerase suspension, D-glucose plus D-fructose standard solution (0.2 mg mL^{-1} of each sugar), and β-fructosidase (pH 4.6). Reagent solutions/suspensions were prepared as described by the assay procedure: $NADP^+$ plus ATP was dissolved in H_2O (22 mL), divided into aliquots, and stored at -10 °C. β-fructosidase was dissolved in H2O (20mL), divided into aliquots, and stored at -10 °C. Sucrose standard solution (0.5 mg mL^{-1}) was prepared by drying crystalline sucrose (0.250 g) overnight in a vacuum oven at 70 °C, then adding to a volumetric flask (500 mL) along with H_2O up to the mark. Sample from previously described extraction of ripe rimu berries for carbohydrate analysis (SS, 1 mg) was dissolved in H_2O (1 mL). The assay was conducted with a D-glucose/D-fructose standard and blank, along with a sucrose standard and blank. The SS samples were analysed in triplicate for both sucrose and D-glucose/D-fructose assays (6 samples total).

The procedure was followed as per the provided assay instructions: β-fructosidase (0.20 mL) was added to the sucrose blank, sucrose standard, and SS sample test tubes. Sample solution (0.10 mL) (SS, sucrose standard, and D-glucose/D-fructose) was added to test tubes, excluding the blanks. The tubes were vortexed and incubated in a water bath at 30 °C for 5 minutes. H_2O was added to the sucrose blank (2.00 mL), sucrose standard (1.90 mL), SS sucrose assay samples (1.90 mL), D-glucose/D-fructose blank (2.20 mL), D-glucose/D-fructose standard (2.10 mL), and SS D-glucose/D-fructose assay samples (2.10 mL). Buffer solution I (0.10 mL), and $NADP^+$/ATP solution (0.10 mL) was added to all tubes. The tubes were vortexed and absorbances (340 nm) of the solutions was read after 5 minutes. The reaction was started by the addition of hexokinase plus glucose-6-phosphate dehydrogenase suspension (0.02 mL) to all tubes. The tubes were mixed and absorbances (340 nm) of the solutions was read after 5 minutes. Phosphoglucose isomerase suspension (0.02 mL) was added to the D-glucose/D-fructose blank, D-glucose/D-fructose standard, and SS D-glucose/D-fructose assay samples. The tubes were vortexed and absorbances (340 nm) of the solutions was read after 10 minutes.

6.7 Total Starch Assay

Assay conducted using Megazyme Total Starch assay kit (Amyloglucosidase/ α-amylase method) following the procedure for the AOAC Official Method 996.11.

MOPS buffer (50 mM, pH 7.0) plus calcium chloride (5 mM), and sodium azide (0.02% w/v) was prepared by adding 2.388 g of MOPS.Na to H_2O (200 mL). The solution was adjusted to pH 7.01 with 1M HCl (6.3 mL). $CaCl_2$ (330 mg) and NaN_3 (45.6 mg) were dissolved in the solution and H_2O (21.2 mL) was added. Sodium acetate buffer (200 mM, pH 4.5) was prepared by adding glacial acetic acid (11.8 mL) to H_2O (900 mL) in a volumetric flask (1 L). 1M NaOH (80 mL) was added to adjust the pH to 4.5, and volume adjusted to 1L with H_2O. GOPOD reagent was prepared by adding the contents of the GOPOD reagent buffer to a volumetric flask (1 L) and making up to the mark with H_2O. GOPOD reagent enzymes were dissolved in the GOPOD reagent buffer solution (20 mL) and then this solution was returned to

the volumetric flask. The GOPOD reagent was divided into 10x aliquots (100 mL) and stored at -20 °C.

Duplicate samples from previously described extraction of ripe rimu berries for carbohydrate analysis (AIR, WWE_Insol, and WWE_Sol) (10.0 mg), and starch control (10.0 mg, 83% starch content) were added to Kimax tubes. Aqueous ethanol (80% v/v, 20 µL) and anhydrous DMSO (200 µL) was added, and the tubes were vortexed. Thermostable α-amylase diluted 30-fold in MOPS buffer (50 mM, pH 7.0) (300 µL, 30 U) was added and the tubes were vortexed and then put in a boiling water bath for 6 minutes with further mixing at 2 minute intervals. The tubes were cooled to 50 °C and sodium acetate buffer (400 µL, 200 mM, pH 4.5) and amyloglucosidase (10 µL, 2 U) were added. The tubes were vortexed before being incubated at 50 °C for 30 minutes. H_2O (5 mL) was added to each tube and the solutions were filtered through syringe filters (0.45 µm) into volumetric flasks (10.0 mL) and made up to the mark with H_2O. The same procedure without the enzymes was repeated for all samples (AIR, WWE_Insol, and WWE_Sol) as a no-enzyme control for determination of free glucose. Sodium acetate buffer (410 µL, 200 mM, pH 4.5) was used in the no-enzyme control samples. GOPOD reagent (3.0 mL) was added, and tubes were vortexed and incubated at 50 °C for 20 minutes. The absorbances (510 nm) of the solutions was read against reagent blanks.

6.8 Extraction of Berries, Foliage, and Seeds of *Dacrydium cupressinum* for Iodine Analysis

Dry KI (overnight lyophilisation, 5.0 mg) was dissolved in water (volumetric flask, 500.0 mL) to produce a bulk solution (0.01 mg mL^{-1}). An aliquot of bulk solution (5.0 µL) was added to a volumetric flask (50 mL) and made up to the mark with aqueous tetramethylammonium hydroxide (TMAH, 25%) to make a spiking solution with a concentration of 1 ng mL^{-1}. Lyophilised plant material (100.0 mg) from berries (ripe), berries (overripe), foliage, and seeds were weighed into falcon tubes in triplicate (duplicate samples and spiked sample). To the duplicate samples and a blank sample, TMAH (2.5 mL) was added. To spiked samples, TMAH spiked with KI at 1

ng mL^{-1} (2.5 mL) was added. The lids of all falcon tubes were screwed on tightly and the vessels were weighed. The lids were sealed with electrical tape, and the tubes were incubated for 20.5 hours at 60 °C. The tubes were allowed to cool, and the electrical tape was removed. The vessels were weighed again to ensure no loss from evaporation. Loss was found to be minimal (0.01 – 0.1%). The tubes were centrifuged at 3000 rpm for 10 minutes at 20 °C. The supernatants (1 mL) were transferred to vials for submission for assay by ICP-MS. The iodine was quantified by ICP-MS at the Campbell Microanalytical Laboratory at the University of Otago by Dr. Malcolm Reid.

6.9 Extracts of Berries, Foliage, Seeds, and Unfertilised Ovules of *Dacrydium cupressinum* for Spectrographic and Bioassay Guided Search for Phytoestrogens

6.9.1 Sequential Double Extractions in Water, Methanol, and Chloroform:

Foliage (63.92 g), berry (overripe) (43.76 g), seed (13.75), and unfertilised ovule (23.56 g) samples of fresh plant material were frozen in $N_{2\,(l)}$ (~ -196 °C) and ground to a fine consistency in a mortar and pestle. Plant material was transferred to individual Schott bottles. H_2O (300 mL) was added to each. The bottles were stirred gently overnight at room temperature. The liquid was decanted through a fine cloth filter (~1 mm pore size) and collected. The plant material and cloth filter were returned to the Schott bottle for a second extraction in H_2O (300 mL) under the same conditions. The plant material was collected, frozen, and lyophilised to remove any water present before proceeding with further extractions. This process was repeated for sequential double extractions in MeOH (2 × 300 mL), and $CHCl_3$ (2 × 300 mL). The H_2O extracts were centrifuged at 4000 rpm for 30 min at 20 °C. The supernatant was decanted into a round-bottomed flask and frozen in a bath of $(CH_3)_2CO/CO_{2\,(s)}$ (~ -77 °C) and lyophilised overnight. Recovered masses for H_2O extracts were 6.02 g for foliage, 3.21 g for berries (overripe), 0.40 g for seeds, and 1.41 g for unfertilised ovules. The MeOH and $CHCl_3$ extracts were filtered through Whatman #4 filter paper and concentrated to dryness. The MeOH extracts generated dried material: 2.75 g

for foliage, 1.88 g for berries (overripe), 0.39 g for seeds, and 0.66 g for unfertilised ovules. Recovered masses for $CHCl_3$ extracts were 0.67 g for foliage, 1.11 g for berries (overripe), 0.16 g for seeds, and 0.16 g for unfertilised ovules.

6.9.2 Double Extraction of Ripe Berries in Methanol

Berries (ripe) (46.79 g) from Anchor Island Southwest were frozen in $N_{2\,(l)}$ (~ -196 °C) and ground to a fine consistency in a mortar and pestle and transferred to a Schott bottle. MeOH (300 mL) was added and was stirred gently overnight at room temperature. The berries were filtered through Whatman #4 filter paper and returned to the Schott bottle with additional MeOH (300 mL) for a second overnight extraction with gentle stirring at room temperature. The MeOH extracts were combined, filtered, and concentrated to dryness with a mass recovery of 4.05 g.

6.10 Cyclic Loading Procedure for Fractionation of *Dacrydium cupressinum* Crude Extracts

HP20 beads (CV = 100 mL for foliage, 100mL for berries (ripe), 80 mL for berries (overripe), 10 mL for seeds, and 40 mL for unfertilised ovules) were loaded into a suitably sized column and were conditioned with H_2O (3 CV), followed by acetone (3 CV), then MeOH (3 CV). MeOH extracts (2.75 g foliage, 4.05 g berries (ripe), 1.88 g berries (overripe), 0.39 g seeds, and 0.66 g unfertilised ovules) were dissolved in minimal MeOH and ran through the column at a flow rate of approximately 10 mL min^{-1}. The eluent was collected and diluted with H_2O (1 CV) then passed through the column again. The eluent was collected and diluted with H_2O (2 CV) and passed through the column and collected, followed by washing the column with H_2O (3 CV). The columns were eluted with 3 CV of (1) 20% acetone/H_2O, (2) 40% acetone/H_2O, (3) 60% acetone/H_2O, (4) 80% acetone/H_2O, (5) 100% acetone. To remove H_2O from the eluents of the 20 – 80% acetone/H_2O fractions, HP20 beads (CV = 0.5 initial CV = 50 mL for foliage, 50mL for berries (ripe), 40mL for berries (overripe), 5 mL for seeds, and 20 mL for unfertilised ovules) were loaded into a column and

conditioned with H_2O (3 CV), followed by acetone (3 CV), then MeOH (3 CV). The 20 – 80% acetone/H_2O fractions were diluted with H_2O (6 CV) and passed through the column. The eluent was further diluted with H_2O (12 CV) and passed through the column. The columns were then eluted with acetone (3 CV). The mass recovered were:

- Foliage fractions 20%: 50 mg, 40%: 400 mg, 60%: 210 mg, 80%: 725 mg, and 100%: 730 mg.
- Berries (ripe) fractions 20%: 145 mg, 40%: 109 mg, 60%: 61 mg, 80%: 315 mg, and 100%: 970 mg.
- Berries (overripe) fractions 20% and 40% combined: 13.2 mg, 60%: 27.2 mg, 80%: 73.7 mg, 100%: 595.6 mg.
- Seed fractions 20%: 1.1 mg, 40%: 3.1 mg, 60%: 8.6 mg, 80%: 24.9 mg, and 100%: 160 mg.
- Unfertilised ovule fractions 20%: 4.0 mg, 40%: 83.8 mg, 60%: 39.6 mg, 80%: 95.6 mg, and 100%: 180 mg.

6.11 Further Fractionation of 80% Me_2CO/H_2O Fractions of *Dacrydium cupressinum* Extracts

6.11.1 80% Me_2CO/H_2O Fraction of Foliage

The 80% Me_2CO/H_2O fraction of foliage (665 mg) was dissolved in 50% MeOH/DCM (2.75 mL) and dry loaded onto silica. The material was separated on Buchi Flashpure FP Si 24g column (25 µm) with a flow rate of 32 mL min^{-1}, and equilibration of 3.0 CV. Run length was 17.2 CV. Mobile phase consisted of: (1) 90% hexane/10% DCM for 3 CV, (2) 95% DCM/5% ethyl acetate for 3 CV, (3) ethyl acetate for 3 CV, (4) 83% ethyl acetate/ 17% MeOH for 3 CV, and (5) MeOH for 5.2 CV. All of the eluent was collected into test tubes. Test tubes were combined to isolate ELSD and UV peaks from the trace producing 5 fractions (F1–F5). Recovered material: (F1) 33 mg, (F2) 109 mg, (F3) 208 mg, (F4) 115 mg, and (F5) 148 mg.

Fractions F2 (sample code: Fol_ME_80%_F2) and F3 (sample code: Fol_ME_80%_F3) were selected for further fractionation.

6.11.1.1 Fol_ME_80%_F2

Sample Fol_ME_80%_F2 (58.2 mg) was dissolved in 50% MeOH/DCM (1.00 mL) and dry loaded onto silica. The material was separated on Buchi flash pure FP Si 12g column (25 µm) with a flow rate of 30 mL min^{-1}, and equilibration of 6.0 CV. Run length was 32.6 CV. Mobile phase consisted of: (1) A gradient from 20% hexane/80% DCM to 100% DCM over 5 CV, (2) a gradient from 95% DCM/5% ethyl acetate to 75% DCM/25% ethyl acetate over 11.2 CV, (3) 5% DCM/95% ethyl acetate for 4 CV. All the eluent was collected into test tubes. Test tubes were combined to isolate ELSD and UV peaks from the trace producing six fractions (F1–F6). Masses recovered from each fraction were: (F1) 2.4 mg, (F2) 28.9 mg, (F3) 11.6 mg, (F4) 2.8 mg, (F5) >1.0 mg, and (F6) >1.0 mg Fractions F2 and F3) were combined (sample code: Fol_ME_80%_F2_F2&3) for further fractionation.

6.11.1.1.1 Fol_ME_80%_F2_F2&3

Sample Fol_ME_80%_F2_F2&3 (40.5mg) was dissolved in 50% MeOH/DCM (1.00 mL) and dry loaded onto silica. The material was separated on Buchi Flashpure FP Si 12g column (25 µm) with a flow rate of 30 mL min^{-1}, and equilibration of 6.0 CV. Run length was 24.9 CV. Mobile phase consisted of: (1) A gradient from 80% hexane/20% DCM to 100% DCM over 15.8 CV, (2) 100% DCM for 3 CV, (3) mistakenly, a gradient from 100% DCM to 50% hexane/50% DCM over 6 CV (supposed to use 50% DCM/50% ethyl acetate). All the eluent was collected into test tubes. Test tubes were combined to isolate ELSD and UV peaks from the trace producing five fractions (F1–F5). The mass in each fraction was: (F1) <1.0 mg, (F2) 11.2 mg, (F3) 5.0 mg, (F4) 6.6 mg, and (F5) 3.8 mg. Fraction F2 (sample code: Fol_ME_80%_F2_F2&3_F2) was selected for further fractionation.

6.11.1.1.1.1 Fol_ME_80%_F2_F2&3_F2

Sample Fol_ME_80%_F2_F2&3_F2 (11.2 mg) was dissolved in 50% MeOH/DCM (1.00 mL) and dry loaded onto silica, followed by freeze drying to ensure full removal of MeOH which was suspected to be the cause of poor chromatographic separation in the prior separation. The material was separated on Buchi Flashpure FP Si 12g column (25 µm) with a flow rate of 30 mL min^{-1}, and equilibration of 6.0 CV. Run length was 24.9 CV. Mobile phase consisted of: (1) A gradient from 80% hexane/20% DCM to 100% DCM over 15.8 CV, (2) 100% DCM for 3 CV, (3) a gradient from 100% DCM to 50% DCM/50% ethyl acetate over 6 CV. All of the eluent was collected into test tubes. Test tubes were combined to isolate ELSD and UV peaks from the trace producing five fractions (F1–F5). Fraction mass recoveries: (F1) <1.0 mg, (F2) <1.0 mg, (F3) 5.5 mg, (F4) 1.8 mg, and (F5) 2.4 mg.

6.11.1.2 Fol_ME_80%_F3

Sample Fol_ME_80%_F3 (208 mg) was dissolved in 50% MeOH/DCM (2.00 mL) and dry loaded onto silica. The material was separated on Buchi Flashpure FP Si 24g column (25 µm) with a flow rate of 32 mL min^{-1}, and equilibration of 6.0 CV. Run length was 36.0 CV. Mobile phase consisted of: (1) A gradient from 100% hexane to 100% DCM over 12.5 CV, (2) 100% DCM for 1 CV, (3) mistakenly, a gradient from 100% DCM to 10% hexane/90% DCM over 8.4 CV (supposed to be 90% DCM/10% ethyl acetate), (4) a gradient from 20% DCM/80% ethyl acetate to 100% ethyl acetate over 13.9 CV. All of the eluent was collected into test tubes. Test tubes were combined to isolate ELSD and UV peaks from the trace producing seven fractions (F1–F7). Material from each solvent evaporated fraction was recorded: (F1) 25.0 mg, (F2) 16.1 mg, (F3) 63.7 mg, (F4) 36.4 mg, (F5) 9.3 mg, (F6) 15.6 mg, (F7) 1.8 mg.

6.11.2 80% Me_2CO/H_2O Fractions of Berries (ripe)

The 80% Me_2CO/H_2O fraction of berries (ripe) (315 mg) was dissolved in 50% MeOH/DCM (2.00 mL) and dry loaded onto silica. The material was separated on

Buchi flash pure FP Si 24g column (25 µm) with a flow rate of 32 mL min^{-1}, and equilibration of 6.0 CV. Run length was 28.2 CV. Mobile phase consisted of: (1) 90% hexane/10% DCM for 5 CV, (2) 95% DCM/5% ethyl acetate for 5 CV, (3) ethyl acetate for 5 CV, (4) 80% ethyl acetate/ 20% MeOH for 5 CV, and (5) MeOH for 8.2 CV. All of the eluent was collected into test tubes. Test tubes were combined to isolate ELSD and UV peaks from the trace producing eight fractions (F1–F8). Recovered masses: (F1) 2.2 mg, (F2) 53.8 mg, (F3) 40.6 mg, (F4) 17.2 mg, (F5) 23.6 mg, (F6) 18.4 mg, (F7) 1.6 mg, (F8) 1.6 mg. Fraction F3 (sample code: Berries (ripe)_ME_80%_F3) was selected for further fractionation.

6.11.2.1 Berries (ripe)_ME_80%_F3

Sample Berries (ripe)_ME_80%_F3 (40.6 mg) was dissolved in 50% MeOH/DCM (1.00 mL) and dry loaded onto silica. The material was separated on Buchi Flashpure FP Si 12g column (25 µm) with a flow rate of 30 mL min^{-1}, and equilibration of 6.0 CV. Run length was 30.0 CV. Mobile phase consisted of: (1) hexane for 7.5 CV, (2) a gradient from 100% hexane to 100% DCM over 7.5 CV, (3) a gradient from 100% DCM to 100% ethyl acetate over 10.0 CV, (4) a gradient from 100% ethyl acetate to 80% ethyl acetate/20% MeOH over 2.5, (5) MeOH for 8.2 CV. All the eluent was collected into test tubes. Test tubes were combined to isolate ELSD and UV peaks from the trace producing fourteen fractions (F1–F14). The mass in each fraction was: (F1) <1.0 mg, (F2) <1.0 mg, (F3) 7.8 mg, (F4) <1.0 mg, (F5) <1.0 mg, (F6) 3.4 mg, (F7) 9.0 mg, (F8) 3.4 mg, (F9) 3.0 mg, (F10) 1.2 mg, (F11) 1.0 mg, (F12) <1.0 mg, (F13) 3.1 mg, (F14) <1.0 mg. Fraction F6 (sample code: Berries (ripe)_ME_80%_F3_F6) was selected for purification by HPLC.

6.11.3 80% Me_2CO/H_2O Fractions of Berries (overripe), Seeds, and Unfertilised Ovules

The 80% Me_2CO/H_2O fraction of berries (overripe) (70 mg), seeds (24.9 mg), and unfertilised ovules (70.6 mg) were separately dissolved in 50% MeOH/DCM (2.00

mL) and dry loaded onto silica. The materials were separated on Buchi Flashpure FP Si 12g column (25 µm) with a flow rate of 30 mL min^{-1}, and equilibration of 6.0 CV. Run length was 23.0 CV. Mobile phase consisted of: (1) hexane for 5.0 CV, (2) a gradient from 100% hexane to 100% DCM over 5.0 CV , (3) a gradient from 100% DCM to 100% ethyl acetate over 5.0 CV, (4) a gradient from 100% ethyl acetate to 100% MeOH over 5.0 CV, and (5) MeOH for 3.0 CV. All the eluent was collected into test tubes. Test tubes were combined to isolate ELSD and UV peaks from the trace. The masses recovered in each fraction was:

- Berries (overripe) produced thirteen fractions (BF1–BF13). (BF1) 2.2 mg, (BF2) 2.6 mg, (BF3) <1.0 mg, (BF4) <1.0 mg, (BF5) 10.4 mg, (BF6) 3.4 mg, (BF7) 1.0 mg, (BF8) <1.0 mg, (BF9) 4.2 mg, (BF10) 7.0 mg, (BF11) 6.4 mg, (BF12) 4.8 mg, and (BF13) 2.2 mg.
- Seeds produced seven fractions (SF1–SF7). (SF1) <1.0 mg, (SF2) <1.0 mg, (SF3) <1.0 mg, (SF4) <1.0 mg, (SF5) 2.8 mg, (SF6) <1.0 mg, (SF7) 1.2 mg.
- Unfertilised ovules produced eleven fractions (UF1–UF11). (UF1) 5.2 mg, (UF2) <1.0 mg, (UF3) 15.6 mg, (UF4) 1.8 mg, (UF5) <1.0 mg, (UF6) 3.8 mg, (UF7) 9.6 mg, (UF8) 5.0 mg, (UF9) <1.0 mg, (UF10) 7.2 mg, (UF11) 5.4 mg.

6.12 Purification of Berries (ripe)_ME_80%_F3_F6 by HPLC

Sample Berries (ripe)_ME_80%_F3_F6 (3.4 mg) was dissolved in MeOH (340 µL) and filtered through a HP-PTFE syringe filter (0.22 µm) into a vial. Scout runs were conducted using a Phenomenex Luna C18(2) (4.6 x 250 mm) column with 100 Å pore size and 5 µm particle size at 25 °C with a flow rate of 0.5, 0.7, and 1 mL min^{-1}. Injection volume was 20 µL. Mobile phases tested during the scout run included (1) 85% acetonitrile/15% H_2O, (2) 95% acetonitrile/5% H_2O, (3) 100% acetonitrile. For the analytical run, the method using 95% acetonitrile/5% H_2O mobile phase was selected with a flow rate of 0.5 mL min^{-1}. The method was scaled up for the semipreparative run increasing loop size from 100 µL to 500 µL, flow rate increased to 2.35 mL min^{-1}, and injection volume increased to 94 µL. Semipreparative run was conducted using a Phenomenex Luna C18(2) (10.0 x 250 mm) column with 100 Å

pore size and 5 µm particle size. The compound of interest had a retention time of 7.1 min.

6.13 GCMS of Phthalate Contaminated Samples from Cyclic Loading Procedure

The 80% acetone/water fractions of methanol extracts of foliage, berries (overripe), seeds, and unfertilised ovules were dissolved in acetonitrile to make 2 mg mL^{-1} solutions. The solutions were filtered through PTFE syringe filters (0.22 µm) and were analysed by GCMS. Measurement conditions: Agilent Technologies GC 6890N equipped with an electron impact MS detector (helium carrier gas, constant flow rate of 1 mL min^{-1}, using splitless mode) was loaded with an Agilent 29091S-433LTM HP-5ms column (length 30 m, I.D. 0.25 mm, film thickness 0.25 µm) with an inlet temperature of 250 °C and a detector temperature of 280 °C. The oven temperature was held at 50 °C for 1 minute then ramped at 25 °C min^{-1} up to 300 °C. The sample injection volume was 5 µL.

Appendix A

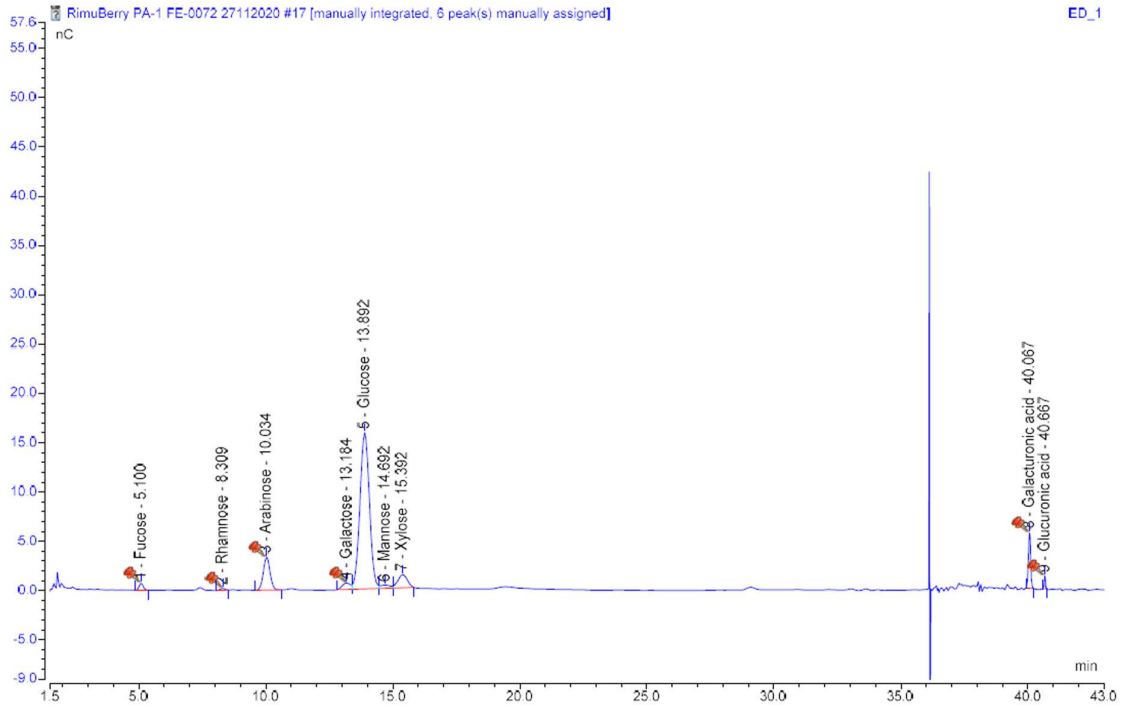

Peak No.	Peak Name	Ret.Time min	Amount	Rel.Area %	Area nC*min	Height nC	Type	Width (50%) min	Asym. EP	Resol. EP	Plates EP
1	Fucose	5.100	0.1633	1.34	0.1294	0.71	BMB*^	0.170	1.06	9.86	4983
2	Rhamnose	8.309	0.1946	0.44	0.0425	0.19	BMB*^	0.214	0.96	4.08	8353
3	Arabinose	10.034	1.6909	10.56	1.0203	3.33	BMB^	0.285	1.04	n.a.	6853
4	Galactose	13.184	0.1614	2.63	0.2545	0.66	BM *^	n.a.	n.a.	n.a.	n.a.
5	Glucose	13.892	18.7798	70.98	6.8572	15.85	M *	0.405	1.01	n.a.	6505
6	Mannose	14.692	0.7976	1.55	0.1498	0.33	M *	n.a.	n.a.	n.a.	n.a.
7	Xylose	15.392	1.0787	5.99	0.5786	1.33	MB*	0.420	n.a.	56.44	7439
8	Galacturonic acid	40.067	2.1213	5.89	0.5691	5.61	BMB*^	0.096	0.96	5.05	967555
9	Glucuronic acid	40.667	0.2279	0.62	0.0596	1.30	BMB*^	0.044	0.93	n.a.	4682301
Maximum			18.7798	70.98	6.8572	15.85		0.420	1.06	56.44	4682301
Minimum			0.1614	0.44	0.0425	0.19		0.044	0.93	4.08	4983
Sum			25.2155	100.00	9.6610	29.30					

HPAEC-PAD trace and raw data of MeHCl/TFA hydrolysis of AIR (one representative sample).

Appendix A

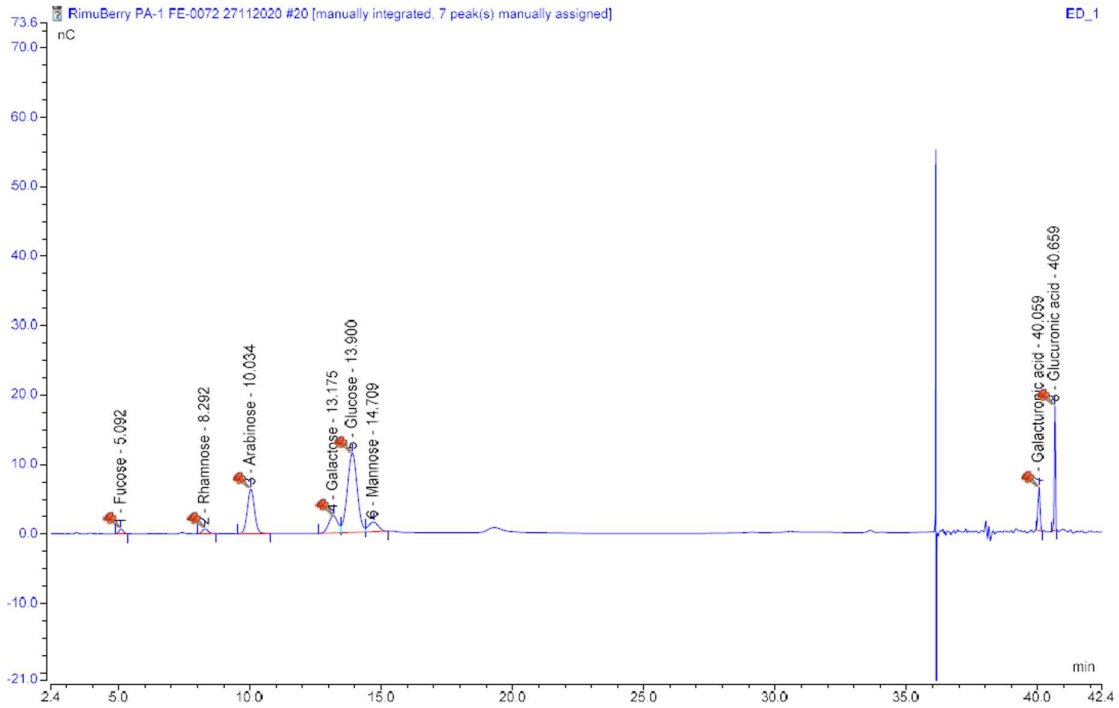

Peak No.	Peak Name	Ret.Time min	Amount	Rel.Area %	Area nC*min	Height nC	Type	Width (50%) min	Asym. EP	Resol. EP	Plates EP
1	Fucose	5.092	0.1669	1.27	0.1323	0.72	BMB*^	0.171	1.07	9.38	4930
2	Rhamnose	8.292	0.8007	1.67	0.1739	0.70	BMB*^	0.232	1.08	3.96	7095
3	Arabinose	10.034	3.4925	19.37	2.0130	6.49	BMB^	0.287	1.05	5.42	6755
4	Galactose	13.175	1.8851	9.75	1.0126	2.53	BM ^	0.396	n.a.	1.07	6131
5	Glucose	13.900	12.3647	47.77	4.9635	11.45	M *^	0.404	n.a.	1.14	6547
6	Mannose	14.709	3.3312	5.83	0.6061	1.40	MB*	0.432	n.a.	57.06	6418
7	Galacturonic acid	40.059	2.2068	5.74	0.5961	6.27	BMB*^	0.092	0.92	5.10	1049080
8	Glucuronic acid	40.659	2.5674	8.60	0.8938	17.98	BMB*^	0.047	0.93	n.a.	4172423
Maximum			12.3647	47.77	4.9635	17.98		0.432	1.08	57.06	4172423
Minimum			0.1669	1.27	0.1323	0.70		0.047	0.92	1.07	4930
Sum			26.8151	100.00	10.3913	47.53					

HPAEC-PAD trace and raw data of MeHCl/TFA hydrolysis of WWE_Sol (one representative sample).

Appendix A

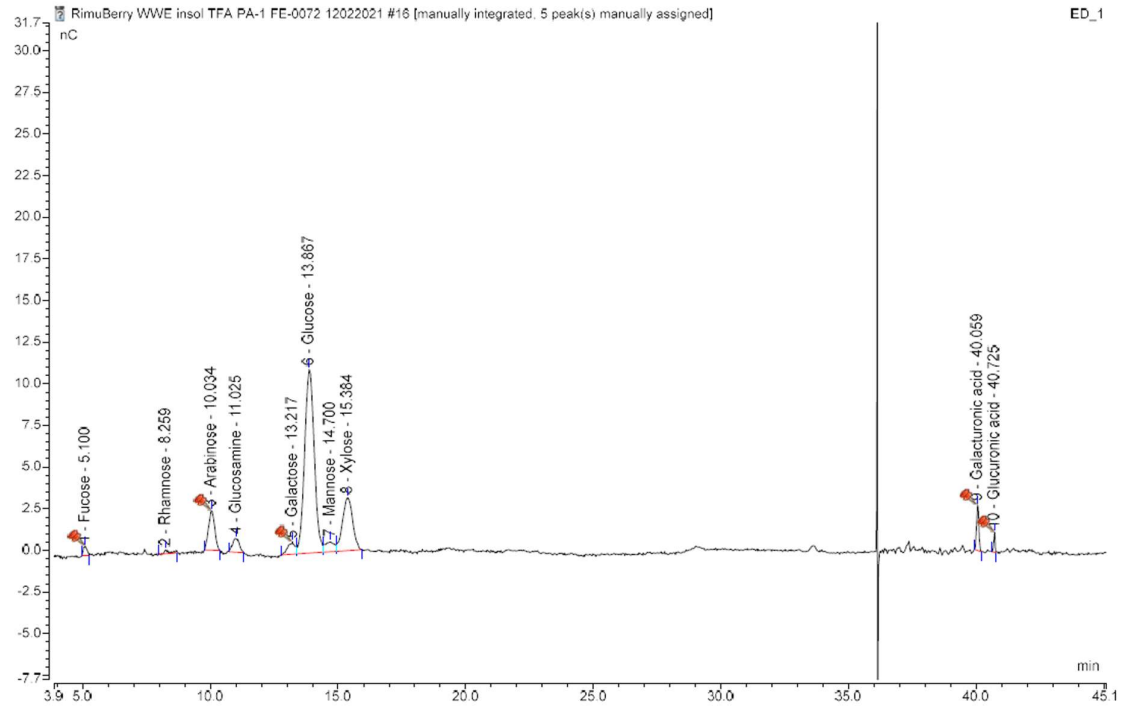

Peak No.	Peak Name	Ret.Time min	Amount	Rel.Area %	Area nC*min	Height nC	Type	Width (50%) min	Asym. EP	Resol. EP	Plates EP
1	Fucose	5.100	0.3445	1.10	0.0991	0.58	BMB*^	0.167	1.09	11.06	5137
2	Rhamnose	8.292	0.4662	0.80	0.0720	0.32	BMB*^	0.173	1.39	4.49	12741
3	Arabinose	10.034	1.7170	8.90	0.8052	2.60	BMB*^	0.285	1.17	n.a.	6869
4	Galactose	13.217	0.4461	3.61	0.3266	0.88	BM *^	n.a.	n.a.	n.a.	n.a.
5	Glucose	13.867	11.9473	55.87	5.0544	11.35	M *	0.416	n.a.	n.a.	6169
6	Mannose	14.659	1.6610	4.99	0.4513	0.91	M *	n.a.	n.a.	n.a.	n.a.
7	Xylose	15.359	4.4632	20.64	1.8674	3.77	MB*	0.459	n.a.	52.34	6214
8	Galacturonic acid	40.067	1.8598	3.41	0.3083	2.97	BMB*^	0.099	0.98	5.14	916627
9	Glucuronic acid	40.734	0.6035	0.68	0.0617	1.10	BMB*^	0.055	0.82	n.a.	3082740
Maximum			11.9473	55.87	5.0544	11.35		0.459	1.39	52.34	3082740
Minimum			0.3445	0.68	0.0617	0.32		0.055	0.82	4.49	5137
Sum			23.5086	100.00	9.0460	24.48					

HPAEC-PAD trace and raw data of MeHCl/TFA hydrolysis of WWE_Insol (one representative sample).

Appendix A

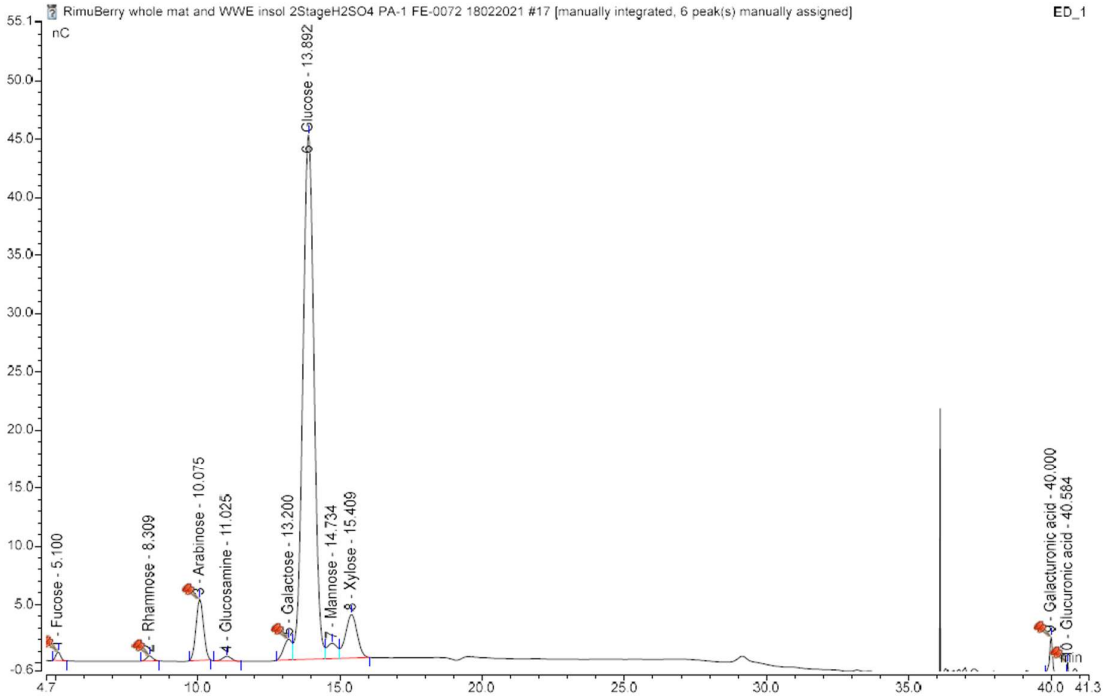

Peak No.	Peak Name	Ret.Time min	Amount	Rel.Area %	Area nC*min	Height nC	Type	Width (50%) min	Asym. EP	Resol. EP	Plates EP
1	Fucose	5.100	0.1834	0.54	0.1387	0.73	BMB*^	0.183	1.08	8.85	4304
2	Rhamnose	8.309	0.4080	0.44	0.1116	0.43	BMB*^	0.245	1.07	3.90	6386
3	Arabinose	10.075	1.2787	6.26	1.6054	5.23	BMB^	0.290	1.02	1.78	6693
4	Glucosamine	11.025	0.0863	0.55	0.1398	0.40	BMB*	0.339	1.06	n.a.	5876
5	Galactose	13.200	n.a.	2.38	0.6102	1.75	BM *^	n.a.	n.a.	n.a.	n.a.
6	Glucose	13.892	23.1281	79.16	20.2901	45.04	M *	0.420	1.01	n.a.	6047
7	Mannose	14.734	1.2484	2.11	0.5420	1.31	M *	n.a.	n.a.	n.a.	n.a.
8	Xylose	15.409	1.0793	6.91	1.7707	3.72	MB*	0.446	n.a.	53.01	6615
9	Galacturonic acid	40.000	1.0463	1.47	0.3760	3.17	BMB^	0.102	0.76	4.87	860292
10	Glucuronic acid	40.584	0.2857	0.19	0.0480	1.20	BMB*^	0.040	0.92	n.a.	5761271
Maximum			23.1281	79.16	20.2901	45.04		0.446	1.08	53.01	5761271
Minimum			0.0863	0.19	0.0480	0.40		0.040	0.76	1.78	4304
Sum			28.7441	100.00	25.6325	62.96					

HPAEC-PAD trace and raw data of two-stage H_2SO_4 hydrolysis of AIR (one representative sample).

Appendix A

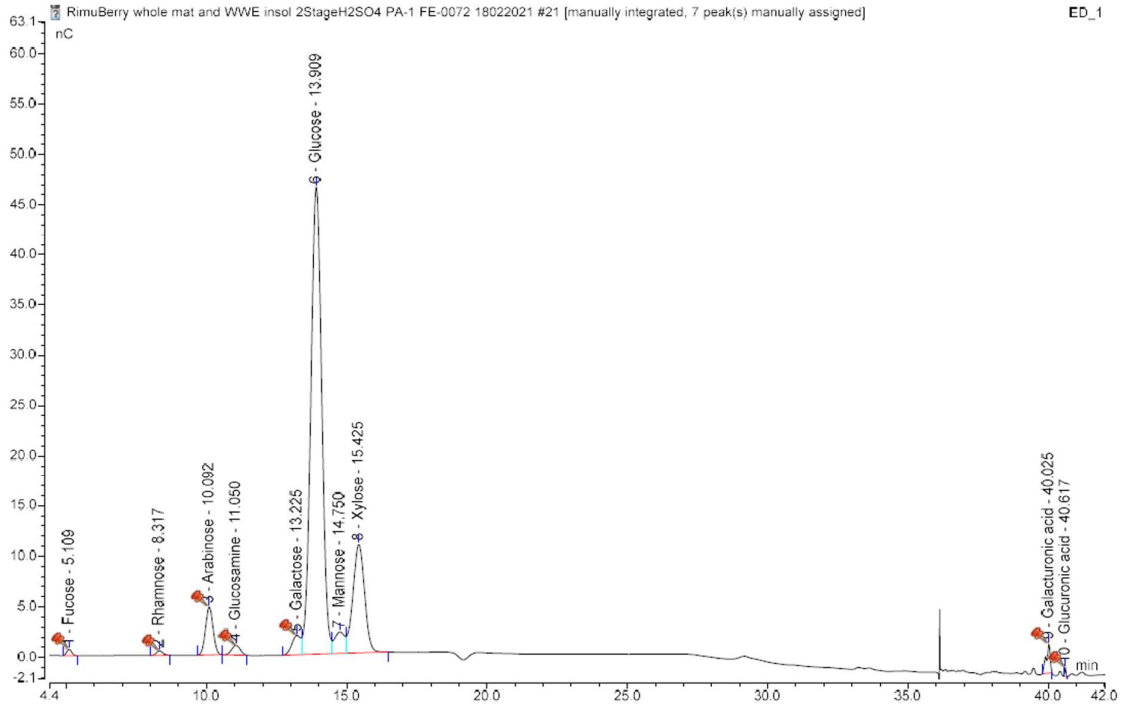

Peak No.	Peak Name	Ret.Time min	Amount	Rel.Area %	Area nC*min	Height nC	Type	Width (50%) min	Asym. EP	Resol. EP	Plates EP
1	Fucose	5.109	0.1742	0.42	0.1267	0.63	BMB*^	0.194	1.05	8.65	3846
2	Rhamnose	8.317	0.4203	0.40	0.1206	0.46	BMB*^	0.244	1.12	3.91	6445
3	Arabinose	10.092	1.1771	4.90	1.4844	4.77	BMB^	0.292	1.05	1.79	6625
4	Glucosamine	11.050	0.1543	1.14	0.3445	0.97	BMB*^	0.339	0.99	n.a.	5903
5	Galactose	13.225	n.a.	2.32	0.7024	1.93	BM *^	n.a.	n.a.	n.a.	n.a.
6	Glucose	13.909	23.8173	69.08	20.9399	46.46	M *	0.421	1.01	n.a.	6056
7	Mannose	14.750	2.1213	3.01	0.9133	2.14	M *	n.a.	n.a.	n.a.	n.a.
8	Xylose	15.425	5.1207	17.07	5.1747	10.78	MB*	0.446	n.a.	52.55	6623
9	Galacturonic acid	40.025	1.2104	1.52	0.4593	2.90	BMB*^	0.106	0.71	4.56	786680
10	Glucuronic acid	40.617	0.2816	0.15	0.0456	0.92	BMB*^	0.047	0.86	n.a.	4178571
Maximum			23.8173	69.08	20.9399	46.46		0.446	1.12	52.55	4178571
Minimum			0.1543	0.15	0.0456	0.46		0.047	0.71	1.79	3846
Sum			34.4771	100.00	30.3117	71.96					

HPAEC-PAD trace and raw data of two-stage H_2SO_4 hydrolysis of WWE_Insol (one representative sample).

Appendix A

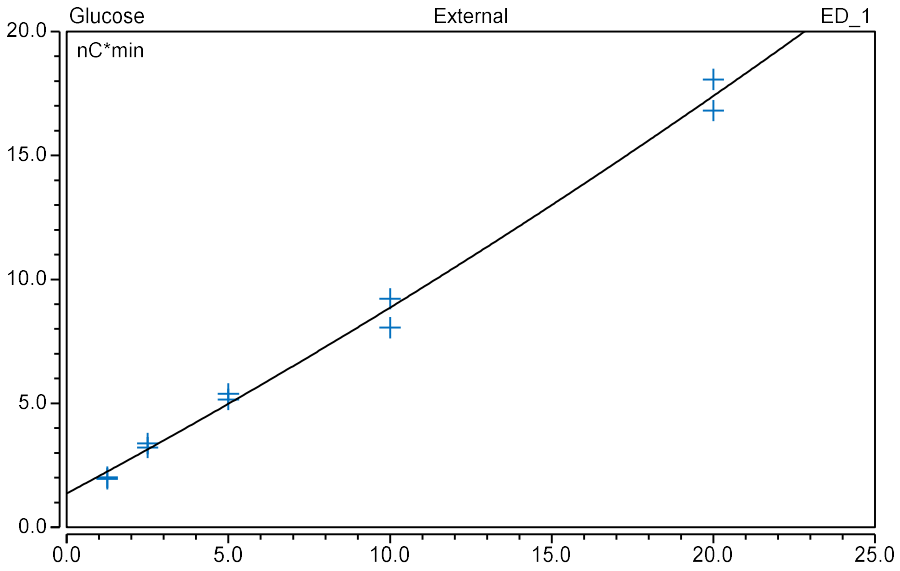

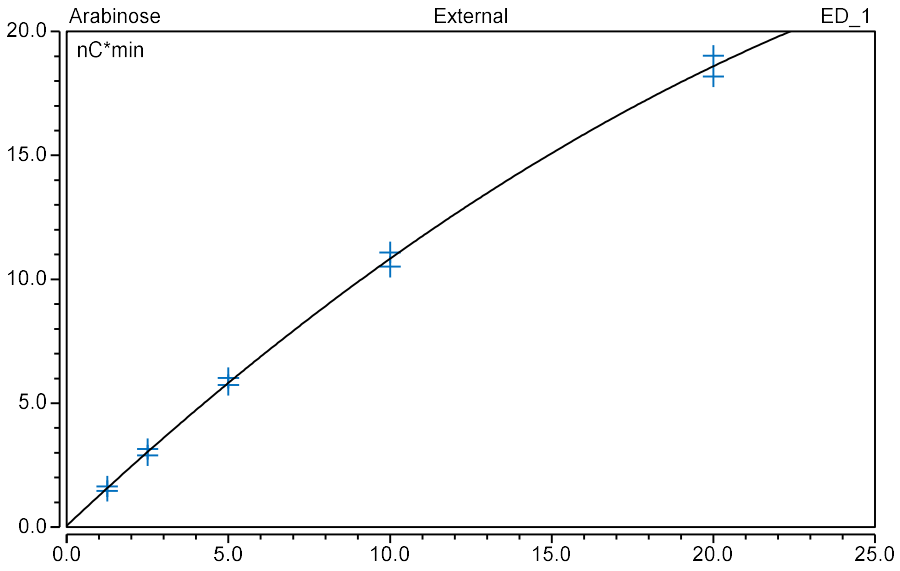

Example standard curves for two monosaccharides in the 12-sugar mix used for quantitation demonstrating notably different non-linear response.

Appendix B

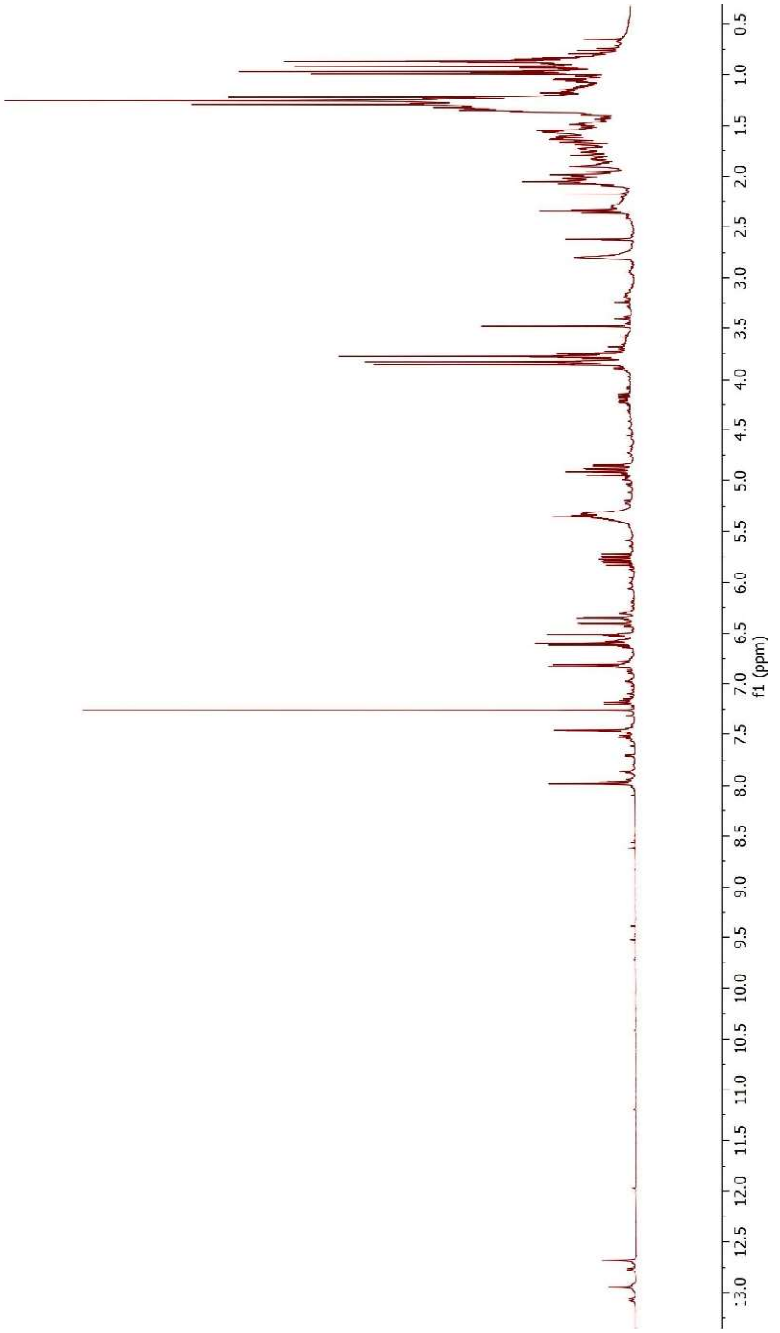

^{1}H NMR spectrum of foliage fraction DSH1_10_80% in $CDCl_3$ (500 MHz).

Appendix B

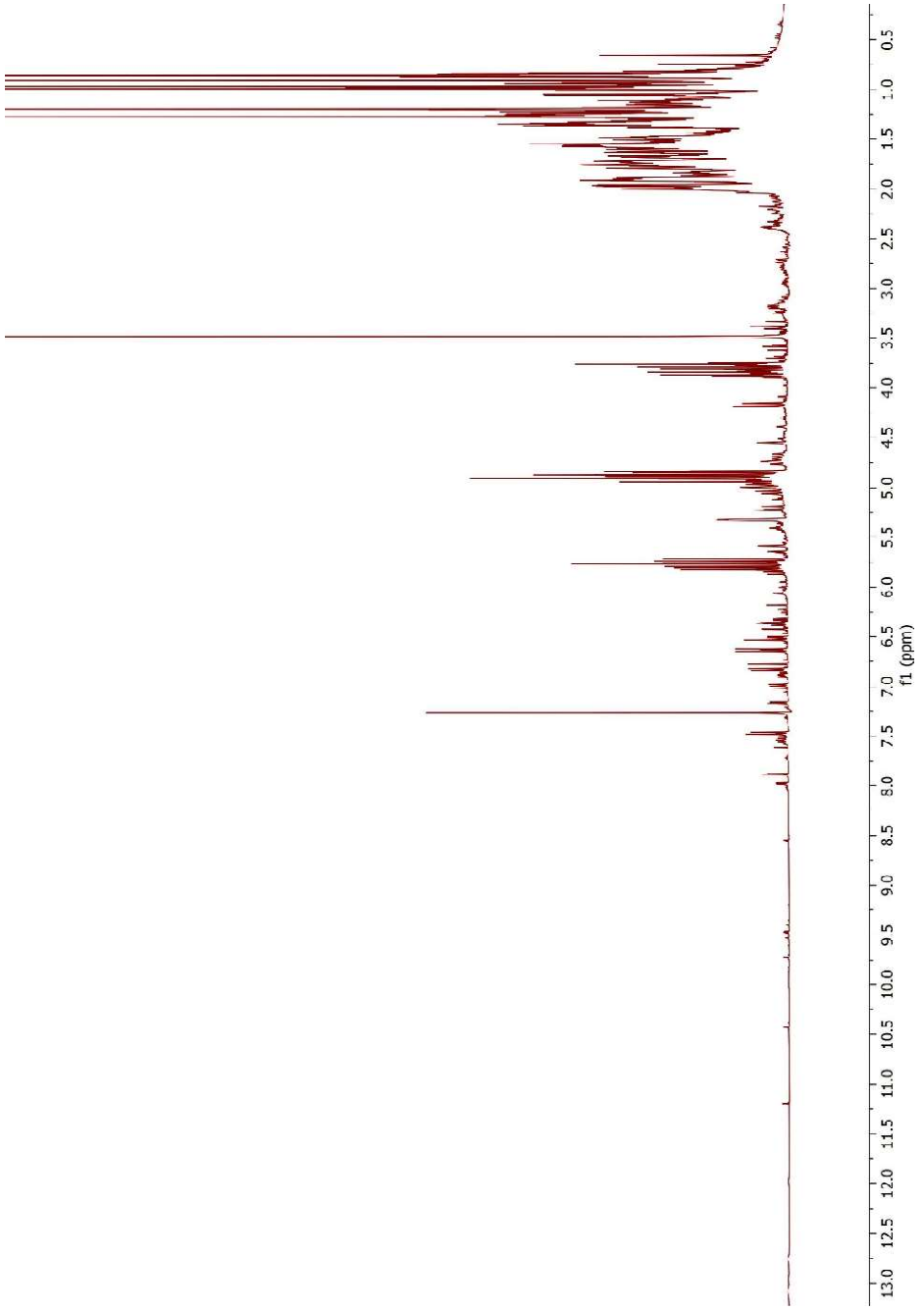

^{1}H NMR spectrum of foliage fraction DSH1_20_F2 in $CDCl_3$ (500 MHz).

Appendix B

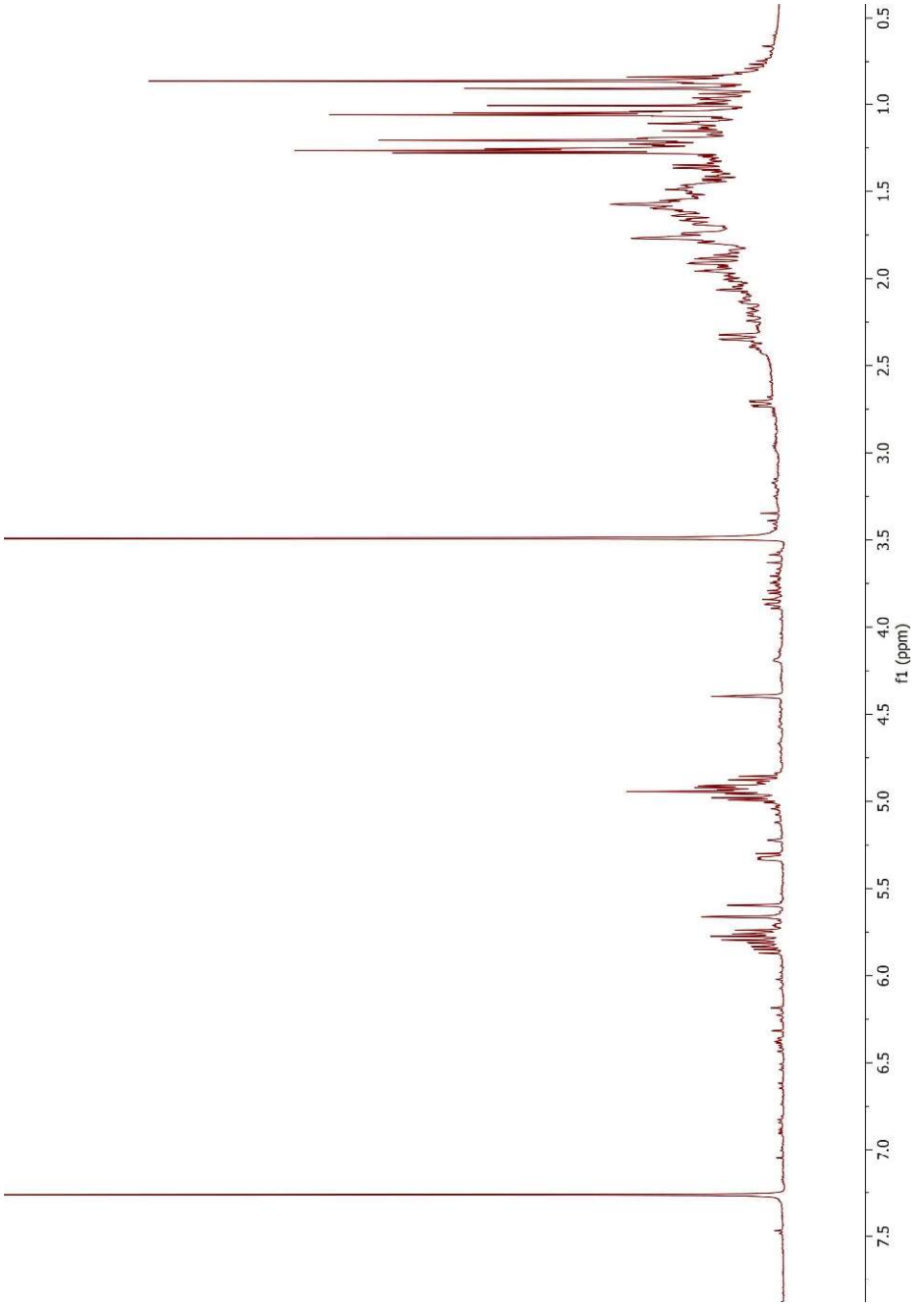

^{1}H NMR spectrum of foliage fraction DSH1_91_F3 in $CDCl_3$ (500 MHz).

Appendix B

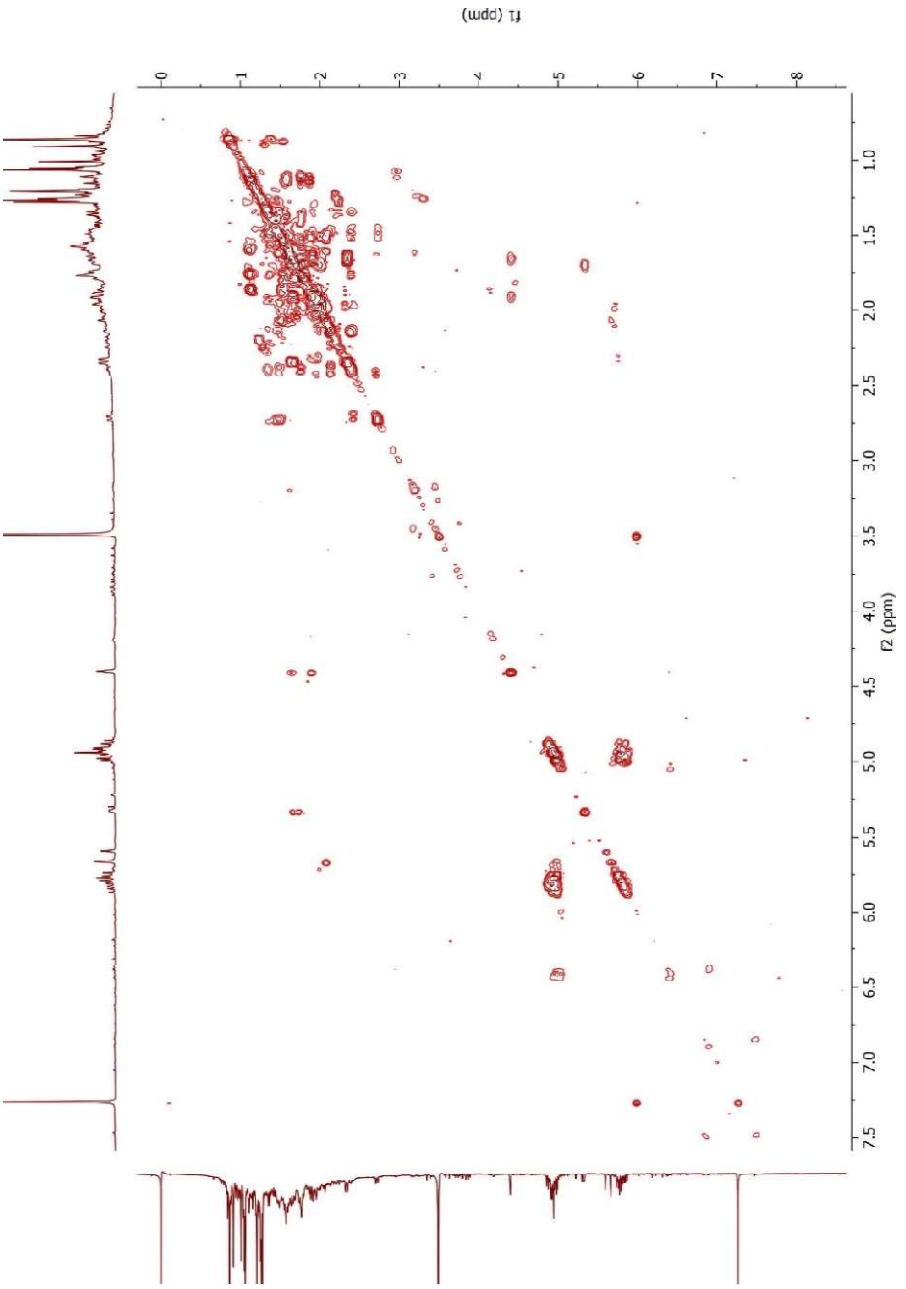

COSY NMR spectrum of foliage fraction DSH1_91_F3 in $CDCl_3$ (500 MHz).

Appendix B

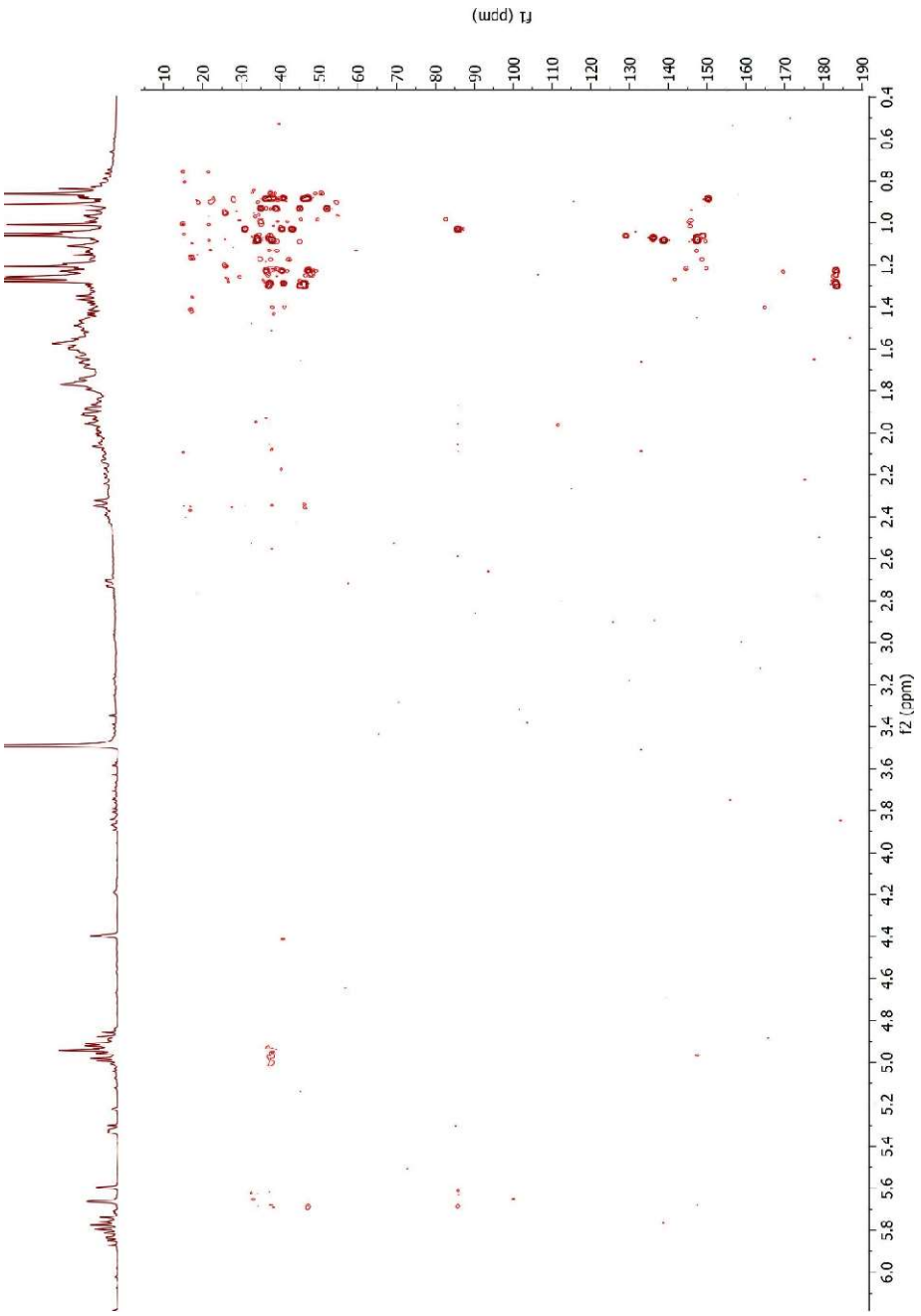

HMBC NMR spectrum of foliage fraction DSH1_91_F3 in $CDCl_3$ (500 MHz).

Appendix B

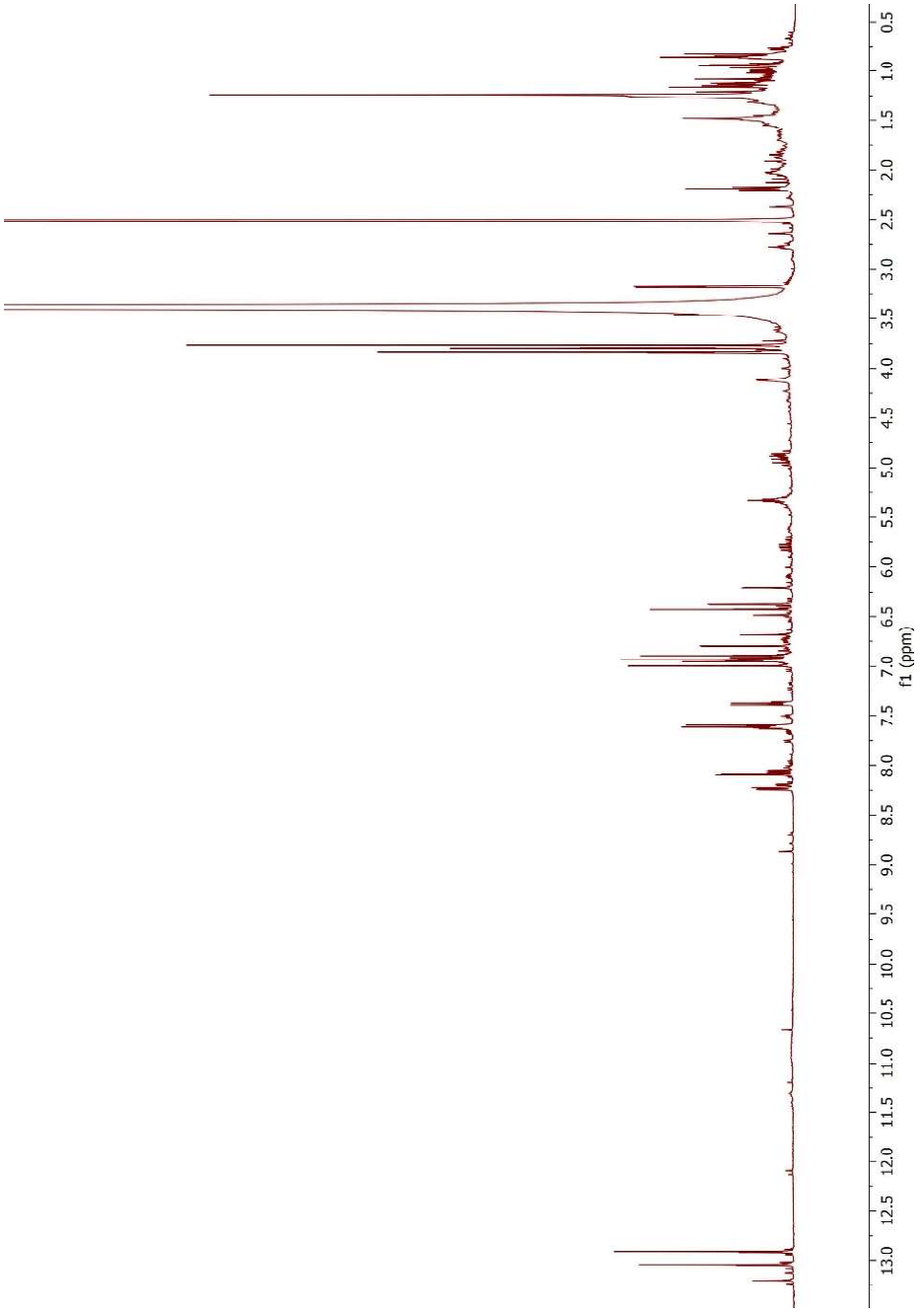

^{1}H NMR spectrum of foliage fraction DSH1_20_F3 in $CDCl_3$ (500 MHz).

Appendix B

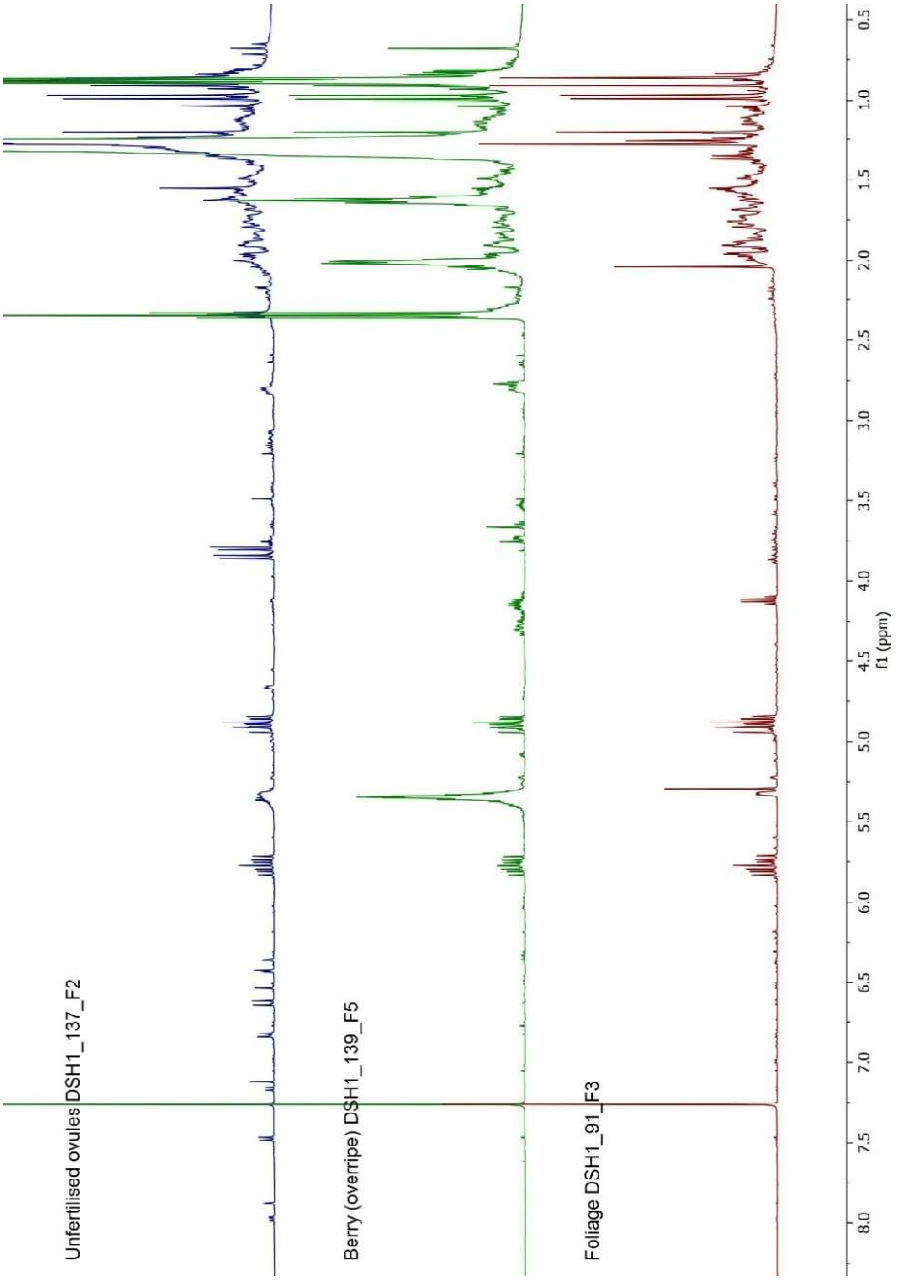

Stacked ^{1}H NMR spectra of unfertilised ovules fraction DSH1_137_F2, berry (overripe) fraction DSH1_139_F5 foliage, and foliage fraction DSH1_91_F3 in $CDCl_3$ (500 MHz).

Appendix B

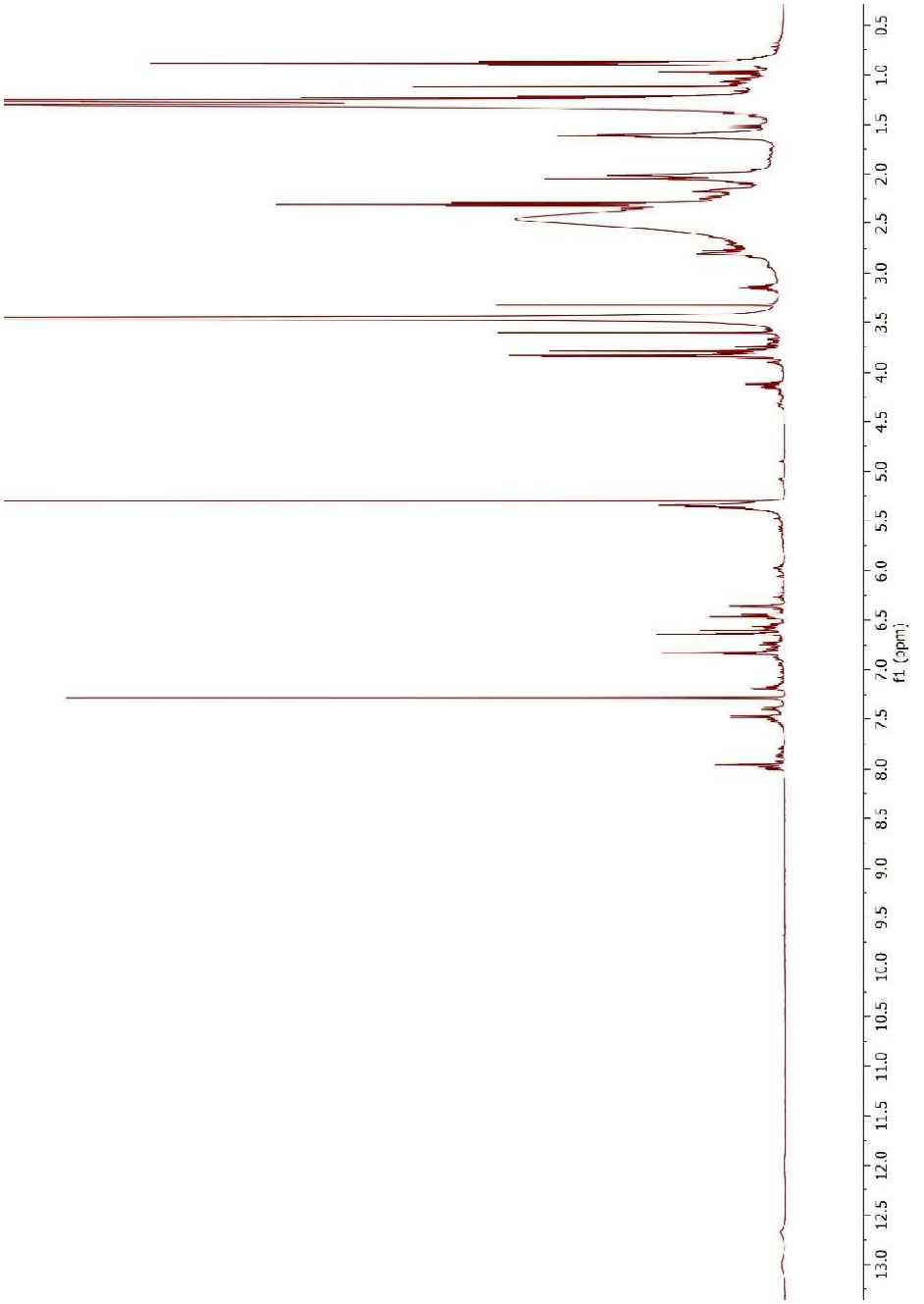

^{1}H NMR spectrum of berry (ripe) fraction DSH1_111_F3 in $CDCl_3$ (500 MHz).

Appendix B

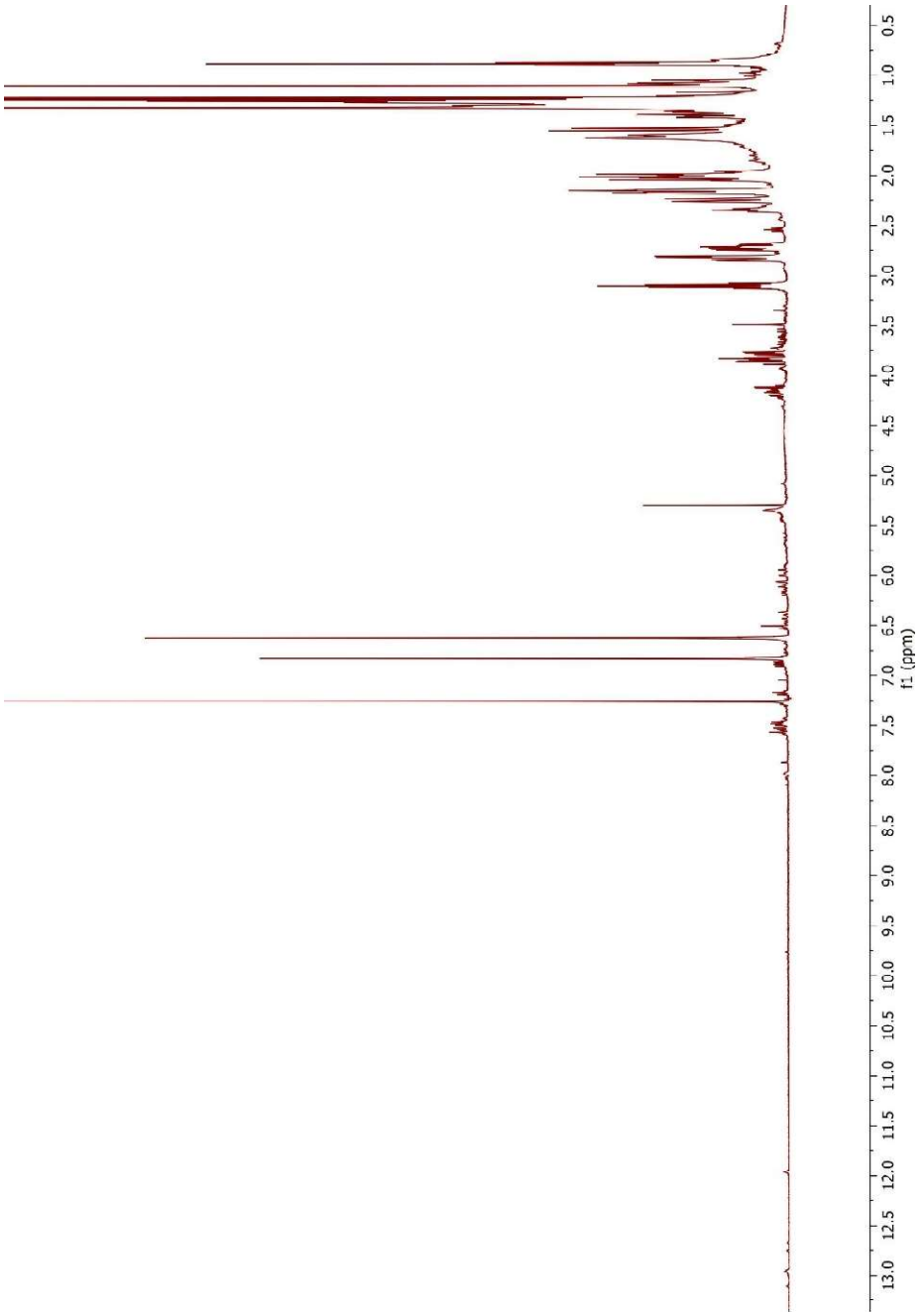

^{1}H NMR spectrum of berry (ripe) fraction DSH1_128_F6 in $CDCl_3$ (500 MHz).

Appendix C

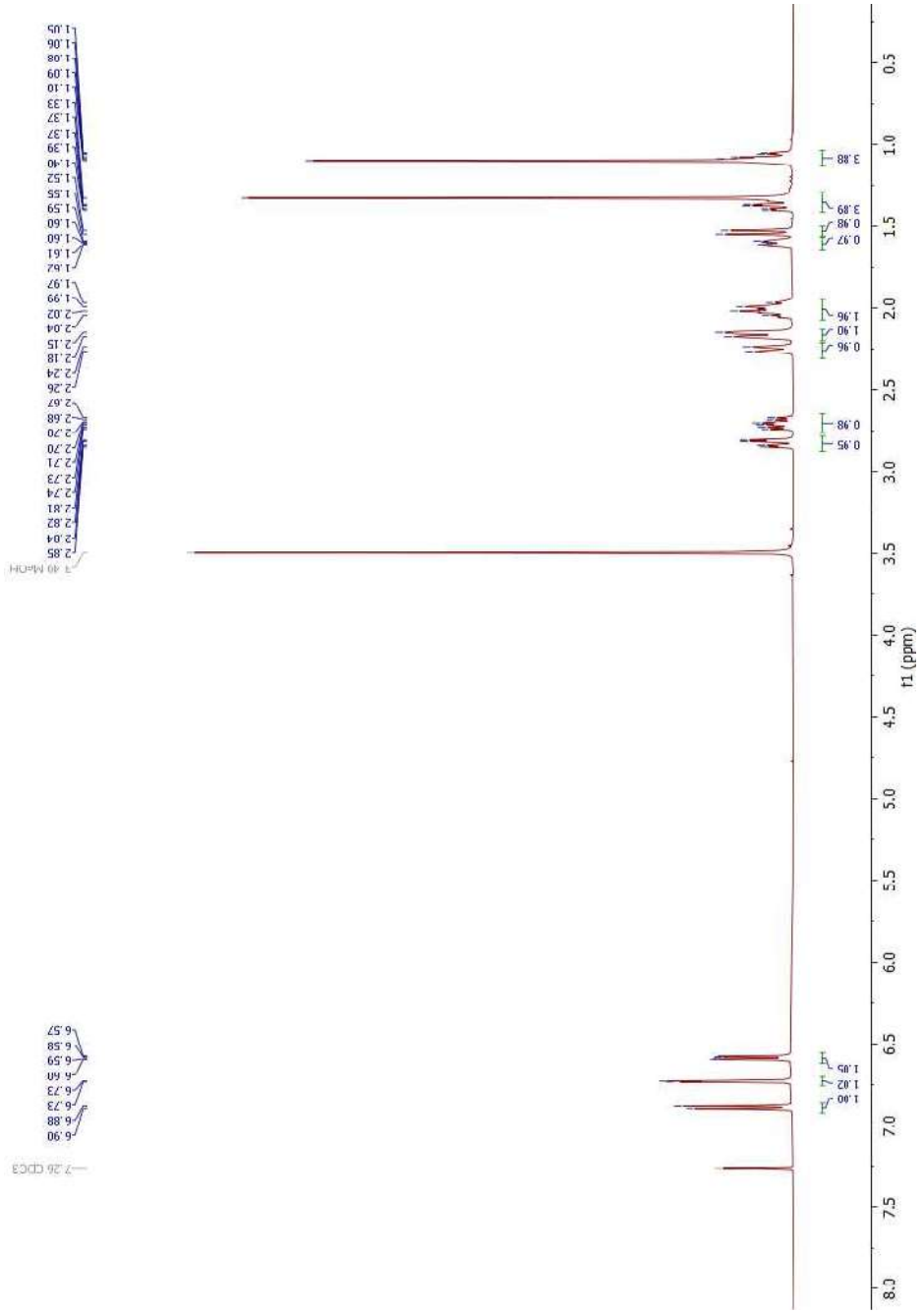

^{1}H NMR spectrum of podocarpic acid in $CDCl_3$ (500 MHz).

Appendix C

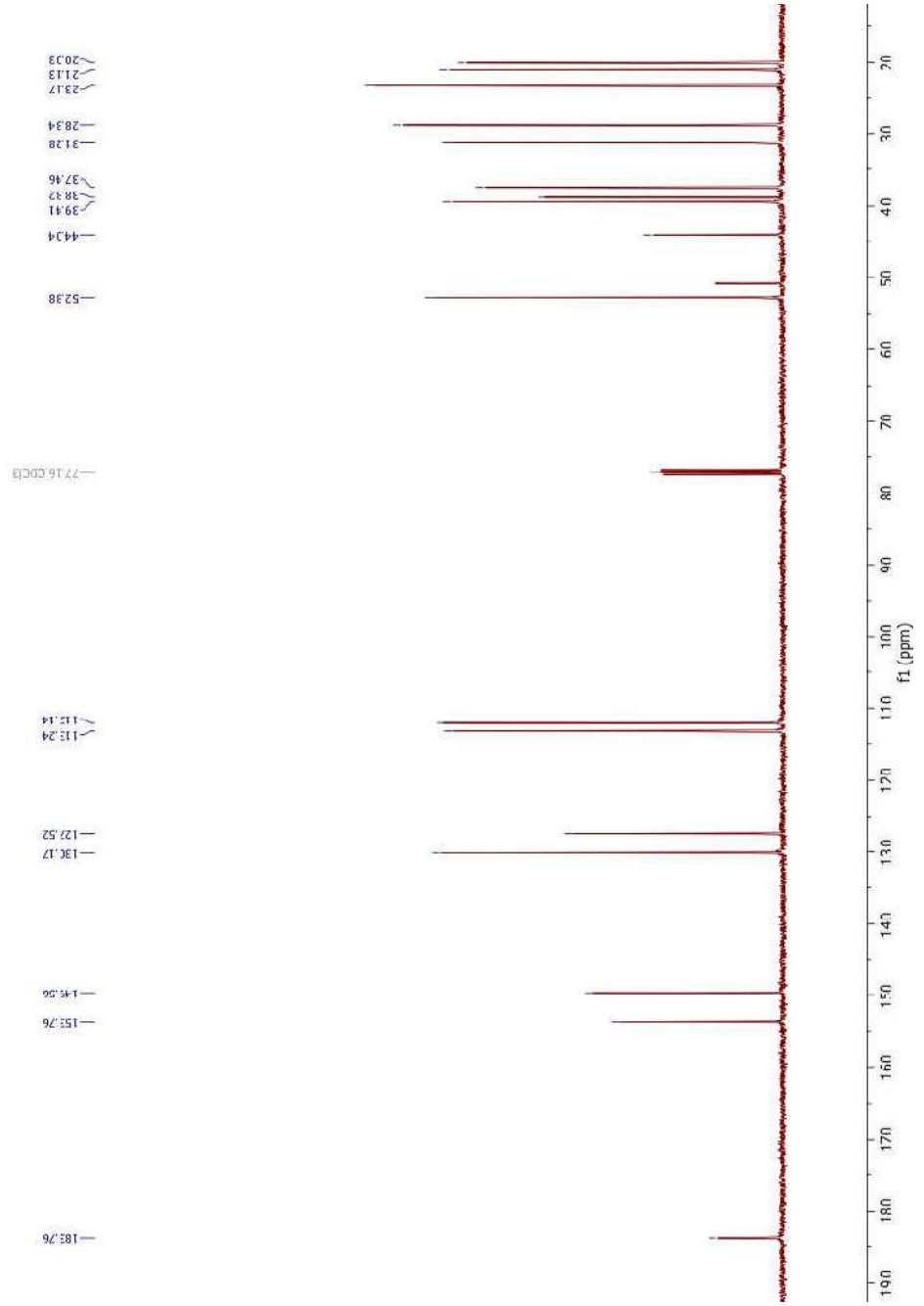

^{13}C NMR spectrum of podocarpic acid in $CDCl_3$ (500 MHz).

Appendix C

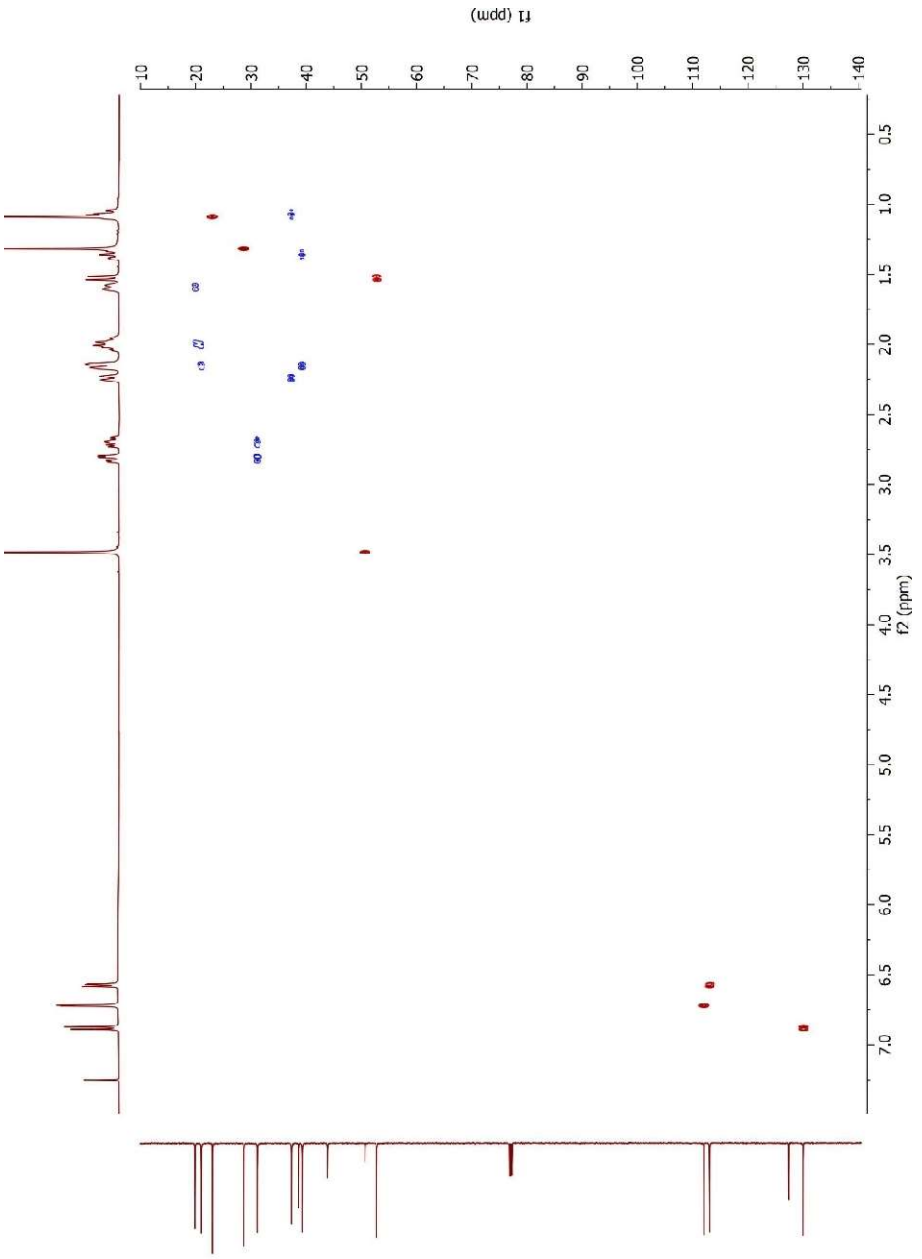

HSQC NMR spectrum of podocarpic acid in $CDCl_3$ (500 MHz).

Appendix C

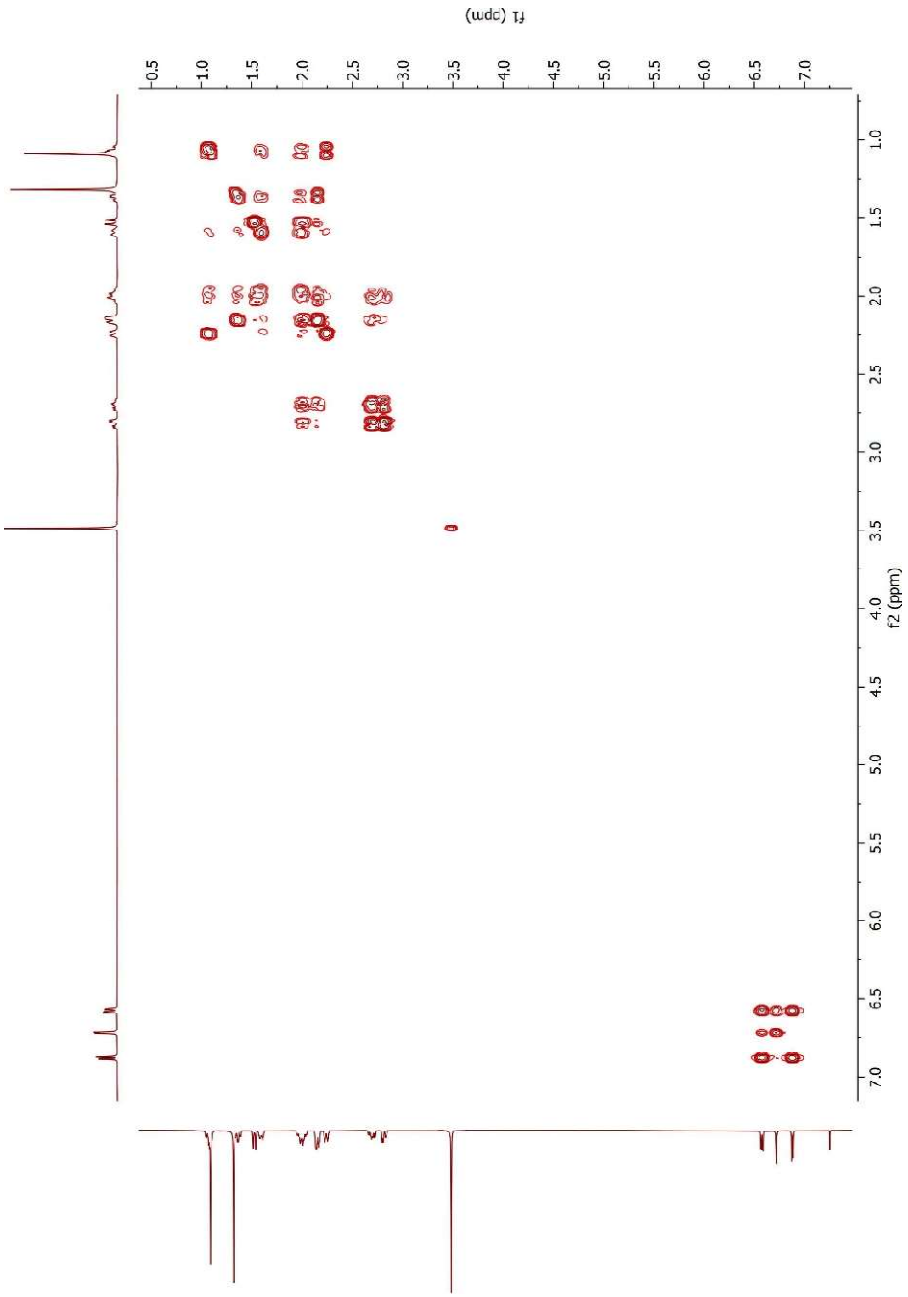

COSY NMR spectrum of podocarpic acid in $CDCl_3$ (500 MHz).

Appendix C

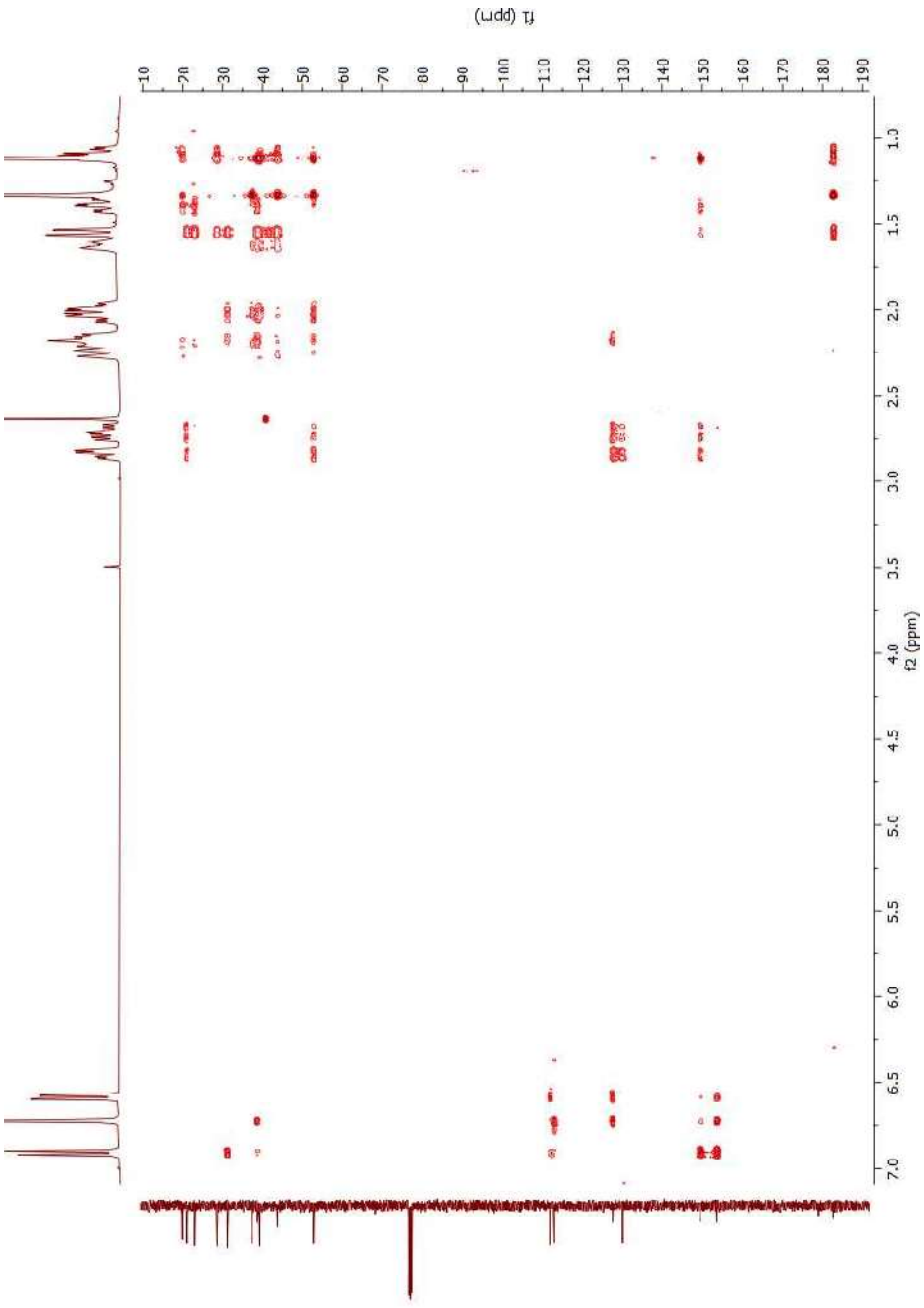

HMBC NMR spectrum of podocarpic acid in $CDCl_3$ (500 MHz).

Appendix D

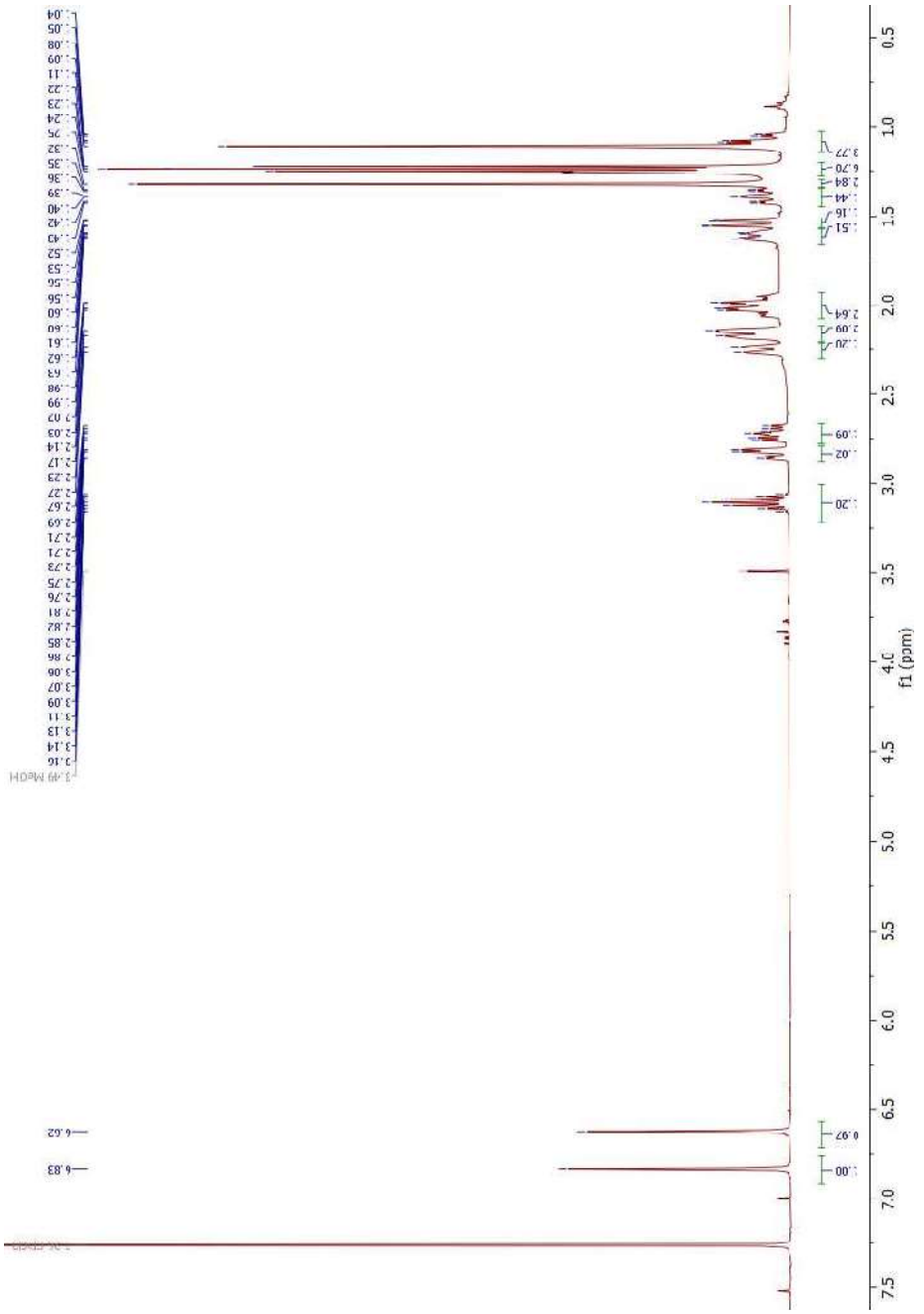

^{1}H NMR spectrum of compound **48** in $CDCl_3$ (400 MHz).

Appendix D

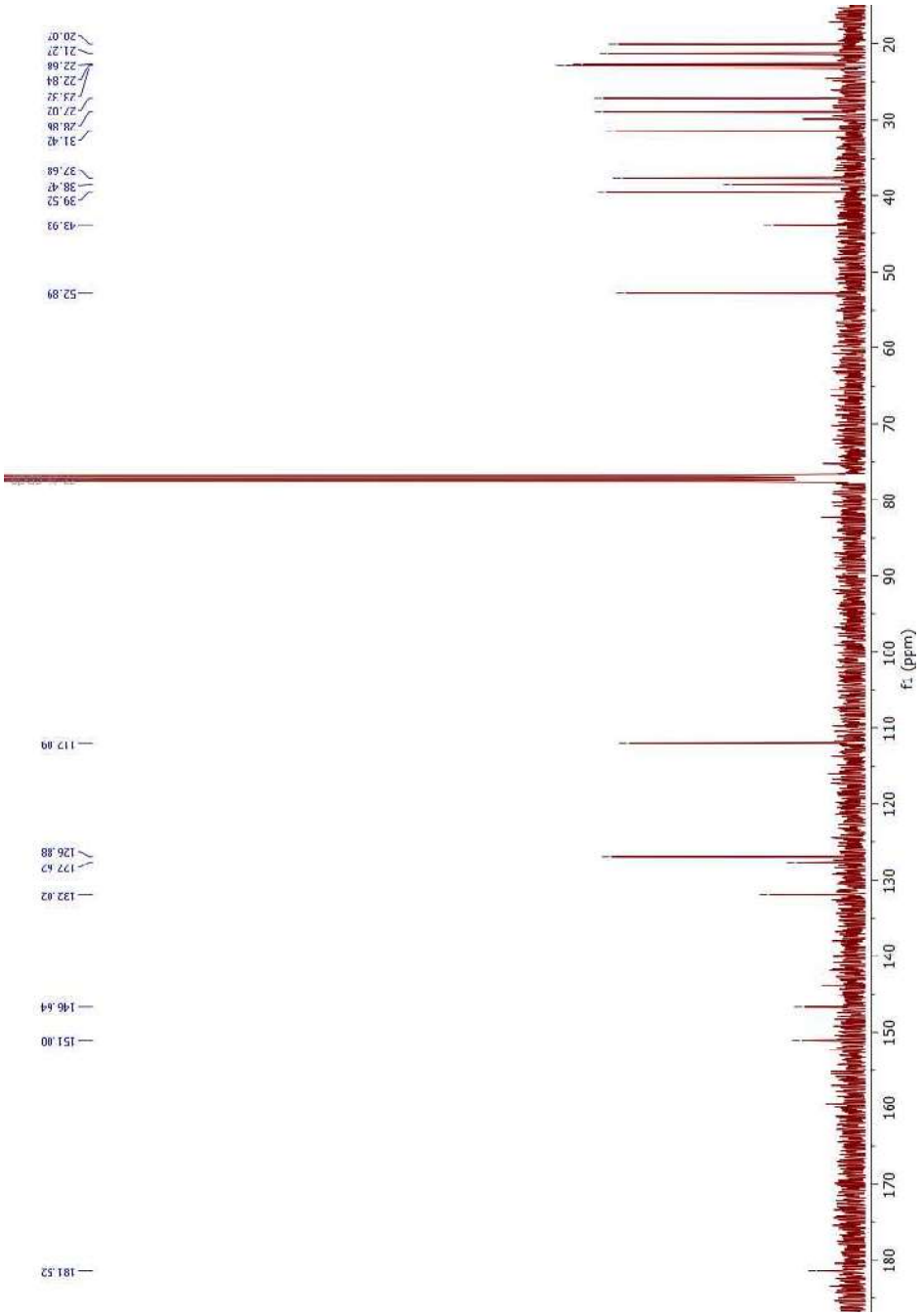

^{13}C NMR spectrum of compound **48** in $CDCl_3$ (400 MHz).

Appendix D

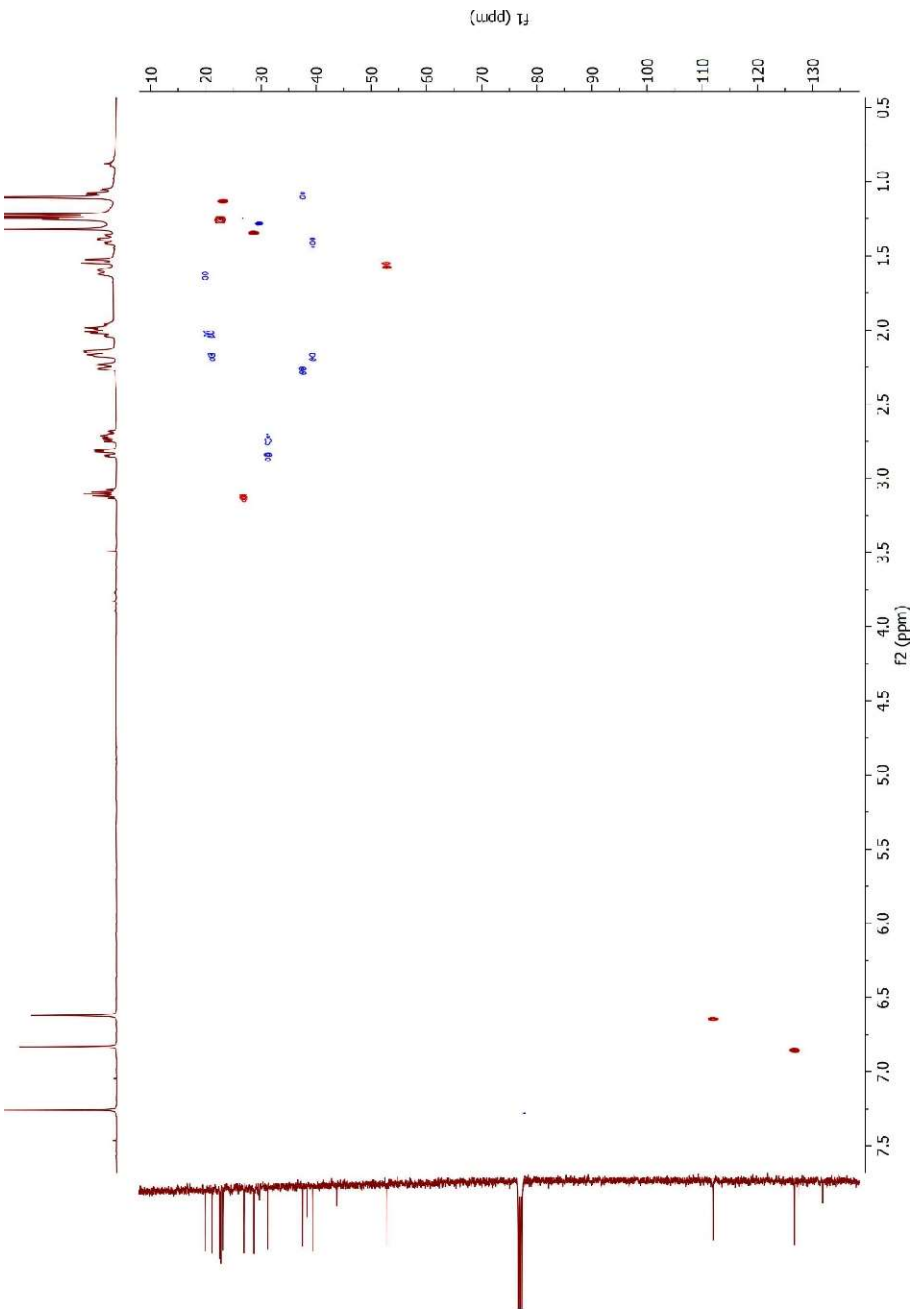

HSQC NMR spectrum of compound **48** in $CDCl_3$ (400 MHz).

Appendix D

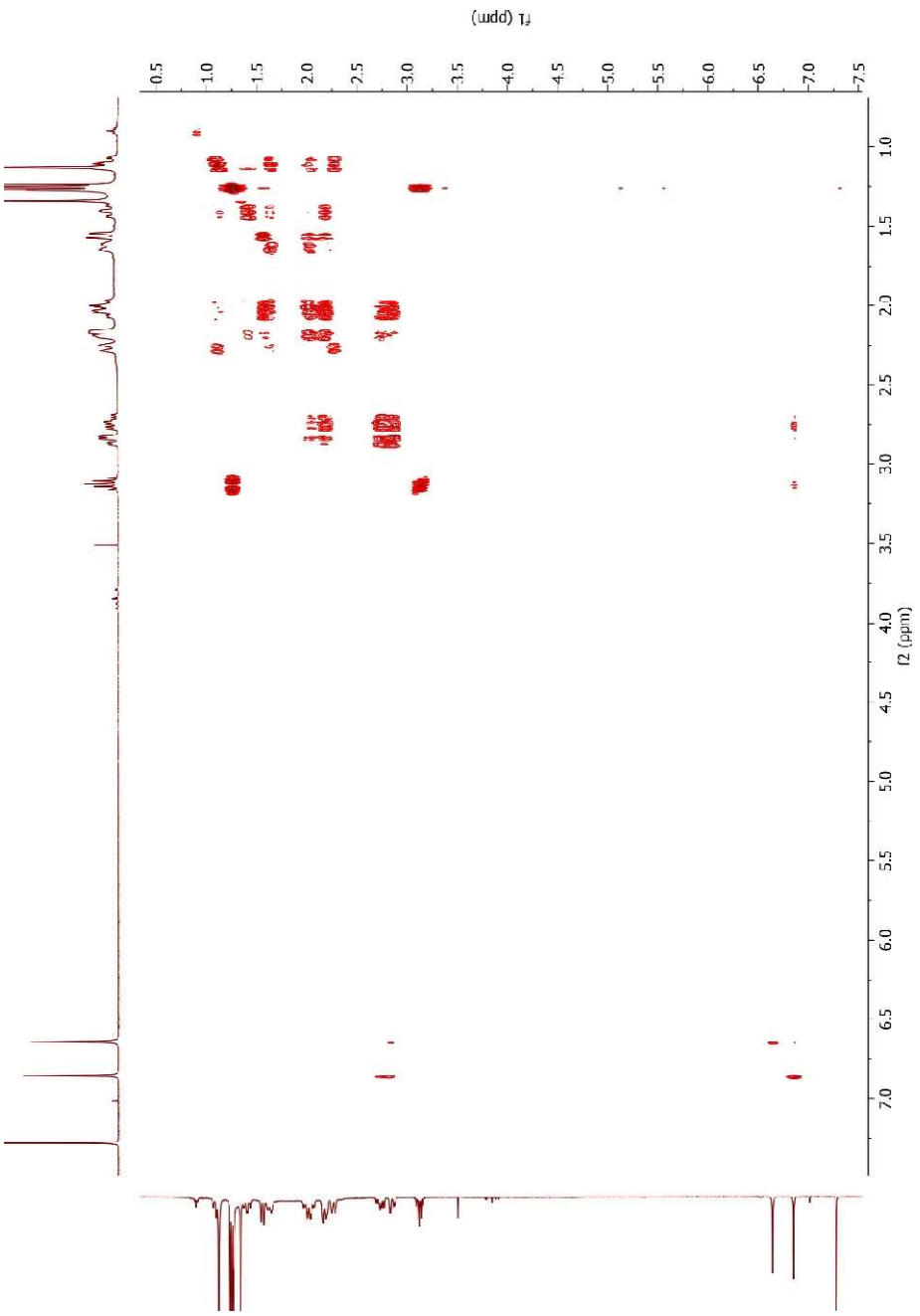

COSY NMR spectrum of compound **48** in $CDCl_3$ (400 MHz).

Appendix D

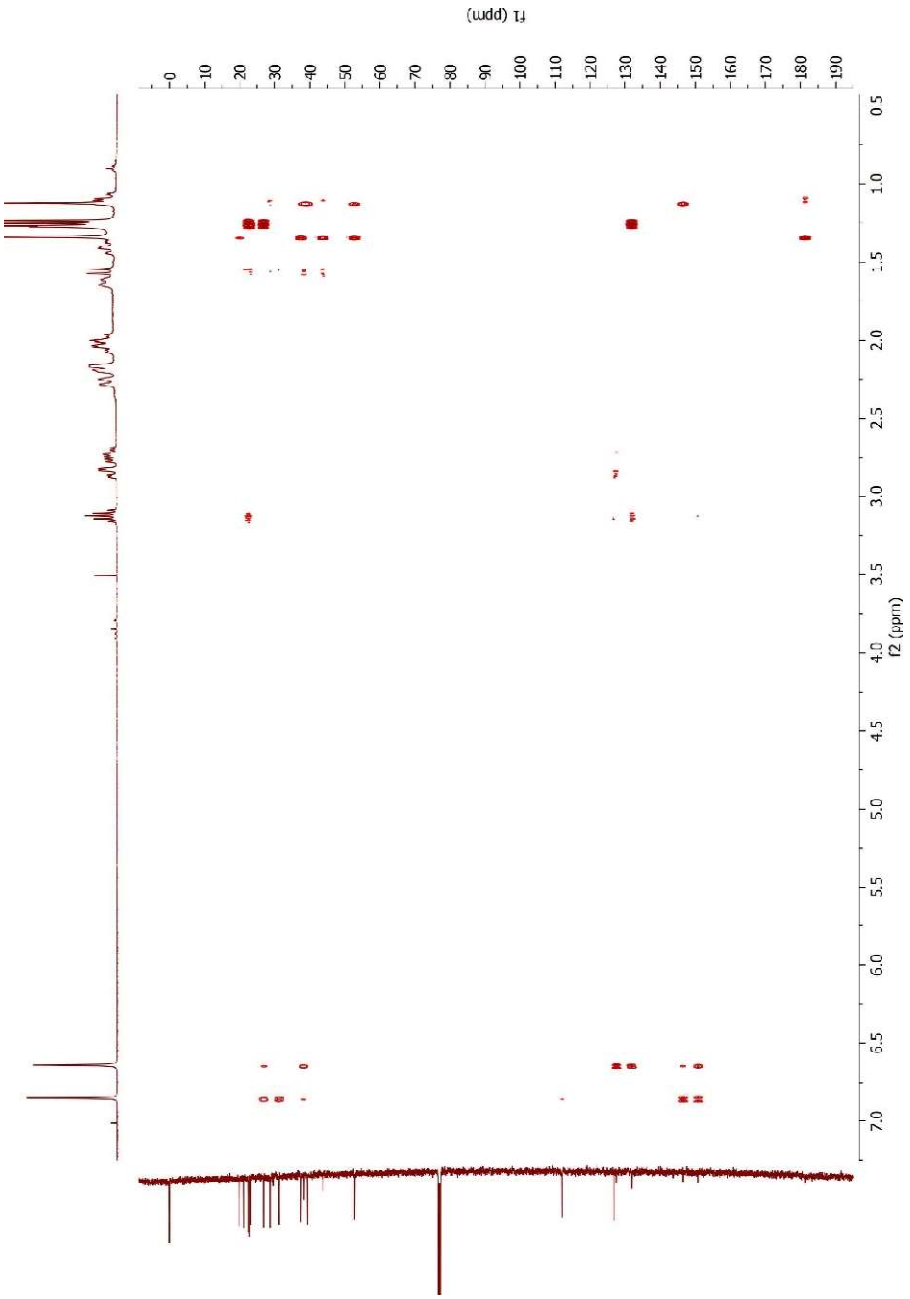

HMBC NMR spectrum of compound **48** in $CDCl_3$ (400 MHz).

Appendix D

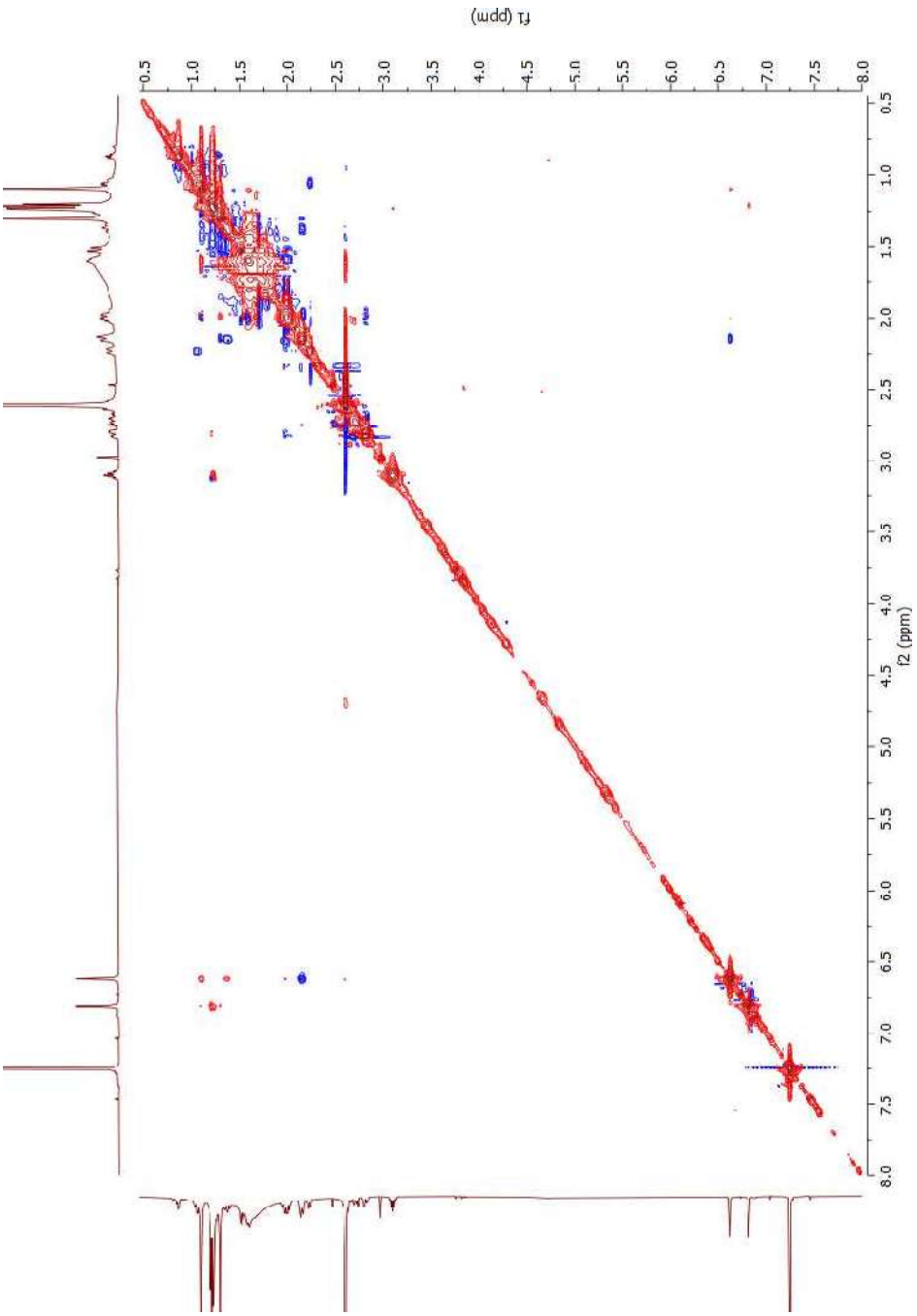

NOESY NMR spectrum of compound **48** in $CDCl_3$ (400 MHz).

Appendix D

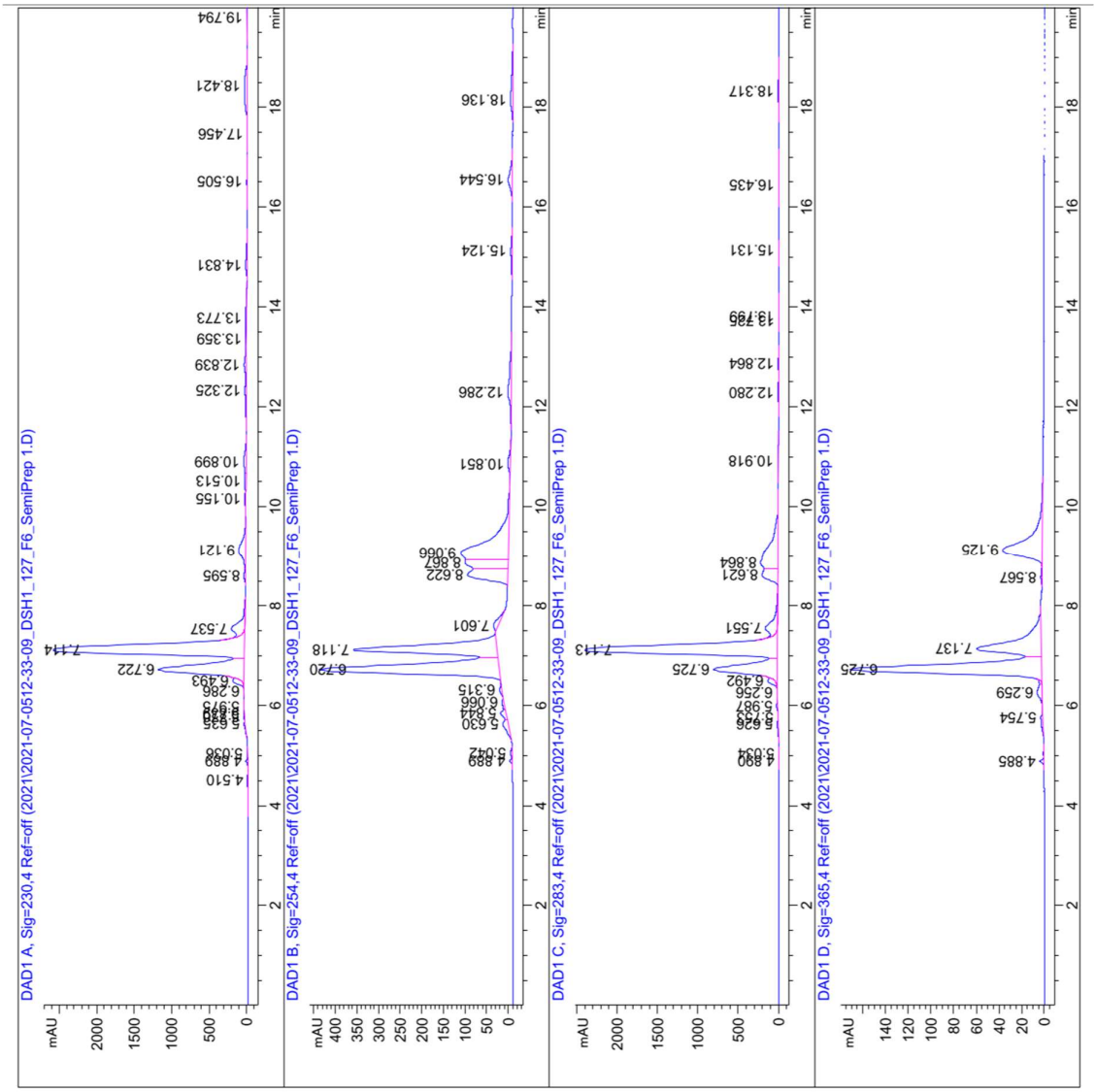

HPLC traces of berry (ripe) fraction DSH1_134_F5&6 leading to isolation of compound **48** having a retention time of 7.1 minutes detected as the second peak on UV detectors at 230, 254, 283, and 365 nm.

Appendix D

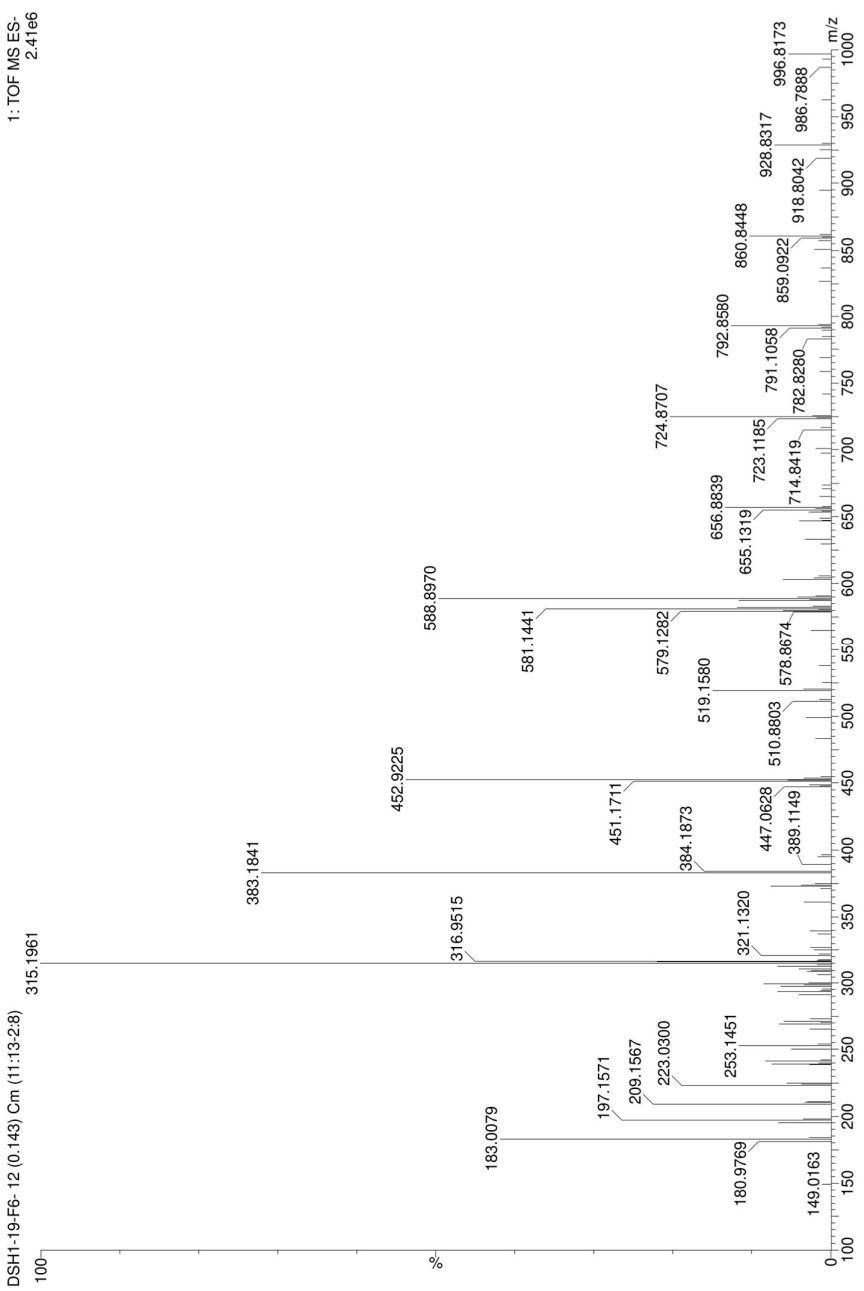

High-resolution MS of compound **48** in negative ion mode.

Appendix D

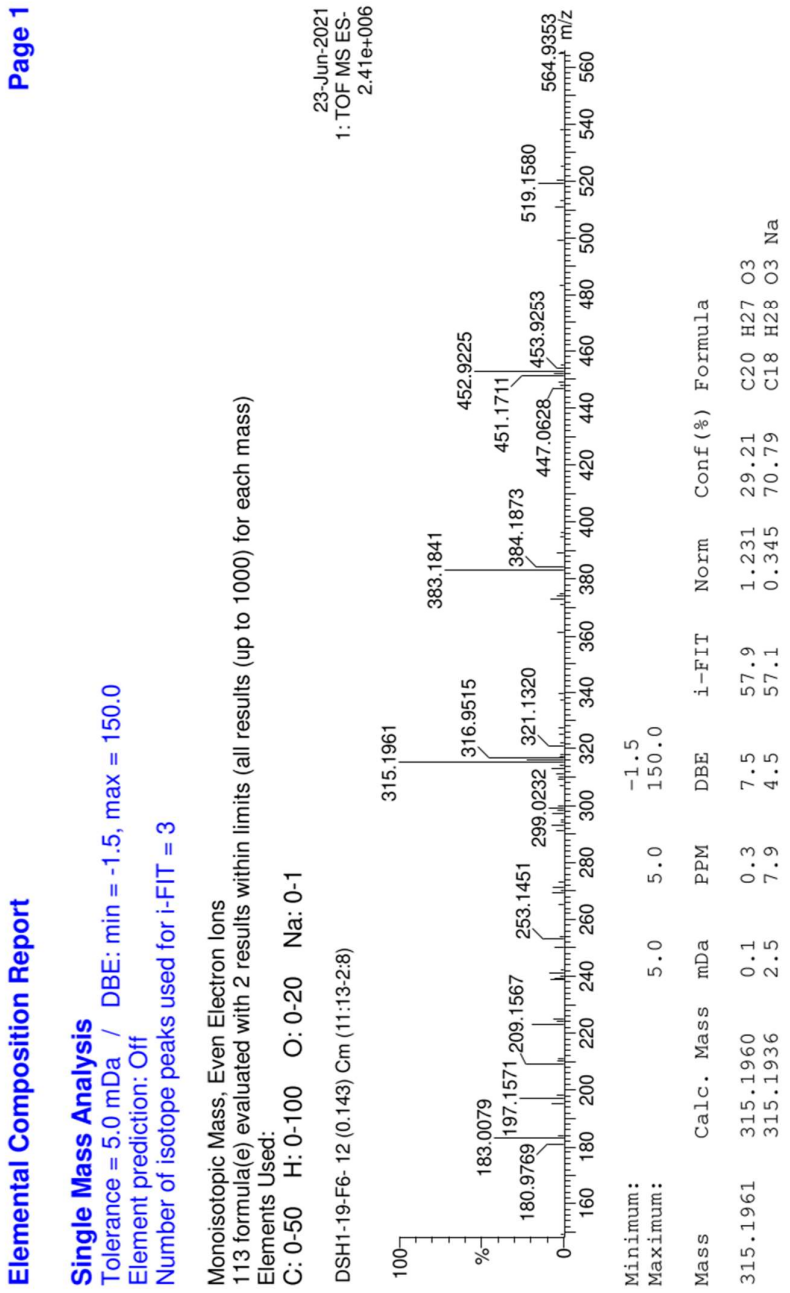

High-resolution MS single mass analysis of compound **48** in negative ion mode.

Appendix E

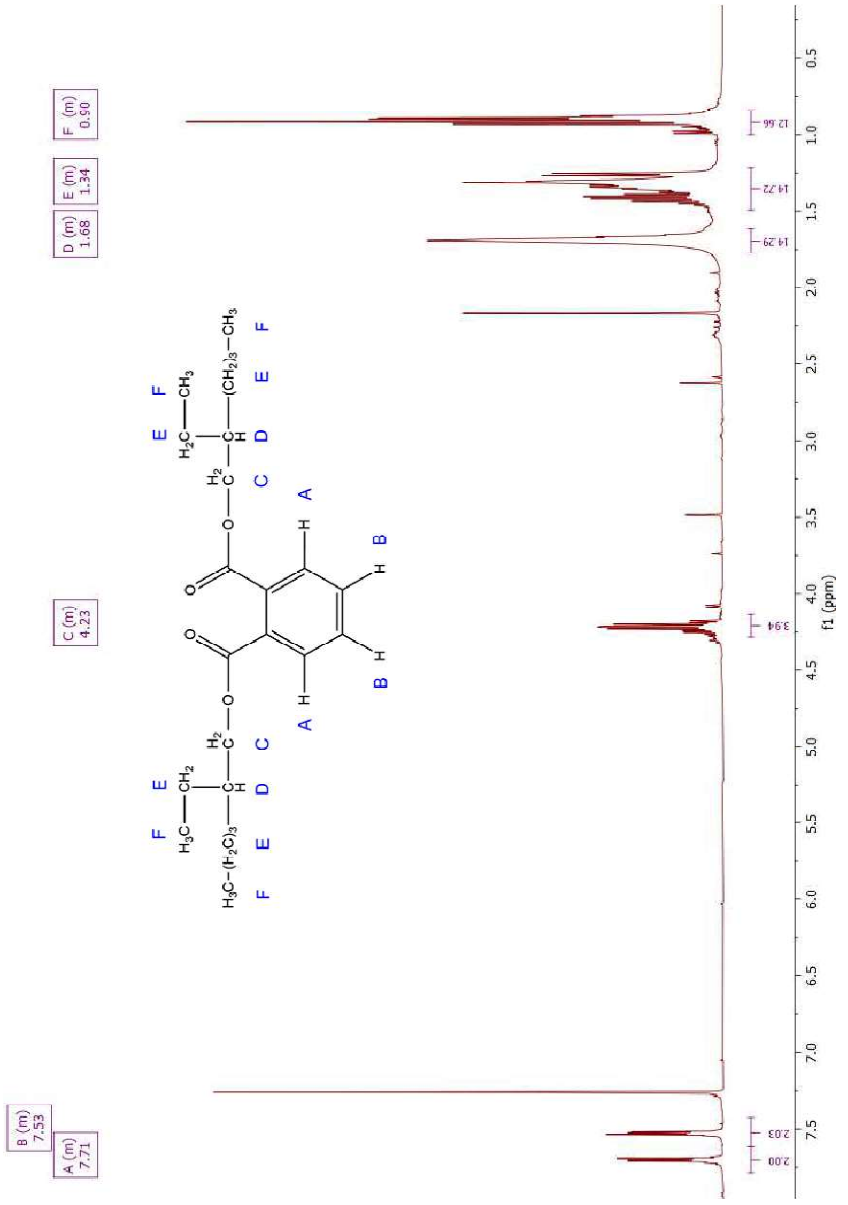

^{1}H NMR spectrum of analytical grade acetone used in cyclic loading procedure displaying the presence of bis(2-ethylhexyl) phthalate along with minor amounts of other unidentified impurities.

Appendix E

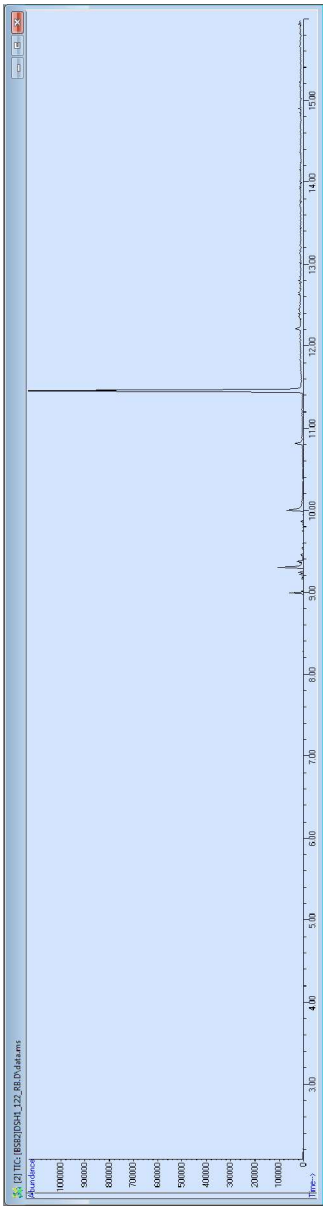

GC-MS total ion chromatogram with background subtracted of 80% acetone/water fraction of methanol extract of rimu berries (overripe) displaying a peak for the phthalate impurity with a retention time of 11.43 min.

Appendix E

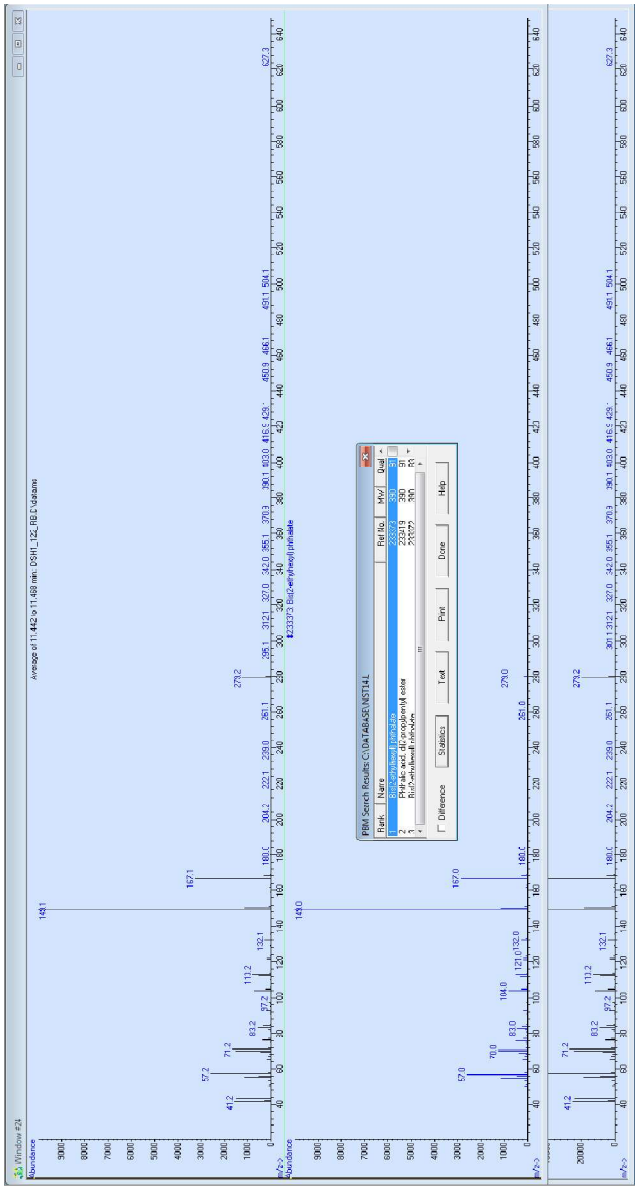

Average mass scan of the 11.43 min peak in the total ion chromatogram with database matching to bis(2-ethylhexyl) phthalate.

References

1. New Zealand Department of Conservation. Kākāpō recovery education resource. https://www.doc.govt.nz/globalassets/documents/getting-involved/students-and-teachers/kakapo-recovery/kakapo-recovery-education-resource.pdf (2018).

2. Cockrem, J. F. & Rounce, J. R. Non-invasive assessment of the annual gonadal cycle in free-living kakapo (Strigops habroptilus) Using Fecal Steroid Measurements. *Auk* **112**, 253–257 (1995).

3. Cockrem, J. F. The timing of breeding in the kakapo (Strigops habroptilus). *Notornis* **53**, 153–159 (2006).

4. Fiske, P., Rintamäki, P. T. & Karvonen, E. Mating success in lekking males: A meta-analysis. *Behav. Ecol.* **9**, 328–338 (1998).

5. Merton, D. V., Morris, R. B. & Atkinson, I. A. E. Lek behaviour in a parrot:the Kakapo Strigops habroptilus of New Zealand. *Ibis (Lond. 1859).* **126**, 277–283 (1984).

6. Whitehead, J., Case, B., Wilson, K.-J. & Molles, L. Breeding variation in female kakapo (Strigops habroptilus) on Codfish Island in a year of low food supply. *N. Z. J. Ecol.* **36**, 64–74 (2012).

7. New Zealand Department of Conservation. Kākāpō population reaches a record high of 213. https://www.doc.govt.nz/news/media-releases/2019/kakapo-population-reaches-a-record-high-of-213/ (2019).

8. Butler, D. J. The habitat, food and feeding ecology of kakapo in Fiordland: A synopsis from the unpublished MSc thesis of Richard Gray. *Notornis* **53**, 55–79 (2006).

9. Best, H. A. The foods of kakapo on Stewart Island as determined from their feeding sign. *N. Z. J. Ecol.* **7**, 71–83 (1984).

10. von Hurst, P. R., Moorhouse, R. J. & Raubenheimer, D. Preferred natural food

of breeding Kakapo is a high value source of calcium and vitamin D. *J. Steroid Biochem. Mol. Biol.* **164**, 177–179 (2016).

11. Wilson, D. J. *Diet of kakapo in breeding and non-breeding years on Codfish Island (Whenua Hou) and Stewart Island. Department of Conservation Science Internal Series 182.* http://www.doc.govt.nz (2004).

12. Cottam, Y. H., Merton, D. V & Hendriks, W. Nutrient composition of the diet of parent-raised kakapo nestlings. *Notornis* **53**, 90–99 (2006).

13. Powlesland, R. G. & Lloyd, B. D. Use of supplementary feeding to induce breeding in free-living kakapo Strigops habroptilus in New Zealand. *Biol. Conserv.* **69**, 97–106 (1994).

14. Clout, M. N., Elliott, G. P. & Robertson, B. C. Effects of supplementary feeding on the offspring sex ratio of kakapo: a dilemma for the conservation of a polygynous parrot. *Biol. Conserv.* **107**, 13–18 (2002).

15. Elliott, G. P., Merton, D. V. & Jansen, P. W. Intensive management of a critically endangered species: The kakapo. *Biol. Conserv.* **99**, 121–133 (2001).

16. Caprio, M., Fabbrini, E., Isidori, A. M., Aversa, A. & Fabbri, A. Leptin in reproduction. *Trends Endocrinol. Metab.* **12**, 65–72 (2001).

17. Pearson, K. Rimu Dacrydium cupressinum. *Herb Federation of New Zealand, herb awareness week* https://herbs.org.nz/wp-content/uploads/2019/01/Rimu-Dacrydium-cupressinum-Monograph-Herb-Awareness-Week-2019-Final-2.pdf (2019).

18. Wassilieff, M. Conifers - Rimu and kahikatea. *Te Ara - the Encyclopedia of New Zealand* http://www.teara.govt.nz/en/conifers/page-3 (2007).

19. Norton, D. A. & Kelly, D. Mast seeding over 33 years by Dacrydium cupressinum Lamb. (rimu) (Podocarpaceae) in New Zealand: The importance of economies of scale. *Funct. Ecol.* **2**, 399–408 (1988).

20. Norton, D. A., Herbert, J. W. & Beveridge, A. E. The ecology of dacrydium

cupressinum: A review. *New Zeal. J. Bot.* **26**, 37–62 (1988).

21. Cambie, R. C. A New Zealand phytochemical register. Part III. *J. R. Soc. New Zeal.* **6**, 307–379 (1976).

22. Cambie, R. C. A New Zealand phytochemical register. Part IV. *J. R. Soc. New Zeal.* **18**, 137–184 (1988).

23. Berry, K. M., Perry, N. B. & Weavers, R. T. Foliage sesquiterpenes of dacrydium Cupressinum: Identification, Variation, and Biosynthesis. *Phytochemistry* **24**, 2893–2898 (1985).

24. Richards, M. P. Trace mineral metabolism in the avian embryo. *Poult. Sci.* **76**, 152–164 (1997).

25. Loukopoulos, P. *et al.* An outbreak of thyroid hyperplasia (goiter) with high mortality in budgerigars (Melopsittacus undulatus). *J. Vet. Diagnostic Investig.* **27**, 18–24 (2015).

26. Merryman, J. I. & Buckles, E. L. The avian thyroid gland. Part two: A review of function and pathophysiology. *J. Avian Med. Surg.* **12**, 238–242 (1998).

27. Sancha, E., Van Heezik, Y., Maloney, R., Alley, M. & Seddon, P. Iodine deficiency affects hatchability of endangered captive kaki (black stilt, Himantopus novaezelandiae). *Zoo Biol.* **23**, 1–13 (2004).

28. Lewis, P. D. Responses of domestic fowl to excess iodine: a review. *Br. J. Nutr.* **91**, 29–39 (2004).

29. Cottam, Y. H. Characteristics of green rimu fruit that might trigger breeding in kakapo. (Massey University, 2010).

30. Corradini, C., Lantano, C. & Cavazza, A. Innovative analytical tools to characterize prebiotic carbohydrates of functional food interest. *Anal. Bioanal. Chem.* **405**, 4591–4605 (2013).

31. Landete, J. M. *et al.* Bioactivation of phytoestrogens: Intestinal bacteria and health. *Crit. Rev. Food Sci. Nutr.* **56**, 1826–1843 (2016).

32. Ivell, R. Mini symposium: The role of carbohydrates in reproduction. *Hum. Reprod. Update* **5**, 277–279 (1999).

33. Siva, N., Thavarajah, P., Kumar, S. & Thavarajah, D. Variability in prebiotic carbohydrates in different market classes of chickpea, common bean, and lentil collected from the american local market. *Front. Nutr.* **6**, 1–11 (2019).

34. Mohnen, D. & Hahn, M. G. Cell wall carbohydrates as signals in plants. *Semin. Cell Biol.* **4**, 93–102 (1993).

35. Voragen, A. G. J., Coenen, G. J., Verhoef, R. P. & Schols, H. A. Pectin, a versatile polysaccharide present in plant cell walls. *Struct. Chem.* **20**, 263–275 (2009).

36. Pettolino, F. A., Walsh, C., Fincher, G. B. & Bacic, A. Determining the polysaccharide composition of plant cell walls. *Nat. Protoc.* **7**, 1590–1607 (2012).

37. Sarkar, P., Bosneaga, E. & Auer, M. Plant cell walls throughout evolution: Towards a molecular understanding of their design principles. *J. Exp. Bot.* **60**, 3615–3635 (2009).

38. Matros, A., Peukert, M., Lahnstein, J., Seiffert, U. & Burton, R. Determination of fructans in plants: Current analytical means for extraction, detection, and quantification. *Annu. Plant Rev. Online* **2**, 1–39 (2019).

39. Pfister, B. & Zeeman, S. C. Formation of starch in plant cells. *Cell. Mol. Life Sci.* **73**, 2781–2807 (2016).

40. Gibson, L. J. The hierarchical structure and mechanics of plant materials. *J. R. Soc. Interface* **9**, 2749–2766 (2012).

41. Yoo, H. D., Kim, D., Paek, S. H. & Oh, S. E. Plant cell wall polysaccharides as potential resources for the development of novel prebiotics. *Biomol. Ther.* **20**, 371–379 (2012).

42. Scheller, H. V. & Ulvskov, P. Hemicelluloses. *Annu. Rev. Plant Biol.* **61**, 263–

289 (2010).

43. Venkatanagaraju, E., Bharathi, N., Hema Sindhuja, R., Roy Chowdhury, R. & Sreelekha, Y. *Extraction and purification of pectin from agro-industrial wastes*. P*ectins - extraction, purification, characterization and applications* (2019). doi:10.5772/intechopen.85585.

44. Prasanna, V., Prabha, T. N. & Tharanathan, R. N. Fruit ripening phenomena-an overview. *Crit. Rev. Food Sci. Nutr.* **47**, 1–19 (2007).

45. Eggleston, G. & Côté, G. L. Oligosaccharides in Food and Agriculture. in *Oligosaccharides in Food and Agriculture (ACS Symposium Series, No. 849)* 1–14 (American Chemical Society, 2003). doi:10.1021/bk-2003-0849.ch001.

46. Martins, G. N., Ureta, M. M., Tymczyszyn, E. E., Castilho, P. C. & Gomez-Zavaglia, A. Technological aspects of the production of fructo and galacto-oligosaccharides. Enzymatic synthesis and hydrolysis. *Front. Nutr.* **6**, 1–24 (2019).

47. Markowiak, P. & Ślizewska, K. The role of probiotics, prebiotics and synbiotics in animal nutrition. *Gut Pathog.* **10**, 1–20 (2018).

48. Wu, H., Shang, H., Guo, Y., Zhang, H. & Wu, H. Comparison of different extraction methods of polysaccharides from cup plant (Silphium perfoliatum L.). *Process Biochem.* **90**, 241–248 (2019).

49. Castellari, Ma; Versari, Aa; Spinabelli, Ua; Galassi, Aa; Amati, A. An improved method for the analysis of organic acids, carbohydrates, and alcohols in grape musts and wines. *J. Liq. Chromatogr. Relat. Technol.* **23**, 2047–2056 (2007).

50. Montañés, F. *et al.* Selective fractionation of disaccharide mixtures by supercritical CO_2 with ethanol as co-solvent. *J. Supercrit. Fluids* **41**, 61–67 (2007).

51. Ruiz-Matute, A. I., Ramos, L., Martínez-Castro, I. & Sanz, M. L. Fractionation of honey carbohydrates using pressurized liquid extraction with activated charcoal. *J. Agric. Food Chem.* **56**, 8309–8313 (2008).

52. Chen, X. *et al.* Applications of asymmetrical flow field-flow fractionation for separation and characterization of polysaccharides: A review. *J. Chromatogr. A* **1635**, 461726 (2021).

53. Kaewjumpol, G., Oruna-Concha, M. J., Niranjan, K. & Thawornchinsombut, S. The production of hydrolysates from industrially defatted rice bran and its surface image changes during extraction. *J. Sci. Food Agric.* **98**, 3290–3298 (2018).

54. Cui, S. Structural analysis of polysaccharides. in *Food carbohydrates: chemistry, physical properties, and applications* (CRC Press, 2005). doi:10.1201/9780203485286.ch3.

55. Herrero, M., Cifuentes, A., Ibáñez, E. & Dolores, M. Advanced analysis of carbohydrates in foods. in *Methods of Analysis of Food Components and Additives* 150–179 (2011). doi:10.1201/b11218-12.

56. De Ruiter, G. A., Schols, H. A., Voragen, A. G. J. & Rombouts, F. M. Carbohydrate analysis of water-soluble uronic acid-containing polysaccharides with high-performance anion-exchange chromatography using methanolysis combined with TFA hydrolysis is superior to four other methods. *Anal. Biochem.* **207**, 176–185 (1992).

57. Panagiotopoulos, C. & Sempéré, R. Analytical methods for the determination of sugars in marine samples: A historical perspective and future directions. *Limnol. Oceanogr. Methods* **3**, 419–454 (2005).

58. Mechelke, M. *et al.* HPAEC-PAD for oligosaccharide analysis—novel insights into analyte sensitivity and response stability. *Anal. Bioanal. Chem.* **409**, 7169–7181 (2017).

59. Nouara, A., Panagiotopoulos, C. & Sempéré, R. Simultaneous determination of neutral sugars, alditols and anhydrosugars using anion-exchange chromatography with pulsed amperometric detection: Application for marine and atmospheric samples. *Mar. Chem.* **213**, 24–32 (2019).

60. Fidler, A. E., Lawrence, S. B. & McNatty, K. P. An hypothesis to explain the linkage between kakapo (Strigops habroptilus) breeding and the mast fruiting of their food trees. *Wildl. Res.* **35**, 1–7 (2008).

61. Hazlerigg, D. G. & Wagner, G. C. Seasonal photoperiodism in vertebrates: from coincidence to amplitude. *Trends Endocrinol. Metab.* **17**, 83–91 (2006).

62. Edinger, R. S., Mambo, E. & Evans, M. I. Estrogen-dependent transcriptional activation and vitellogenin gene memory. *Mol. Endocrinol.* **11**, 1985–1993 (1997).

63. Brandt, C. W. & Ross, D. J. Podocarpic acid as a source of an œstrogenic hormone. *Nature* vol. 161 892 (1948).

64. Fidler, A. E. *et al.* Screening foods of the endangered Kakapo parrot (Strigops habroptilus) for oestrogenic activity using a recombinant yeast bioassay. *Br. Poult. Sci.* **41**, 48–54 (2000).

65. Amenyogbe, E. *et al.* A review on sex steroid hormone estrogen receptors in mammals and fish. *Int. J. Endocrinol.* (2020) doi:10.1155/2020/5386193.

66. Michel, T., Halabalaki, M. & Skaltsounis, A. L. New concepts, experimental approaches, and dereplication strategies for the discovery of novel phytoestrogens from natural sources. *Planta Med.* **79**, 514–532 (2013).

67. Li, L. *et al.* The molecular mechanism of bisphenol A (BPA) as an endocrine disruptor by interacting with nuclear receptors: Insights from molecular dynamics (MD) simulations. *PLoS One* **10**, 1–18 (2015).

68. Davis, C. E. J. Kākāpō reproduction: Identification of steroid receptors and oestrogenic activity in native flora. (Victoria University of Wellington, 2013).

69. Rochester, J. R. & Millam, J. R. Phytoestrogens and avian reproduction: Exploring the evolution and function of phytoestrogens and possible role of plant compounds in the breeding ecology of wild birds. *Comp. Biochem. Physiol. - A Mol. Integr. Physiol.* **154**, 279–288 (2009).

70. Bacciottini, L. *et al.* Phytoestrogens: Food or drug? *Clin. Cases Miner. Bone Metab.* **4**, 123–130 (2007).

71. Panche, A. N., Diwan, A. D. & Chandra, S. R. Flavonoids: An overview. *J. Nutr. Sci.* **5**, 1–15 (2016).

72. Havsteen, B. H. The biochemistry and medical significance of the flavonoids. *Pharmacol. Ther.* **96**, 67–202 (2002).

73. Liu, H., Zhang, C., Liu, Y. & Duan, H. Total flavonoid contents in bamboo diets and reproductive hormones in captive pandas: Exploring the potential effects on the female giant panda (Ailuropoda melanoleuca). *Conserv. Physiol.* **7**, 1–10 (2019).

74. Akdemir, F. & Sahin, K. Genistein supplementation to the quail: Effects on egg production and egg yolk genistein, daidzein, and lipid peroxidation levels. *Poult. Sci.* **88**, 2125–2131 (2009).

75. Dixon, R. A. Phytoestrogens. *Annu. Rev. Plant Biol.* **55**, 225–261 (2004).

76. Teponno, R. B., Kusari, S. & Spiteller, M. Recent advances in research on lignans and neolignans. *Nat. Prod. Rep.* **33**, 1044–1092 (2016).

77. Li, Y., Xie, S., Ying, J., Wei, W. & Gao, K. Chemical structures of lignans and neolignans isolated from Lauraceae. *Molecules* **23**, 1–18 (2018).

78. Tou, J. C. L., Chen, J. & Thompson, L. U. Flaxseed and its lignan precursor, secoisolariciresinol diglycoside, affect pregnancy outcome and reproductive development in rats. *J. Nutr.* **128**, 1861–1868 (1998).

79. Kennedy, A. K. Effects of flaxseed lignans on laying hen reproductive parameters. (Texas A&M University, 1997).

80. Nikolić, I., Savić-Gajić, I., Tačić, A. & Savić, I. Classification and biological activity of phytoestrogens: A review. *Adv. Technol.* **6**, 96–106 (2017).

81. Bickoff, E. M. *et al.* Coumestrol, a new estrogen isolated from forage crops. *Science.* **126**, 969–970 (1957).

82. Blomquist, C. H., Lima, P. H. & Hotchkiss, J. R. Inhibition of 3α-hydroxysteroid dehydrogenase (3α-HSD) activity of human lung microsomes by genistein, daidzein, coumestrol and C 18-, C19- and C21-hydroxysteroids and ketosteroids. *Steroids* **70**, 507–514 (2005).

83. Kuiper, G. G. J. M. *et al.* Interaction of estrogenic chemicals and phytoestrogens with estrogen receptor β. *Endocrinology* **139**, 4252–4263 (1998).

84. Ashby, J., Tinwell, H., Soames, A. & Foster, J. Induction of hyperplasia and increased DNA content in the uterus of immature rats exposed to coumestrol. *Environ. Health Perspect.* **107**, 819–822 (1999).

85. Reinisalo, M., Kårlund, A., Koskela, A., Kaarniranta, K. & Karjalainen, R. O. Polyphenol stilbenes: Molecular mechanisms of defence against oxidative stress and aging-related diseases. *Oxid. Med. Cell. Longev.* **2015**, 1–24 (2015).

86. Kwasniewski, S. P., Claes, L., Francois, J. P. & Deleuze, M. S. High level theoretical study of the structure and rotational barriers of trans-stilbene. *J. Chem. Phys.* **118**, 7823–7836 (2003).

87. Dou, Y. & Allen, R. E. Detailed dynamics of a complex photochemical reaction: Cis – trans photoisomerization of stilbene. *J. Chem. Phys.* **119**, 10658–10666 (2003).

88. Ziaullah & Rupasinghe, H. P. V. Application of NMR spectroscopy in plant polyphenols associated with human health. in *Applications of NMR Spectroscopy* (eds. Choudhary, A.-R. & Iqbal, M.) vol. 2 3–92 (Bentham Science Publishers, 2015).

89. Henry, L. A. & Witt, D. M. Effects of neonatal resveratrol exposure on adult male and female reproductive physiology and behavior. *Dev. Neurosci.* **28**, 186–195 (2006).

90. Englyst, H. N., Quigley, M. E. & Hudson, G. J. Determination of dietary fibre as

non-starch polysaccharides with gas-liquid chromatographic, high-performance liquid chromatographic or spectrophotometric measurement of constituent sugars. *Analyst* **11**, 1497–1509 (1994).

91. Van Soest, P. J., Robertson, J. B. & Lewis, B. A. Methods for dietary fiber, neutral detergent fiber, and nonstarch polysaccharides in relation to animal nutrition. *J. Dairy Sci.* **74**, 3583–3597 (1991).

92. Tobimatsu, Y. *et al.* Coexistence but independent biosynthesis of catechyl and guaiacyl/syringyl lignin polymers in seed coats. *Plant Cell* **25**, 2587–2600 (2013).

93. Vispo, C. & Karasov, W. H. The Interaction of avian gut microbes and their host: An elusive symbiosis. in *Gastrointestinal Microbiology* 116–155 (1997). doi:10.1007/978-1-4615-4111-0_5.

94. Guo, M. Q., Hu, X., Wang, C. & Ai, L. Polysaccharides: Structure and solubility. in *Solubility of Polysaccharides* (2017). doi:10.5772/intechopen.71570.

95. Pelletier, S. *et al.* Drying procedures affect non-structural carbohydrates and other nutritive value attributes in forage samples. *Anim. Feed Sci. Technol.* **157**, 139–150 (2010).

96. Shimizu, N. & Andres, A. Characterisation of fructans by size-exclusion chromatography: A Review. in *Agricultural Research Updates* (ed. Gorawala, P.) vol. 29 209–236 (Nova Science Publishers, 2020).

97. Balto, A. S. *et al.* On the use of differential solubility in aqueous ethanol solutions to narrow the DP range of food-grade starch hydrolysis products. *Food Chem.* **197**, 872–880 (2016).

98. Strachan, J. Solubility of cellulose in water. *Nature* **141**, 332–333 (1938).

99. Deguchi, S., Tsujii, K. & Horikoshi, K. Cooking cellulose in hot and compressed water. *Chem. Commun.* 3293–3295 (2006) doi:10.1039/b605812d.

100. Wang, R. S. *et al.* Solubility difference between pectic fractions from creeping fig seeds. *Polymers (Basel).* **11**, 1–11 (2019).

101. Basanta, M. F., Ponce, N. M. A., Rojas, A. M. & Stortz, C. A. Effect of extraction time and temperature on the characteristics of loosely bound pectins from Japanese plum. *Carbohydr. Polym.* **89**, 230–235 (2012).

102. Gawkowska, D., Cybulska, J. & Zdunek, A. Structure-related gelling of pectins and linking with other natural compounds: A review. *Polymers (Basel).* **10**, (2018).

103. Glibowski, P. & Bukowska, A. The effect of pH, temperature and heating time on inulin chemical stability. *Acta Sci. Pol. Technol. Aliment.* **10**, 189–196 (2011).

104. Böhm, A., Kaiser, I., Trebstein, A. & Henle, T. Heat-induced degradation of inulin. *Eur. Food Res. Technol.* **220**, 466–471 (2005).

105. Liu, H., Yu, L., Xie, F. & Chen, L. Gelatinization of cornstarch with different amylose/amylopectin content. *Carbohydr. Polym.* **65**, 357–363 (2006).

106. Megazyme. Sucrose/D-Fructose/D-Glucose Assay Kit. *Sucrose, D-Frutose and D-Glucose Assay Procedure* (2018).

107. Chaimanee, P. & Suntornwat, O. Changes in carbohydrate content during fruit ripening - A new approach of teaching of carbohydrate chemistry in biochemistry course. *Biochem. Educ.* **22**, 101–102 (1994).

108. Megazyme. Total starch assay procedure (amyloglucosidase/ α-amylase method). (2020).

109. Alves, L. A., Silva, J. B. A. & Giulietti, M. Solubility of D-glucose in water and ethanol/water mixtures. *J. Chem. Eng. Data* **52**, 2166–2170 (2007).

110. Saeman, J. F., Moore, W. E., Mitchell, R. L. & Millett, M. A. Techniques for the determination of pulp constituents by quantitiative paper chromatography. *Tappi J.* **37**, 336–343 (1954).

111. Becker, M. *et al.* Comparative hydrolysis analysis of cellulose samples and aspects of its application in conservation science. *Cellulose* **28**, 8719–8734 (2021).

112. Fazio, S. A., Uhlinger, D. J., Parker, J. H. & White, D. C. Estimations of uronic acids as quantitative measures of extracellular and cell wall polysaccharide polymers from environmental samples. *Appl. Environ. Microbiol.* **43**, 1151–1159 (1982).

113. Conner, A. H., Harris, J. F., Wood, B. F. & Hill, C. G. Kinetic model for the dilute sulfuric acid saccharification of lignocellulose. *J. Wood Chem. Technol.* **5**, 461–489 (1985).

114. Silva, J., Ferraz, R., Dupree, P., Showalter, A. M. & Coimbra, S. Three decades of advances in arabinogalactan-protein biosynthesis. *Front. Plant Sci.* **11**, 1–18 (2020).

115. Philip, J., T, T. & S, B. Occurrence of cellulose degraders in fruit and vegetable decaying wastes. *J. Bioremediation Biodegrad.* **7**, 1–5 (2016).

116. Hartemink, R. Prebiotic effects of non-digestible oligo- and polysaccharides. (Wageningen Agricultural University, 1997).

117. Keithley, J. & Swanson, B. Glucomannan and obesity: A critical review. *Altern. Ther. Health Med.* **11**, 30–34 (2005).

118. Baker, J. T., Duarte, M. E., Holanda, D. M. & Kim, S. W. Friend or foe? Impacts of dietary xylans, xylooligosaccharides, and xylanases on intestinal health and growth performance of monogastric animals. *Animals* **11**, 1–28 (2021).

119. Mirzadeh, M., Keshavarz Lelekami, A. & Khedmat, L. Plant/algal polysaccharides extracted by microwave: A review on hypoglycemic, hypolipidemic, prebiotic, and immune-stimulatory effect. *Carbohydr. Polym.* **266**, 118–134 (2021).

120. Raubenheimer, D. & Simpson, S. J. The challenge of supplementary feeding:

Can geometric analysis help save the kakapo? *Notornis* **53**, 100–111 (2006).

121. Singh, R. P. *et al.* Generation of structurally diverse pectin oligosaccharides having prebiotic attributes. *Food Hydrocoll.* **108**, 105988 (2020).

122. Jensen, H. *et al.* Environmental Parameters affecting the concentration of iodine in New Zealand pasture. *J. Environ. Qual.* **48**, 1517–1523 (2019).

123. Mann, J. I. & Aitken, E. The re-emergence of iodine deficiency in New Zealand? *N. Z. Med. J.* **116**, 1–5 (2003).

124. Vannort, R., Cressey, P. & Silvers, K. *1997/98 New Zealand total diet survey - Part 2: elements - selected contaminants and nutrients*. https://www.moh.govt.nz/notebook/nbbooks.nsf/0/ac68dd275c26fd3f4c2568b10070f6d2/$FILE/ElementsFinal.pdf (2000).

125. Tagami, K., Uchida, S., Hirai, I., Tsukada, H. & Takeda, H. Determination of chlorine, bromine and iodine in plant samples by inductively coupled plasma-mass spectrometry after leaching with tetramethyl ammonium hydroxide under a mild temperature condition. *Anal. Chim. Acta* **570**, 88–92 (2006).

126. Yamada, H., Kiriyama, T. & Yonebayashi, K. Determination of total iodine in soils by inductively coupled plasma mass spectrometry. *Soil Sci. Plant Nutr.* **42**, 859–866 (1996).

127. Haldimann, M., Alt, A., Blanc, A. & Blondeau, K. Iodine content of food groups. *J. Food Compos. Anal.* **18**, 461–471 (2005).

128. Carlsen, M. H., Andersen, L. F., Dahl, L., Norberg, N. & Hjartåker, A. New iodine food composition database and updated calculations of iodine intake among Norwegians. *Nutrients* **10**, 1–13 (2018).

129. Sarker, S. D., Latif, Z. & Gray, A. I. *Natural products isolation*. *Natural product reports* (Humana Press, 2006). doi:10.1039/b700306b.

130. Walker, J. M. *Natural products isolation Methods and protocols*. *Life Sciences* (Humana Press, 2009).

131. Levin, E. R. Plasma membrane estrogen receptors. *Trends Endocrinol Metab* **20**, 477–482 (2009).

132. Lipinski, C. A., Lombardo, F., Dominy, B. W. & Feeney, P. J. Experimental and computational approaches to estimate solubility and permeability in drug discovery and development settings. *Adv. Drug Deliv. Rev.* **64**, 4–17 (2001).

133. Frimurer, T. M., Bywater, R., Naerum, L., Lauritsen, L. N. & Brunak, S. Improving the idds in discriminating “drug-Like” from “non drug-like” compounds. *J. Chem. Inf. Comput. Sci.* **40**, 1315–1324 (2000).

134. Singh, Ameet, J. Secondary metabolites from the New Zealand marine sponge Mycale hentscheli. (Victoria University of Wellington, 2007).

135. West, L. M. The isolation of secondary metabolites from New Zealand marine sponges. (Victoria University of Wellington, 2001).

136. Chemicalbook. Bis(2-ethylhexyl) phthalate(117-81-7) 1H NMR. https://www.chemicalbook.com/SpectrumEN_117-81-7_1HNMR.htm.

137. Chen, X. *et al.* Toxicity and estrogenic endocrine disrupting activity of phthalates and their mixtures. *Int. J. Environ. Res. Public Health* **11**, 3156–3168 (2014).

138. Gogoi, J. *et al.* Isolation and characterization of bioactive components from Mirabilis jalapa L. radix. *J. Tradit. Complement. Med.* **6**, 41–47 (2016).

139. Sorensen, T. S. On the non-equivalence of isopropyl CH_3 nuclear magnetic resonance signals. *Can. J. Chem.* **45**, 1585–1588 (1967).

140. Tikka, C. *et al.* Isolation and characterization of ethanol tolerant yeast strains. *Bioinformation* **9**, 421–425 (2013).

141. Mota, M. N., Martins, L. C. & Sá-Correia, I. The identification of genetic determinants of methanol tolerance in yeast suggests differences in methanol and ethanol toxicity mechanisms and candidates for improved methanol tolerance engineering. *J. Fungi* **7**, 1–28 (2021).

142. Sadowska-Bartosz, I., Paczka, A., Moloń, M. & Bartosz, G. Dimethyl sulfoxide induces oxidative stress in the yeast Saccharomyces cerevisiae. *FEMS Yeast Res.* **13**, 820–830 (2013).